Developing cancer immunotherapy by activating macrophage tumoricidal activity

by

Ajna Avdagic]

Thesis for Master´s Degree in Molecular Bioscience

60 study points

Department of Molecular Biosciences

The Faculty of Mathematics and Natural Sciences

University of Oslo

August 2017

Developing cancer immunotherapy by activating macrophage tumoricidal activity

by

Ajna Avdagic

Master Program in Molecular Biology

Department of Molecular Biosciences

The Faculty of Mathematics and Natural Sciences

University of Oslo

Master Thesis 60 study points

Supervised by Alexandre Corthay

Performed at the Department of Pathology

Oslo University Hospital, Rikshospitalet

August 2017

August 2017

Developing cancer immunotherapy by activating macrophage tumoricidal activity

Ajna Avdagic

http://www.duo.uio.no

Trykk: Reprosentralen, Universitetet i Oslo

TABLE OF CONTENTS

Acknowledgments

The work presented in this master thesis was performed within the Tumor Immunology group, at the Department of Pathology, Oslo University Hospital, Rikshospitalet, during the period August 2015 to August 2017.

First of all, I would like to thank my supervisor Alexandre Corthay for giving me the opportunity to do my master in his amazing group. Thank you for giving me great advice whenever I ran into a trouble spot. Thank you for the support and feedback during my master work. My sincere thanks goes to Inger Øyenbraten for helping me in the lab.

I want to express my greatest gratitude to Elisabeth Müller for teaching me the techniques and for sharing her knowledge. Thank you for all your help and feedback during my writing process even on your busy schedule.

My deepest gratitude goes to Branislava Stankovic for patiently teaching me how to work with mice. Thank you for all your ideas and encouragements.

Furthermore, I am also grateful to our Panagiotis Christopoulos for always giving me advice and helping me to be a better student. My sincere thanks also goes to Henrik Aamot for teaching me the basic protocols in the operating theatre and working with mice.

I am also grateful to Baiba Ķūrēna for always helping me in the lab and for the feedback on my writing.

I would like to thank my two amazing friends and Master students Asha A Nur Gutale and Renate Skarshaug. Thank you girls for always laughing and stressing together. Thank you for always being there for me.

My gratitude goes to Martin Speth for making the nanoparticles whenever I needed them and giving me ideas for further experiments. Many thanks to Peter Lundbäck for explaining me how HMGB1 works.

Last but not least, I would like to thank my parents for supporting me spiritually throughout my years of study and my life in general. This would not have been possible without you.

Abbreviations

Ag	Antigen
APC	Antigen-presenting cell
BCG	Bacillie Calmete-Guérin
BMDM	Bone marrow derived macrophages
CM	L929-derived conditioned medium
CML	Chronic myeloid leukemia
CREB	Cyclic-AMP-response-element-binding protein
DAMPs	Damage-associated molecular patterns
DMSO	Dimethyl sulfoxide
DPBS	Dulbecco´s phosphate-buffered saline
FBS	Fetal bovine serum
FDA	Food and Drug Administration
HMGB1	High mobility group box protein 1
IFNα	Interferon alpha
IFNβ	Interferon beta
IFNγ	Interferon gamma
IFNAR	Interferon alpha receptor
IFNAR1	Interferon alpha receptor 1
IFNAR2	Interferon alpha receptor 2
IFNGR1	Interferon gamma receptor 1
IKKβ	IkB kinase beta
IL	Interleukin
iNOS	Induced nitric oxide synthase
IRAKs	IL-1R-associated kinases
IRF	Interferon-regulatory factor
IRF3	Interferon-regulatory factor 3
IRF5	Interferon-regulatory factor 5
IRF7	Interferon-regulatory factor 7
JAK	Janus kinases
JNK	Jun kinase
LLC	Lewis Lung Carcinoma
LRR	Leucine-rich repeats
MAPKs	Mitogen-activated protein kinases
MHC	Major histocompatibility complex
MPS	Mononuclear phagocytic system
MyD88	Myeloid differentiation primary response factor 88
NED	N-(I-napthyl)ethylenediamine dihydrochloride
NEMO	NF-kappa B essential modulator
NF-κB	Nucelar factor kappa-light-chain-enhancer of activated B cells
NK	Natural killer cells
NO	Nitric oxide
NO_2^-	Nitrite
NSG	non-obses diabetic severe combined immunodeficiency gamma
PAMPs	Pattern-associated molecular patterns
PBS+/+	Phosphate-buffered saline with Calsium and Magnesium chloride
PBS-/-	Phosphate-buffered saline without Calsium and Magnesium chloride

PD-1	Programmed cell death 1
PEG	Polyethylene glycol
pIC-NPs	poly(I:C) encapsulating chitosan-nanoparticles
PLGA	Poly(lactic-co-glycolic) acid
Poly(I:C)	polyinosinic-polycytidylic acid
PRR	Pattern-recognition receptors
PS	Phosphatidylserine
RAGE	Receptor for advanced glycation end products
s.c	Subcutaneously
scid	Severe combined immunodeficiency
SMT	S-Methylisothiourea hemisulfate salt
SN	Supernatant
STAT	Signal transducer and activator of transcription
STAT 1	Signal transducer and activator of transcription 1
STAT3	Signal transducer and activator of transcription 3
TAK1	Transforming growth factor beta-activated kinase
TAMs	Tumor-associated macrophages
TB	Tuberculosis
TGFβ	Transforming growth factor-β
T_H1	T helper 1 cells
T_H2	T helper 2 cells
TIR	Toll/IL-1 receptor
TLRs	Toll-like receptors
TNF	Tumor necrosis factor
TNFα	Tumor necrosis factor alpha
TNFR1	Tumor necrosis factor receptor 1
TNFR2	Tumor necrosis factor receptor 2
TRAF6	TNFα receptor-associated factor 6
TRAM	TRIF-related adaptor molecule
TRAIL	TNF-related apoptosis-inducing ligand
T_{reg}	regulatory T cells
TRIF	TIR-domain-containing adaptor protein induction IFN-β

Abstract

Immunotherapy is considered one of the most promising novel strategies to cure cancer by taking advantage of the infiltrated tumor innate immune cells. TLR agonists are popular immunotherapeutic agents used to activate tumoricidal activity in macrophages and dendritic cells (DCs). The requirement of the cytokine interferon (IFN)-γ is know to be necessary for the optimal activation of the tumoricidal activity in M1-type macrophages. In this study we investigated the potential of new molecular combinations that could replace IFN-γ involvement in macrophage tumoricidal activation. For this purpose we used the *in vitro* cancer cell growth inhibition assay with murine bone marrow derived macrophages as effector cells. Lewis Lung carcinoma (LLC) cell line was used as the target cells. The production of nitric oxide (NO) was quantified during the main *in vitro* method. TLR3 agonist, Poly(I:C) encapsulated in chitosan-based nanoparticles (pIC-NP) showed to be a potent activator for rendering macrophages tumoricidal. This cancer cell growth inhibition seems to be NO mediated. However, this activation required a second stimulus, provided by the TLR1/2 agonist Pam3. Furthermore, the alarmin HMGB1 synergizes with Pam3 in order to activate macrophages towards an antitumor phenotype. No indication of single TLR macrophage-induced activation was found in any performed experiments. Further experiments revealed the potential of replacing type II interferon with type I for the induction of tumoricidal M1 macrophage phenotype. On the other hand, the cytokine TNF-α showed to be inefficient for macrophage activation. Taken together, the new discovered molecular combinations may be used as new strategies for novel immunotherapeutic protocols against cancer.

1 Introduction

1.1 The Immune system

The immune system has developed in order to protect, limit and eradicate the invasion of the host by microorganisms [1]. The most sophisticated and advanced form of immune defense is found in mammalians, which is divided into two cross-reacting branches: innate and adaptive immunity [2]. Innate immunity is considered to be the first line of defense, which employs anatomical barriers (both physical and chemical), phagocytes like macrophages and dendritic cells, and several serum proteins known as the complement system [1]. The innate immunity is always ready to act, and is capable of sensing and clearing most microorganisms by using germline-encoded pattern-recognition receptors (PRRs) expressed by all innate immune cells [3]. PRRs recognize different but conserved pathogen structures necessary for the pathogen survival, known as pathogen-associated molecular patterns (PAMPs) [2, 4]. Interactions between PRRs and PAMPs induce specific intracellular signaling pathways, which in return lead to different anti-pathogenic responses such as pro-inflammatory cytokine production [2,4]. The goal of these anti-pathogenic responses is to induce destruction of the pathogen in a short time frame such as minutes or hours, and to restore tissue homeostasis by removing damaged or dead cells produced during the infection [1]. New findings indicate that PRRs can also be activated through interactions with damage-associated molecular patterns (DAMPs) [5]. These immune stimulators are defined as endogenous molecules that are released from damaged and stressed cells [4].

In contrast to the innate immunity, which lacks immunological memory and displays limited specificity in terms of PRRs, the adaptive immunity has a high antigen dependent specificity that leads to clonal selection and expansion of pre-existing T- and B-lymphocytes and development of immunological memory [1-4]. The adaptive immune responses require time in order to develop but are very efficient in the later phases of the infection as well as against reoccurring pathogens [1-4].

---

[1] Murphy K: *Janeway´s Immunobiology* 9th Edition: Garland Science; 2017

[2] Akira S, Uematsu S, Takeuchi O: Pathogen recognition and innate immunity. *Cell* 2006, **124 (4)**: 783-801

[3] Schenten, D. and R. Medzhitov: Chapter 3 : The control of adaptive immune responses by the innate immune system. *Advances in Immunology* 2011, **109**: p. 87-124.

[4] Takeuchi O, Akira S: Pattern recognition receptors and inflammation. *Cell* 2010, **140 (6)**: 805-820

[5] McComb S, Thiriot A, Krishnan L, Stark F: Chapter 1: Introduction to the Immune System. *Methods in Molecular Biology* 2013, **1061**: 1-20

1.2 Macrophages

Macrophages are innate immune cells that are part of the mononuclear phagocytic system (MPS), originating from the hematopoietic stem cells in the bone marrow [6]. Monocytes are macrophage precursor cells that circulate in the blood and migrate into a specific tissue where they undergo differentiation into macrophages [6,7]. The differentiation is dependent on the hematopoietic stimulation signals found in the tissue microenvironment [7]. Depending on the activation factors within microenvironment, tissue-resident macrophages are able to display a high functionally heterogeneity and plasticity [7].

Mature macrophages are found in almost all tissues and are involved in immune surveillance and maintenance of tissue homeostasis [6]. They are considered to be professional phagocytic cells that eliminate any signs of damage or pathogenic invasion [6]. In order to be able to carry out its fundamental function, macrophages express a variety of surface receptors such as Toll-like receptors (TLRs), scavenger receptors, complement receptors and Fc receptors for recognizing and binding different PAMPs or DAMPs [6,7]. Macrophages also remove apoptotic or necrotic cells and cell debris, and thereby maintain the tissue homeostasis [6]. An additional role of macrophages is to present pathogen-derived antigens to T lymphocytes on major histocompatibility complexes (MHC) [7].

Macrophages are able to secrete a huge range of different effector molecules including nitric oxide and cytokines after recognition of PAMPs or DAMPs [8]. Upon activation, macrophages change their gene expression, which leads to the polarization of macrophages [8]. Polarized macrophages are divided into two main subtypes: classical (M1) and alternative (M2) [8].

[6] Murray P.J, Wynn T.A : Protective and pathogenic functions of macrophage subsets. *Nature Reviews Immunology* 2011, **11(11)**: 723-737.
[7] Billack B: Macrophage Activation: Role of Toll-like Receptors, Nitric Oxide and Nuclear Factor kappa B. *Americal Journal of Pharmaceutical Education* 2006, **70(5)** Article 102; 1-10
[8] Hume D.A : The Many Alternative Faces of Macrophage Activation. *Frontiers in Immunology* 2015, **6 (370)**: 1-10

1.2.1 M1/M2 characterization

The classical activation of macrophages towards M1 phenotype requires interferon-(IFN)-γ secreted by either natural killer (NK) cells or by T helper 1 (T_H1) cells [9]. The activation also requires TLR agonists that signal either through myeloid differentiation primary response factor 88 (MyD88)-signaling pathway (like LPS) or through TIR-domain-containing adaptor protein inducing IFN-β (TRIF)- dependent pathway [9,10,11]. MyD88-signaling pathway leads to production of tumor necrosis factor (TNF) that can activate macrophages together with IFN-γ in an autocrine manner, whereas IFN-β, which is the production of TRIF-signaling pathway, is able to replace IFNγ and enhance M1 polarization through signal transducer and activator of transcription (STAT)- 1 and IFN-regulatory factor (IRF)- 5 [9,11].

M1 macrophages are characterized by production of a variety of pro-inflammatory cytokines such as interleukin (IL)-1, IL-6, IL-23 and TNF-alpha (TNF-α) (Figure 1), which are associated with T_H1 and T_H17 development [9].

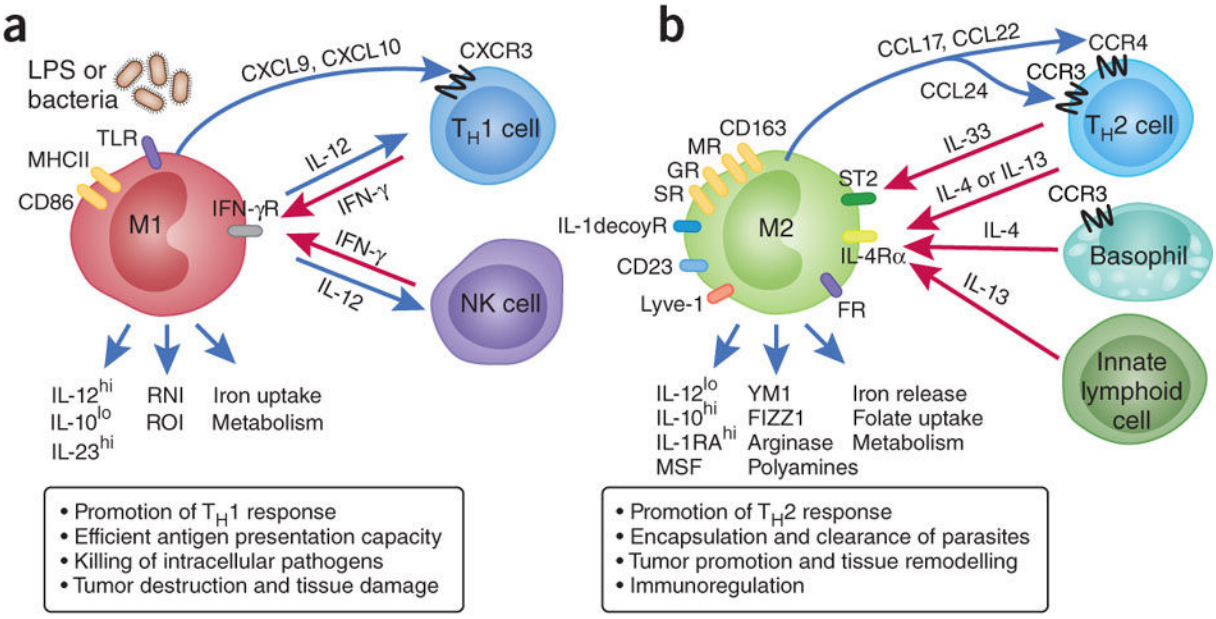

Figure 1. M1 and M2 macrophages. Figure adopted and modified from [10]

[9] Mosser D.M, Edwards J.P: Exploring the full spectrum of macrophage activation. *Nature Review Immunology* 2008, **8 (12)**: 958-969

[10] Biswas S.K, Mantovani A: Macrophage plasticity and interaction with lymphocyte subsets: cancer as a paradigm. *Nature Review Immunology* 2010, **11 (10)**: 889-896

[11] Porta C, Riboldi E, Ippolito A, Sica A: Molecular and epigenetic basis of macrophage polarized activation. *Seminars in Immunology* 2015, **27(4)**: 237-248

Classically activated macrophages also secrete T_H1 –attracting chemokines such as CXCL9 and CXCL10 [9]. Another hallmark of M1 macrophages is increased antigen presentation to CD4+ T cells as a result of up-regulated expression of MHC class II molecules [9,10]. M1 macrophages are also characterized by enhanced expression of induced nitric oxide synthase (iNOS) (Table 1) and production of high levels of reactive nitrogen and oxygen intermediates [9,10]. All these unique attributes make M1 macrophages the perfect mediators of cytotoxic and tumoricidal activity against pathogens and cancer cells [10,11].

M2 polarization, in contrast, is induced by T_H2 cytokines IL-4 and IL13, and results in production of the anti-inflammatory cytokine IL-10 (Figure 1) [10]. M2 macrophages are characterized by elevated expression of scavenger receptors and thereby display higher phagocytic activity [10,11]. They also use arginase pathways, which leads to the production of ornithine and polyamines [9]. In this way, the alternative activated macrophages can contribute to the extracellular matrix (Table 1) [9]. Compared to M1 macrophages, M2 are able to secrete chemokines such as CCL17, CCL18, CCL22 and CCL24, which attract T_H2, T regulatory cells (T_{reg}), eosinophils and basophils [11]. The end result of M2 polarization is amplification of T_H2 responses such as parasite clearance, allergic reaction and damping inflammation[10,11].

[9] Mosser D.M, Edwards J.P: Exploring the full spectrum of macrophage activation. *Nature Review Immunology* 2008, **8 (12)**: 958-969

[10] Biswas S.K, Mantovani A: Macrophage plasticity and interaction with lymphocyte subsets: cancer as a paradigm. *Nature Review Immunology* 2010, **11 (10)**: 889-896

[11] Porta C, Riboldi E, Ippolito A, Sica A: Molecular and epigenetic basis of macrophage polarized activation. *Seminars in Immunology* 2015, **27(4)**: 237-248

Table 1. Characteristics of M1 (classically activated) and M2 (alternatively activated or wound-healing) macrophages. Table adopted and modified from [9]

Marker	Function	Expression
Classically activated macrophages		
IL-12	Induces T_H1-cell development	Induced by IFNγ
iNOS	Produces NO and citrulline from arginine to kill microorganisms	Depends on IFNγ
CCL15	Attracts monocytes, lymphocytes and eosinophils	Upregulated by IFNγ
CCL20	Chemoattractant for DC and T cells	Upregulated by IFNγ
CXCL9	Involved in T-cell trafficking	Induced by IFNγ
CXCL10	Attracts NK and T cells; signals through CXCR3	Induced by IFNγ
CXCL11	Attracts NK and T cells; signals through CXCR3	Induced by IFNγ
Wound-healing macrophages		
CCL18	Attracts lymphocytes, immature DCs and monocytes	Induced by IL-4
YM1	Chitinase-like protein that can bind to extracellular matrix	Strongly induced by IL-4
RELMα	Can promote deposition of extracellular matrix	Strongly induced by IL-4
CCL17	Attracts T cells and macrophages	Induced by IL-4 and suppressed by IFNγ
IL-27Rα	Inhibits pro-inflammatory cytokine production	Upregulated by IL-4
IGF1	Stimulates fibroblast proliferation and survival	Induced by IL-4
CCL22	Attracts T_H2 cells and other CCR4-expressing cells	Induced by IL-4
DCIR	C-type lectin containing an ITIM motif	Induced by IL-4
Stabilin 1	Endocytic receptor that may be involved in lysosomal sorting	Induced by IL-4
Factor XIII-A	Can bind to extracellular matrix proteins and contribute to wound healing	Induced by IL-4 and suppressed by IFNγ

1.2.2 Role of Toll-like receptors in macrophage activation

Toll-like receptors (TLRs) are PRRs that have a crucial role in initiating innate immune responses by recognizing a variety of conserved pathogen-derived compounds [12]. These receptors are conserved both in invertebrates and vertebrates [12,13]. Until now, 12 different TLRs in mice (TLR1-TLR13) and 10 in humans due to the deletion of TLR11-TLR13 from the human genome have been reported [12,13]. Based on their location, TLRs can be divided into surface (TLR1, TLR2, TLR4, TLR5, TLR6 and TLR10) and endosomal (TLR3, TLR7, TLR9, TLR11, TLR12 and TLR13) TLRs [12,13].The surface TLRs can recognize lipoproteins and proteins while the endosomal ones recognize microbial nucleic acid[13].

[9] Mosser D.M, Edwards J.P: Exploring the full spectrum of macrophage activation. *Nature Review Immunology* 2008, **8 (12)**: 958-969

[12] Botos I, Segal D.M, Davies D.R: The Structural Biology of Toll-like Receptors. *Structure* 2011, **19(4)**: 447-459

[13] Pandey S, Kawai T, Akira S: Microbial Sensing by Toll-like Receptors and Intracellular Nucleic Acid Sensors. *Cold Spring Harbor Perspectives in Biology* 2015, **7 (1)**:a016246; 1-18

TLRs are transmembrane receptors consisting of a horseshoe-shaped ectodomain with leucine-rich repeats (LRRs) motifs and cytosolic Toll/IL-1 receptor (TIR) domains [12,13]. The LRRs motifs are involved in ligand recognition and binding, while TIR domains interact with downstream adaptor molecules that also contain TIR-domains [12,13].

Ligand binding leads to either homo- or heterodimerization of the receptor, which induces conformational changes [12,13]. This dimerization allows to recruit adaptor molecules to the receptor TIR-domains, thereby activating the first step in the signaling cascade [12,13]. Collectively, there are four TIR-domain containing adaptor molecules: MyD88, TRIF, TRIF-related adaptor molecule (TRAM) and MyD88 adaptor-like protein (MAL/TIRAP) [12,13]. Each of these adaptor molecules interacts with different TLRs [14,15]. However, the TLR-signaling pathway is divided into two based on the use of MyD88 or TRIF as the primary adaptor molecule [12,13,15]. They are referred to as MyD88-dependent and TRIF-dependent signaling pathways [12,13,15].

All TLRs, except the endosomal TLR3, signal through MyD88. MyD88 activates interactions between IL-1R-associated kinases (IRAKs) in order to form the Myddosome [12,13]. This complex reacts with TNF receptor-associated factor 6 (TRAF6), which activates transforming growth factor beta-activated kinase 1 (TAK1) [12,13]. The next stage is the phosphorylation of IkB kinase (IKK)-β and mitogen-activated protein kinases (MAPKs) (consisting of Jun kinases (JNK), p38 and cyclic-AMP-response-element-binding protein (CREB)) [12,13]. Furthermore, the IKK complex consisting of IKK-α, IKK-β and nuclear factor kappa-light-chain-enhancer of activated B cells (NF-κB) essential modulator (NEMO) is involved in activation of NF-κB by phosphorylating its inhibitory protein IkBα and preparing it for proteosomal degradation [13]. As a consequence of NFκB´s translocation into the nucleus, the production of pro-inflammatory cytokines, chemokines and iNOS is induced (Figure 2) [13].

[12] Botos I, Segal D.M, Davies D.R: The Structural Biology of Toll-like Receptors. *Structure* 2011, **19(4)**: 447-459

[13] Pandey S, Kawai T, Akira S: Microbial Sensing by Toll-like Receptors and Intracellular Nucleic Acid Sensors. *Cold Spring Harbor Perspectives in Biology* 2015, **7 (1)**:a016246; 1-18

[14] Trinchieri G, Sher A: Cooperation of Toll-like receptor signals in innate immune defense. *Nature Reviews Immunology* 2007, **7(3)**: 179-190

[15] Joosten L.A.B, Abdollahi-Roodsaz S, Dinarello C.A, O´Neill L, Netea M.G: Toll-like receptors and chronic inflammation in rheumatic diseases: new developments. *Nature Reviews Rheumatology* 2016, **12(6)**: 344-357.

In contrast, the endosomal TLR3 uses TRIF-dependent pathway to induce the production of type I IFN (IFN-α and IFN-β) upon recognition of synthetic analog such as polyinosinic-polycytidylic acid (poly I:C) [4,13,16]. TRIF interacts with TRAF3 and TRAF6, which leads to activation of NF-κB and production of type I IFNs through phosphorylation of IRF3 and IRF7, respectively [13,16]. TLR4 receptor is also reported to be able to act through the TRIF-dependent pathway [4,13,16]. To be able to activate TRIF-pathway, TLR4 needs to use other adopter molecule, TRAM [13].

Activation of TLR-signaling in macrophages leads to induction of pro-inflammatory cytokines such as TNF-α and IFN-γ and enhances phagocytosis [17,18]. This is a result of the increased production of iNOS, an enzyme that catalyzes the oxidoreductase reaction for producing NO from L-arginine in the presence of oxygen [17,18,19]. High NO- production is the hallmark of macrophages with killer- or M1-phenotype and is used as a strategy to induce tumor cell apoptosis [17,18]. Besides its involvement in innate immune responses, TLR-signaling can stimulate T cell activation through enhanced antigen presentation by antigen-presenting cells (APCs), up-regulate the expression of co-stimulatory molecules CD80/CD86, and inhibit IL-6 production [17,18].

---

[4] Takeuchi O, Akira S: Pattern recognition receptors and inflammation. *Cell* 2010, **140 (6)**: 805-820

[13] Pandey S, Kawai T, Akira S: Microbial Sensing by Toll-like Receptors and Intracellular Nucleic Acid Sensors. *Cold Spring Harbor Perspectives in Biology* 2015, **7 (1)**:a016246; 1-18

[16] Blasius A.L, Beutler B: Intracellular Toll-like Receptors. *Immunity* 2010, **32(3)**: 305-315

[17] Rakoff-Nahoum S, Medzhitov R: Toll-like receptors and cancer. *Nature Reviews Cancer* 2009, **9(1)**: 57-63

[18] Rahat M.A, Hemmerlein Bernhard : Macrophage-tumor cell interactions regulate the function of nitric oxide. *Frontiers in Physiology* 2013, **4(144)**: 1-15

[19] Bogdan C : Nitric oxide synthase in innate and adaptive immunity: an update. *Trends in immunology* 2015, **36(3)**: 161-178

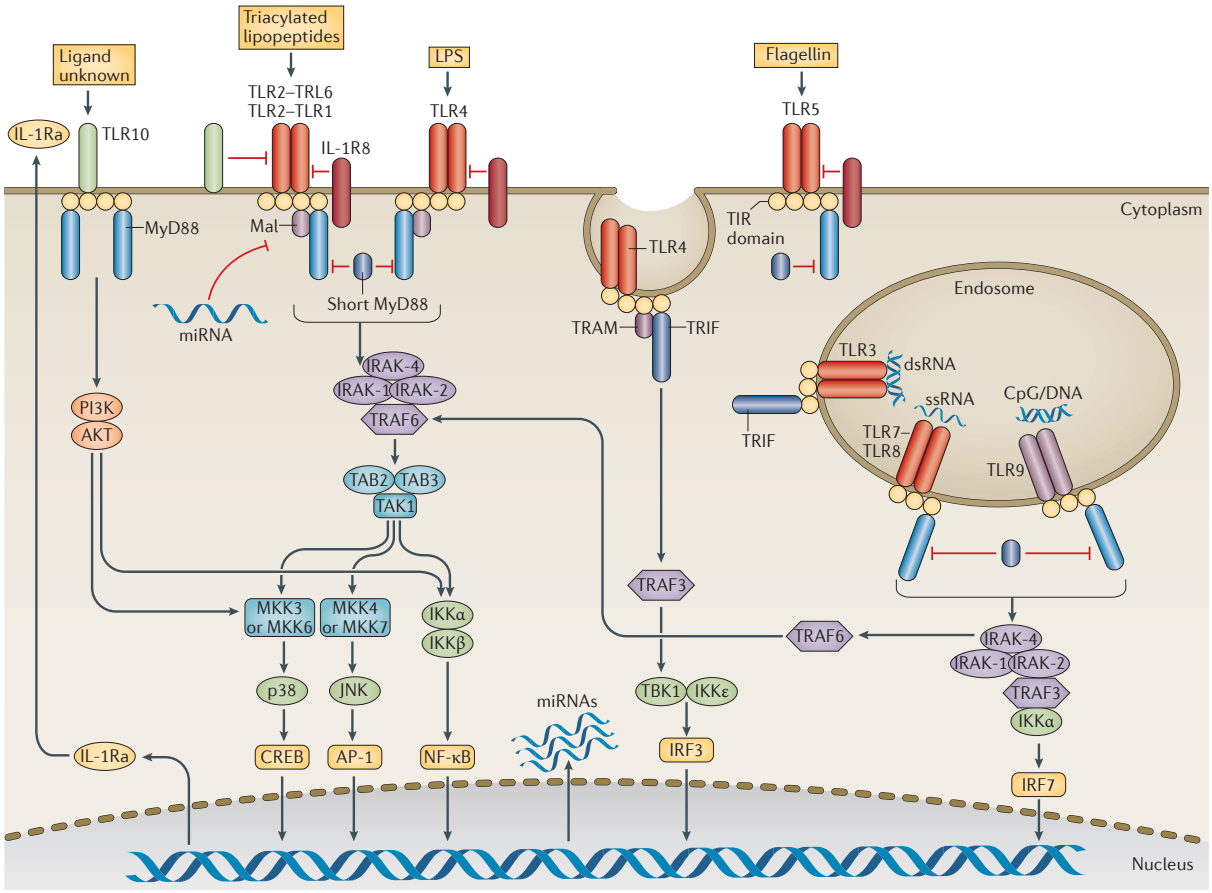

Figure 2. Cellular locations and signaling pathways of TLRs. Figure adopted from [15].

1.3 Cytokines

Cytokines are the major cell signaling molecules produced by both innate and adaptive immune cells [20]. They can be found in either secreted or membrane-bound form and their broad immunological functions include inflammatory, cytostatic, cytotoxic and antiviral activities [20, 21]. They are also involved in the growth and differentiation of immune cells [22].

[15] Joosten L.A.B, Abdollahi-Roodsaz S, Dinarello C.A, O´Neill L, Netea M.G: Toll-like receptors and chronic inflammation in rheumatic diseases: new developments. *Nature Reviews Rheumatology* 2016, **12(6)**: 344-357
[20] Lee S, Margolin K: Cytokines in Cancer Immunotherapy. Cancers 2011, **3(4)**: 3856-3893
[21] Ikram N, Hassan K, Tufail S: Cytokines. International Journal of Pathology 2004, **2(1)**: 47-58
[22] Dranoff G: Cytokines in cancer pathogenesis and cancer therapy. Nature Reviews Cancer 2004, **4 (1)**: 11-22

The secretion of cytokines is induced in response to cellular stress such as carcinogen-induced damage, inflammation or infection [20,21,22]. There is also evidence indicating continuous cytokine secretion independently of stimulation [20, 22].

The biological effects of cytokines are initiated by binding of cytokines to specific cell-surface receptors found on their targets, which results into cytokine internalization [20,21]. Overall, there are seven identified cytokine receptor families, where Type I and Type II cytokine receptors have the most promising clinical potential [20]. Type I cytokine receptors are characterized by a common signaling subunit, γc, which can induce signaling through JAK-STAT pathway [20]. These receptors recognize cytokines such as IL-2, IL-4, IL-5 and IL-13 [20]. On the other hand, Type II cytokine receptors, which recognize IFN-α, IFN-β, IFN-γ and IL-10, are heterodimers resembling immunoglobulin-like receptors [20]. The intracellular signaling domain of these cytokine receptors is associated with JAK-STAT signaling like Type I receptors [20].

Cytokines can act in a short or long distance in relation to the cells that secreted them [21]. For example, a cytokine can induce a response on the same cell that produced it leading to an autocrine effect or it can influence a cell in close proximity and give a paracrine effect [21]. The third option is an endocrine or systemic effect [21]. The effects of cytokines are considered to be both pleiotropic (diverse functions on different cell types and sometimes opposing effects) and redundant (similar effects by different cytokines) [20,21]. On the other hand, cytokines can also have antagonistic effects such as IFN-γ and IL-10 in the context of macrophage activation versus suppression, respectively [20,21].

[20] Lee S, Margolin K: Cytokines in Cancer Immunotherapy. Cancers 2011, **3(4)**: 3856-3893
[21] Ikram N, Hassan K, Tufail S: Cytokines. International Journal of Pathology 2004, **2(1)**: 47-58
[22] Dranoff G: Cytokines in cancer pathogenesis and cancer therapy. Nature Reviews Cancer 2004, **4 (1)**: 11-22

1.3.1 Type I interferon versus Type II interferon

The IFN family consists of type I, type II and the recently discovered type III IFNs [20,23]. They link the two branches of immunity (innate and adaptive), especially in fighting against cancer [23]. Type I IFN, IFN-α and IFN-β, have previously been described as antiviral modulators [20,23]. They are produced by almost all cell types upon viral infections and bind to surface- receptors interferon alpha receptor (IFNAR) 1 and IFNAR2, which activates the JAK-STAT signaling pathway (Figure 3) [23,24].

Recent studies propose involvement of Type I IFNs in anti-tumor responses, including cytotoxic effects and anti-angiogenic effects on tumor cells [25,26]. Moreover, Type I IFNs are able to activate dendritic cells, macrophages and NK cells in order to produce IL-15 and enhance antigen presentation due to increased MHC class I expression leading to T cell activation [23].

US Food and Drug Administration (FDA) has approved Type I IFNs, particularly IFN-α for clinical treatment of different cancer types including AIDS-related Kaposi´s sarcoma, chronic myeloid leukemia (CML) and melanoma [23]. IFN-α has shown good survival prognostics with minimum cancer relapse in certain cancer types such as melanoma [20,23]. Comparison between the antitumor effects induced from Type I IFNs, showed that IFN-β has a more potent anti-proliferative effect in preclinical trials [20]. Moreover, IFN-β is also approved for treatment of autoimmune diseases such as multiple sclerosis [20].

Compared to type I IFNs, IFN-γ is only produced by mature innate cells (Table 2) [23]. This cytokine uses another receptor, interferon gamma receptor 1 (IFNGR1) but acts through JAK-STAT pathway (Figure 3) [20,23].

---

[20] Lee S, Margolin K: Cytokines in Cancer Immunotherapy. Cancers 2011, **3(4)**: 3856-3893

[23] Dunn G.P, Koebel C.M, Schreiber R.D: Interferons, immunity and cancer immunoediting. Nature Reviews Tumor Immunology 2006, **6(11)**: 836-848

[24] Hervas-Stubbs S, Perez-Gracia J.L, Rouzat A, Sanmamed M.F, Le Bon A, Melero I: Direct Effects of Type I Interferons on Cells of the Immune System. Clinical Cancer Research 2011, **17(9)**: 2619-2627

[25] Marschall Z, Scholz A, Cramer T, Schafer G, Schirner M, Oberg K, Wiedenmann B, Höcker M, Rosewicz Stefan: Effects of Interferon Alpha on Vascular Endothelial Growth Factor Gene Transcription and Tumor Angiogenesis. Journal of the National Cancer Institute 2003, **95(6)**: 437-448

[26] Liang S, Wei H, Sun R, Tian Z : IFNalpha regulates NK cell cytotoxicity through STAT1 pathway. Cytokine 2003, **23(6)**: 190-199

IFN-γ leads to up-regulation of MHC class II and I molecules and thereby increases antigen presentation on macrophages and dendritic cells [23]. Macrophage activation by IFN-γ leads to increased production of nitrogen reactive intermediates [20,27].

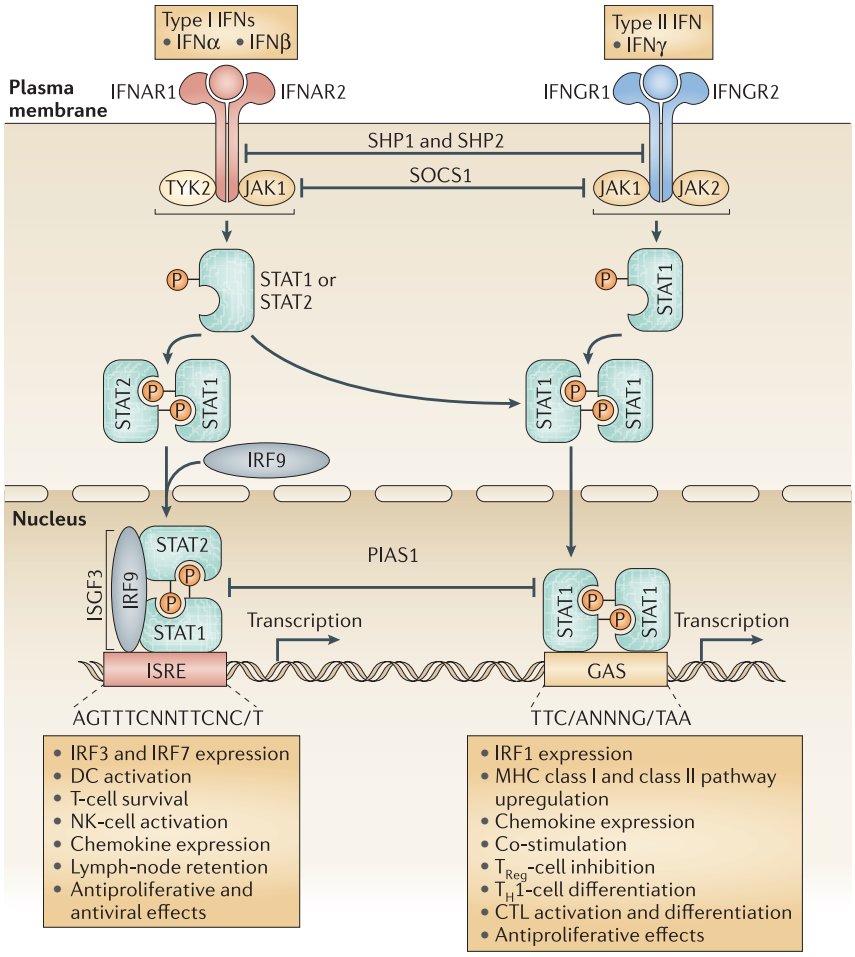

Figure 3. Signaling pathways of Type I and Type II interferons. Figure adopted and modified from [23].

There are some implications of IFN-γ for cancer treatment [23]. Immunoincompetent mice without p53 and IFN-γ recognition are more prone to tumor development than mice deficient only in p53 [23]. Another mice study demonstrated IFN-γ teamwork with other cytokines in tumor prevention while IFN-γ-insensitive mice were more prone to lung adenocarcinoma

[20] Lee S, Margolin K: Cytokines in Cancer Immunotherapy. Cancers 2011, **3(4)**: 3856-3893
[23] Dunn G.P, Koebel C.M, Schreiber R.D: Interferons, immunity and cancer immunoediting. Nature Reviews Tumor Immunology 2006, **6(11)**: 836-848
[27] Boehm U, Klamp T, Groot M, Howard JC : Cellular responses to interferon gamma. Annual Review Immunology 1997, **15**:749-795

development [23]. However, clinical studies in small-cell lung cancer and advanced colon cancer did not improve the survival rate significantly [23].

Table 2. Comparison of Type I and Type II interferon production and signaling. Figure adopted and modified from [23].

Property	Type I IFNs	Type II IFN
	IFNα and IFNβ	**IFNγ**
Stimuli	• Viruses • Other microorganisms	• Antigen–MHC complexes • Activating NK-cell ligands • IL-12 plus IL-18 • TLRs
Cells producing IFN	• All nucleated cells (especially IPCs)	• NK cells • NKT cells • T cells
Number of proteins	• IFNα: 12 (mice) and 12–13 (humans) • IFNβ: 1 (mice and humans)	• 1 (mice and humans)
Cells expressing IFN receptors	• All nucleated cells	• All nucleated cells
Type of IFN receptor	• IFNAR: IFNAR1–IFNAR2	• IFNGR: IFNGR1–IFNGR2
Signalling molecules	• JAK1 and TYK2 • STAT1–STAT2–IRF9 complexes • STAT1–STAT1 complexes	• JAK1 and JAK2 • STAT1–STAT1 complexes
Transcription-factor-binding sites	• ISRE • GAS	• GAS

1.3.2 The pro-inflammatory cytokine TNF-α

TNF-α is a multifunctional cytokine mostly produced by monocytic cell lines such as macrophages [28,29]. TNF-α can bind to two high-affinity transmembrane receptors: TNF receptor 1 (TNFR1) expressed on most cells, and TNF receptor 2 (TNFR2) expressed on immune cells [29]. TNFR1 signaling induces a broad range of TNF-α cellular responses including NF-κB activation, cytotoxicity and up-regulation of cytokine production [29]. On the other hand, TNFR2 signaling is involved in T and B cell proliferation and activation [28,29].

When it comes to the role of TNF-α in cancer, literature presents both tumor promoting and suppressive functions. The anti-tumor properties of TNF-α comprise ability to induce hemorrhagic necrosis of solid tumors and ability to stimulate tumor-specific T cells (Figure 4)

[23] Dunn G.P, Koebel C.M, Schreiber R.D: Interferons, immunity and cancer immunoediting. Nature Reviews Tumor Immunology 2006, **6(11)**: 836-848
[28] Haabeth O.A.W, Bogen B, Corthay A: A model for cancer-suppressive inflammation. Oncolmmunology 2012, **1(7)**: 1146-1155
[29] Parameswaran N, Patial S: Tumor Necrosis Factor-α Signaling in Macrophages. Crit Rev Eukaryot Gene Expr. 2010, **20(2)**: 87-103

[28]. Moreover, TNF-α may synergize with IFN-γ to enhance the tumoricidal activity of murine macrophages [28]. The synergistic effect for induced anticancer effect can also be achieved with the production of IFN-β [29]. TNF-α signaling, which gives NF-κB activation, may induce an autocrine loop and give a low but sustained production of IFN-β [29]. Together, these two cytokines combine the MyD88-dependent and TRIF-dependent pathways so that the production of inflammatory molecules is induced, and primes innate immune cells, such as macrophages, for activation [29].

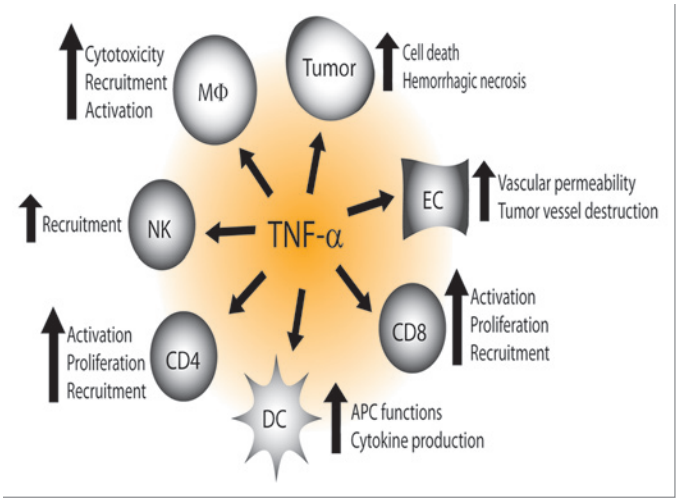

Figure 4. TNF-α and its anti-tumor properties. Figure adopted and modified from [28].

TNF-α cytotoxic ability can also be applied on various human cancer cell lines e.g. melanoma, breast and cervix carcinoma [28,29]. However, high blood levels of TNF-α in CML, is associated with shorter survival prognosis [28].

Collectively, both pro- and anti-tumor effects of TNF-α illustrate different ways in which this cytokine operates. It can be used as an advantage for therapeutical approaches [30]. The focus should be on TNF-α ability to induce tumor- cell apoptosis while suppressing its pro-tumor effects (Figure 4) [22,30].

[22] Dranoff G: Cytokines in cancer pathogenesis and cancer therapy. Nature Reviews Cancer 2004, **4 (1)**: 11-22
[28] Haabeth O.A.W, Bogen B, Corthay A: A model for cancer-suppressive inflammation. Oncolmmunology 2012, **1(7)**: 1146-1155
[29] Parameswaran N, Patial S: Tumor Necrosis Factor-α Signaling in Macrophages. Crit Rev Eukaryot Gene Expr. 2010, **20(2)**: 87-103
[30] Balkwill F: Tumor necrosis factor and cancer. Nature Reviews Cancer 2009, **9(5)**: 361-370

1.3.3 High mobility group box protein 1 (HMGB1)

It was recently discovered that the evolutionary ancient protein HMGB1 has cytokine features[31]. HMGB1 is a ubiquitously expressed protein found in most nucleated cells [31,32]. It has the function of a DNA-binding protein, involved in the nucleosome stabilization and transcription regulation (Figure 5) [31]. In the nucleus, HMGB1 binds loosely to the DNA causing its bending and giving access to several regulatory proteins including V(D) recombinases [31].

In 1999, it was discovered that activated macrophages are able to actively secrete HMGB1 in order to induce a delayed form of inflammation [31]. This happened after the secretion of the usual pro-inflammatory cytokines such as TNF-α [31]. The exogenous HMGB1 might induced the activation of STAT1 and STAT3 and thereby sends signals to inflammatory cells about tissue damage [31]. Later on, it was discovered that other innate immune cells including mature dendritic cells and NK cells, are also able to secrete HMGB1 [31].

HMGB1 can be released into the extracellular environment through two main ways [31,32]. The active strategy results from inflammatory stimulations such as LPS, TNF-α and transforming growth factor-β (TGF-β) [31]. In contrast, the passive diffusion happens during necrosis but not during apoptosis, due to the loosely binding of HMGB1 to DNA in necrotic cells [31,32]. In apoptotic cells, HMGB1 binds strongly to newly formed DNA after post-translational modifications, which makes for it difficult to leak out and thus HMGB1 stays sequestered in the nucleus [31,32]. Other processes, which lead to the translocation of HMGB1 to the cytosol, include hypoxia and ischemia or reperfusion injury of parenchymal cells [32].

Since HMGB1 functions as a alarmin, it can induce intracrine effects but also make immune complexes with cytokines in order to stimulate the innate system [31-33].
HMGB1 is considered to be a pleiotropic cytokine, which has a broad repertoire of immune effects, including cytokine production, cell proliferation and differentiation, chemotaxis, and angiogenesis (Figure 5) [32]. The cytokine production is induced by HMGB1 binding to TLR2

[31] Lotze M.T, Tracey K.J: High-mobility group box 1 protein (HMGB1): nuclear weapon in the immune arsenal. Nature Reviews Immunology 2005, **5(4)**: 331-342
[32] Harris H.E, Andersson U, Pisetsky D.S: HMGB1: A multifunctional alarmin driving autoimmune and inflammatory disease. Nature Reviews Rheumatology 2012, **8(4)**: 195-202
[33] Hreggvidsdottir H.S, östberg T, Wähämaa H, Schierbeck H, Aveberger A-C, Klevenvall L, Palmblad K, Ottosson L, Andersson U, Harris H.E: The alarmin HMGB1 acts in synergy with endogenous and exogenous danger signals to promote inflammation. Journal of Leukocyte Biology 2009, **86(3)**: 655-662

or TLR4 while the chemotactic effects require signaling through the receptor for advanced glycation end products (RAGE) [32].

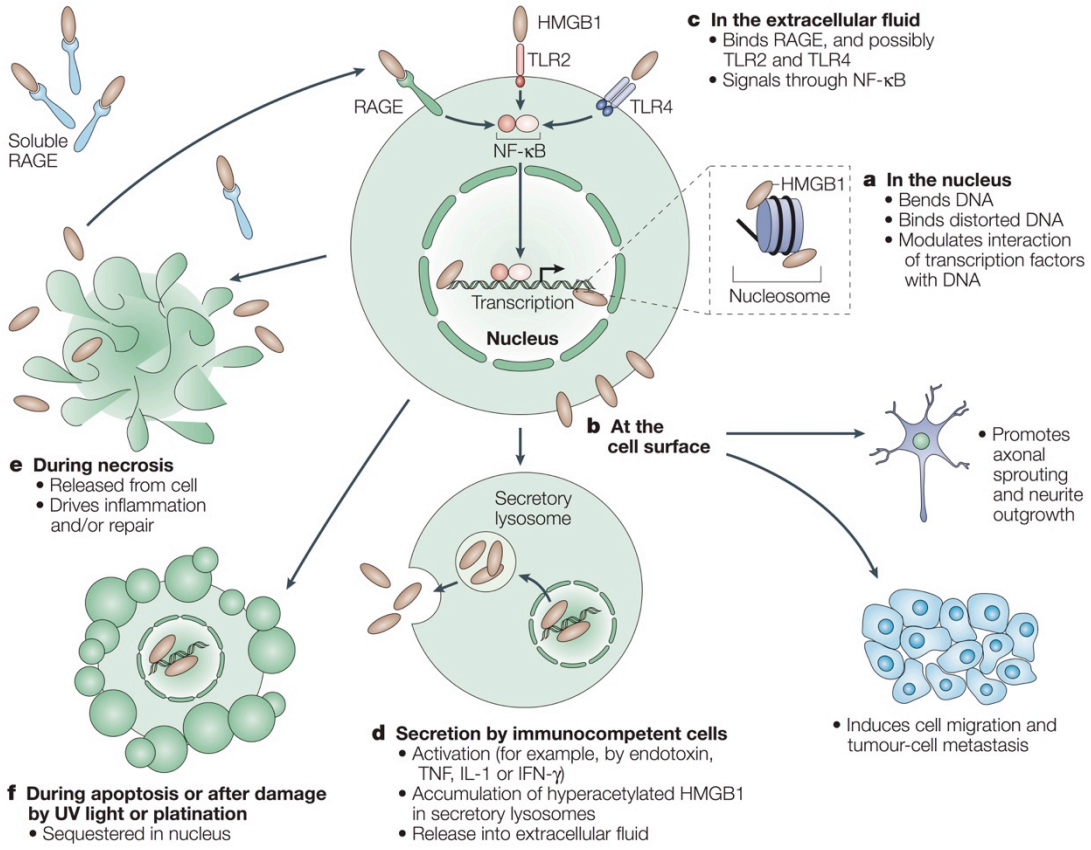

Figure 5. The different functions of HMGB1. Figure adopted and modified from [31].

It is believed that post-translational redox modifications of cysteine residues in HMGB1 can dictate the receptor interactions and inflammatory effects [34]. HMGB1 consists of two DNA-binding domains (A-box and B-box) and an acidic tail (Figure 6) [31]. This cytokine has tree highly conserved redox-sensitive cysteins in positions C23 (A-box), C45 (A-box) and C106 (B-box) [34]. C23 and C45 are bound to each other through an intramolecular disulfide bond in oxidative extracellular environment or in response to intracellular oxidative stress [34]. The third cysteine at position C106, is unpaired and its thiol form is necessary for the TLR4

[31] Lotze M.T, Tracey K.J: High-mobility group box 1 protein (HMGB1): nuclear weapon in the immune arsenal. Nature Reviews Immunology 2005, **5(4)**: 331-342

[32] Harris H.E, Andersson U, Pisetsky D.S: HMGB1: A multifunctional alarmin driving autoimmune and inflammatory disease. Nature Reviews Rheumatology 2012, **8(4)**: 195-202

[34] Yang H, Lündbäck P, Ottosson L, Erlandsson-Harris H, Venereau E, Bianchi M.E, Al-Abed Y, Andersson U, Tracey K.J, Antoine D.J: Redox Modification of Cysteine Residues Regulates the Cytokine Activity of High Mobility Group Box-1 (HMGB1). Molecular Medicine 2012, **18**:250-259

binding [34]. The intermolecular disulfide bond stabilizes the folded HMGB1 protein [34]. Yang et al study suggests that the cytokine-inducing effects of HMGB1 require both the disulfide bond and the thiol form of the third cysteine in order to bind to the TLRs [34].

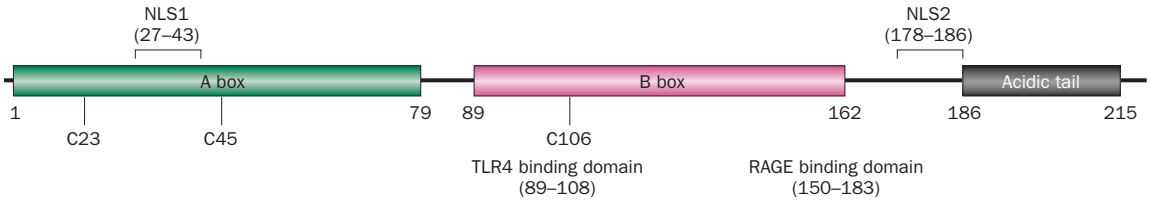

Figure 6. HMGB1 structure. Figure adopted and modified from [32].

The interactions between HMGB1 and TLR4 or TLR2 were first suggested by Park et.al in 2004 [35]. HMGB1 signaling through TLR4 requires co-receptors MD2 and CD14 [35,36]. As a consequence of activating the MyD88-dependent pathway, HMGB1 is able to induce the production of pro-inflammatory cytokines [31,32]. Until now, no connections between HMGB1 and TRIF-dependent pathway (IFNβ-production) has been reported [31,32].

HMGB1 has a dual nature in tumor pathogenesis, which depends on the cytokine binding receptor, its target cells and redox state [37]. The extracellular HMG1 is known to enhance tumor development and metastasis through its binding to RAGE and TLR4 [37]. There are also some indications that HMGB1 favours the rapid metabolism of cancer cells or so called "Warburg effect" by increasing ATP production [37]. The intracellular HMGB1, on the other hand, is known for its antitumor functions for instance in breast cancer [37]. The tumor-

[31] Lotze M.T, Tracey K.J: High-mobility group box 1 protein (HMGB1): nuclear weapon in the immune arsenal. Nature Reviews Immunology 2005, **5(4)**: 331-342
[32] Harris H.E, Andersson U, Pisetsky D.S: HMGB1: A multifunctional alarmin driving autoimmune and inflammatory disease. Nature Reviews Rheumatology 2012, **8(4)**: 195-202
[34] Yang H, Lündbäck P, Ottosson L, Erlandsson-Harris H, Venereau E, Bianchi M.E, Al-Abed Y, Andersson U, Tracey K.J, Antoine D.J: Redox Modification of Cysteine Residues Regulates the Cytokine Activity of High Mobility Group Box-1 (HMGB1). Molecular Medicine 2012, **18**:250-259
[35] Park J.S, Svetkauskaite D, He Q, Kim J.V., Strassheim D, Ishizaka A, Abraham E: Involvement of Toll-like receptors 2 and 4 in cellular activation by high mobility group box 1 protein. Journal of Biological Chemistry 2004, **279 (9)**: 7370-7377
[36] Yang H, Wang H, Ju Z, Ragab A.A, Lündbäck P, Long W, Valdes-Ferrer S.I, He M, Pribis J.P, Li J, Lu B, Gero D, Szabo C, Antoine D.J, Harris H.E, Golenblock D.T, Meng J, Roth J, Chavan S.S, Andersson U, Billiar T.R, Tracey K.J, Al-Abed Y: MD-2 is required for disulfide HMGB1-dependent TLR4 signaling. The Journal of Experimental Medicine 2015, **212(1)**: 5-14
[37] Kang R, Zhang Q, Zeh J.H III, Lotze M.T, Tang D: HMGB1 in Cancer: Good, Bad, or Both? Clinical Cancer Research 2013, **19(15)**: 4046-4057

suppressive functions of HMGB1 are mostly focusing on inducing autophagy, which prevents genome instability and reduces angiogenesis [37].

1.4 Cancer and Immune system

1.4.1 Cancer immunoediting and immunosurveillance

Cancer development is characterized by upregulated proliferation of progeny and transformed cells, and by their spreading to other body parts [1]. Mutations causing these changes are either germline or somatic [38]. Many environmental causes, including pollution and also lifestyle factors such as tobacco smoking and obesity, contribute to the carcinogenic mutations and tumor pathogenesis [38].

More than 50 years ago, Lewis Thomas and Frank MacFarlane Burnet formulated the concept of immune system´s involvement in cancer prevention and eradication, known as immunological surveillance [39]. The immune system is able to recognize tumor cells and initiates tumor eradication [39]. However, the selective pressure from the immune system can lead to re-shaping of tumor-associated antigens thereby avoiding immune destruction, which is one of the hallmark of cancer [40,41]. Conclusively, all pro-tumor abilities of the immune system are focusing on suppressing the protective immune mechanisms and making the tumor less immunogenic [23,42].

The tumor microenvironment includes not only cancer cells and surrounding stroma but also innate immune cells such as macrophages, dendritic cells and natural killer cells and cells of the adaptive immune system, T- and B-lymphocytes respectively [38]. The cytokine and chemokine production within the tumor microenvironment can influence the balance between pro-tumor and anti-tumor immunity [38]. In 2001, Frances Balkwill and Alberto Mantovani proposed that immune cells and cytokine production within the tumor microenvironment

[1] Murphy K: *Janeway´s Immunobiology* 9th Edition: Garland Science; 2017
[23] Dunn G.P, Koebel C.M, Schreiber R.D: Interferons, immunity and cancer immunoediting. Nature Reviews Tumor Immunology 2006, **6(11)**: 836-848
[37] Kang R, Zhang Q, Zeh J.H III, Lotze M.T, Tang D: HMGB1 in Cancer: Good, Bad, or Both? Clinical Cancer Research 2013, **19(15)**: 4046-4057
[38] Grivennikov S.I, Greten F.R, Karin M: Immunity, Inflammation and Cancer, Cell 2010, **140(6)**: 883-899
[39] Corthay A: Does the immune system naturally protect against cancer? Frontiers in Immunology 2014, **5(197)**: 1-8
[40] Pecorino L: Molecular biology of cancer-mechanisms, targets and therapeutics. **Fourth edition** 2016, Oxford University press
[41] Hannah D, Weinberg R.A: Hallmarks of cancer: The next generation. Cell 2011, **144(5)**: 646-672
[42] Dunn G.P, Old L.J, Schreiber R.D: The three Es of cancer immunoediting. Annual Review of Immunology 2004, 22:329-360

might rather promote tumor progression [43,44]. However, there are several lines of evidence that support the immune system´s anti-tumor activity [39]. It is known that the quantity and quality of tumor infiltrated immune cells can be used as a prognostic factor for cancer survival [39]. The cooperation between tumor-infiltrating CD8+ cytotoxic and CD4+ (mostly T_H1) T cells showed an increased survival in non-small cell lung cancer and esophageal squamous cell carcinoma [39].

Mice experiments between 1970s and 1990s demonstrated evidence for immunosurveillance concept [45]. Endogenously produced IFN-γ provided protection against implanted tumors while mice, which are insensitive to perforin or IFN-γ, developed tumors compared to wildtype [45].

Overall, the dual role of immune system in cancer pathogenesis (protection and promotion) forms the basis of immunoediting [23,42]. Cancer immunoediting has three stages: elimination, equilibrium and escape (Figure 7) [23,42]. In the first phase, elimination, the immune system recognizes and destroys cancer cells [23,42]. If the elimination phase is not enough to remove the tumor cells, the dynamic cancer-immunoediting process proceeds with the equilibrium phase [23,44]. Here the tumor progression is contained with the help of lymphocytes and IFN-γ [23,44]. During the equilibrium phase, some cancer cells bearing new mutations can arise and go to the escape phase where tumor growth is favored [23,44]. This phase is associated with uncontrollable proliferation and spread of tumor cells that eventually leads to tumor sizes that are clinically detectable [23,44].

[23] Dunn G.P, Koebel C.M, Schreiber R.D: Interferons, immunity and cancer immunoediting. Nature Reviews Tumor Immunology 2006, **6(11)**: 836-848
[39] Corthay A: Does the immune system naturally protect against cancer? Frontiers in Immunology 2014, **5(197)**: 1-8
[42] Dunn G.P, Old L.J, Schreiber R.D: The three Es of cancer immunoediting. Annual Review of Immunology 2004, **22**:329-360
[43] Balkwill F, Mantovani A: Inflammation and cancer: back to Virchow? Lancet 2001, 357**(9255)**: 539-545
[44] Mantovani A, Allavena P, Sica A, Balkwill F: Cancer-related inflammation. Nature 2008, **454 (7203)**: 436-444
[45] Dunn G.P, Bruce A.T, Ikeda H, Old L.J, Schreiber R.D: Cancer immunoediting: from immunosurveillance to tumor escape. Nature Immunology 2002, 3(11): 991-998

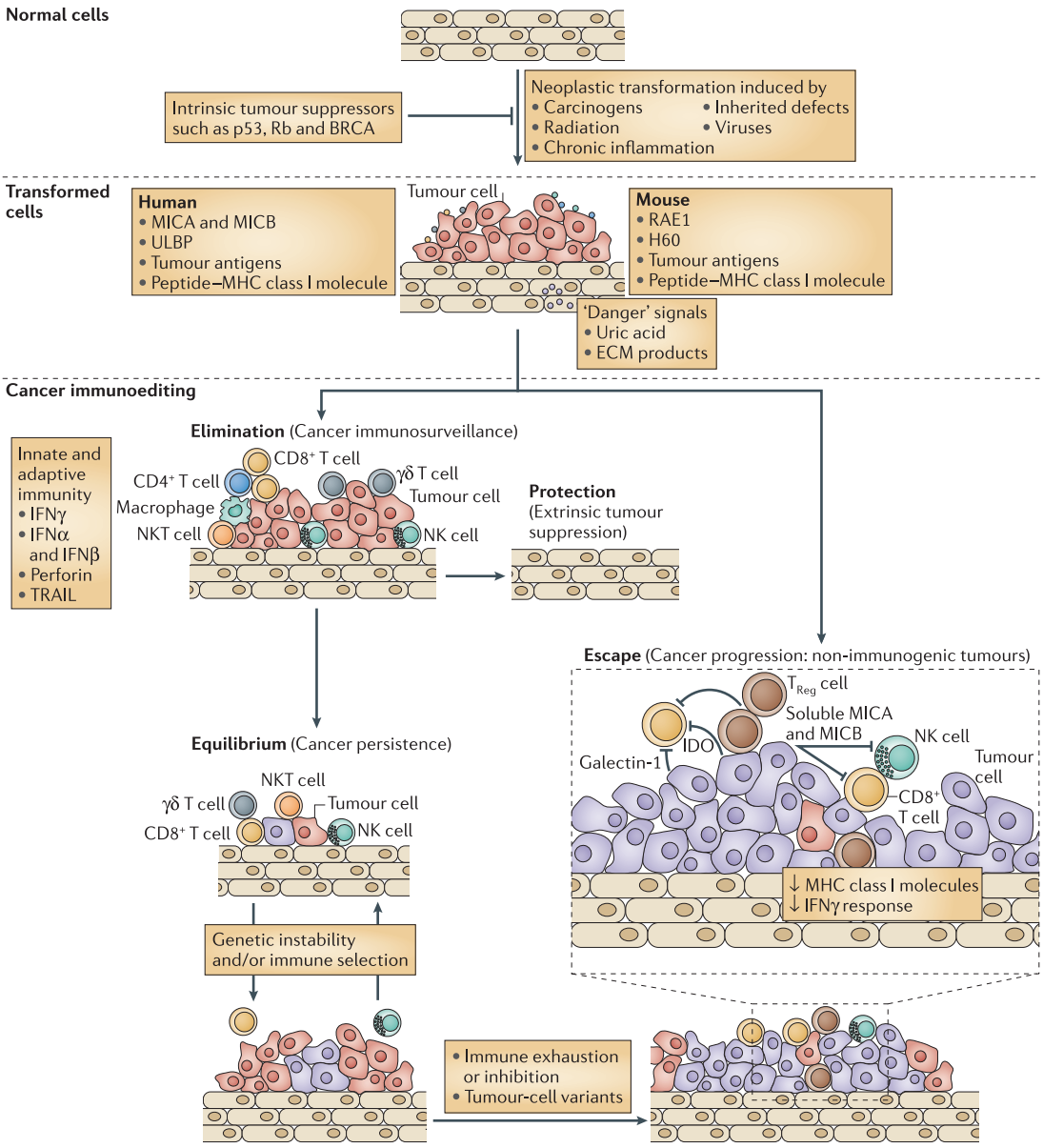

Figure 7. The three phases of cancer immunoediting. Figure modified and adopted from [23]

[23] Dunn G.P, Koebel C.M, Schreiber R.D: Interferons, immunity and cancer immunoediting. Nature Reviews Tumor Immunology 2006, **6(11)**: 836-848

1.4.2 Tumor-associated macrophages

Tumor-associated macrophages (TAMs) are localized in the tumor stroma [46]. They are most frequently known for its tumor-promoting effects by having a role in angiogenesis, tumor growth, metastasis, resistance to chemotherapy and immunosuppression [46,47]. Their phenotype can resemble both M1 and M2 macrophages but they are functionally different [46,47].

The polarization of recruited macrophages from circulation into tumor stroma is dependent on different stimuli produced by the tumor cells [46,47]. As a consequence, each tumor could have its own characteristic TAMs [47]. All this makes TAMs to a highly heterogenic group [46]. In addition, high infiltration of TAMs has been correlated with a poor survival rate in many cancer types including Hodgkin's lymphoma, glioma, ovarian and breast cancer [46].

[46] Petty A.J, Yang Y: Tumor-associated macrophages: implications in cancer immunotherapy. Immunotherapy 2017, **9(3)**: 289-302

[47] Mantovai A, Sozzani S, Locati M, Allavena P, Sica A: Macrophage polarization: tumor-associated macrophages as a paradigm for polarized M2 mononuclear phagocytes. Trends in Immunology Review 2002, **23(11)**: 549-555

1.4.3 Cancer immunotherapy

Cancer immunotherapy is considered to be the ultimate personalized but experimental approach for fighting cancer [48]. It focuses on boosting the patient's own immune system for antitumor responses [48]. However, there are many complications such as reduced immunity due to chemotherapy [48]. The FDA- approved immune-checkpoint inhibitors, anti- cytotoxic T lymphocyte- associated protein 4 (anti-CTLA-4) and anti- programmed cell death 1 (anti-PD-1/PD-1) respectively, have shown a significant clinical improvement in metastatic tumors such as non-small-cell lung cancer, melanoma, and Hodgkin lymphoma [48,49]. This therapeutic effect depends on a timeline of approximately 6 months, which sometimes represents an unrealistic survival timeframe for metastatic cancer patients [48,49]. Consequently new therapeutics and delivery strategies are necessary for improved cancer treatment [48]. Among them, nanoparticles seem to have a promising future for cancer immunotherapy [50].

1.4.3.1 Nanoparticles- a promising therapeutic approach for cancer immunotherapy

The nanoparticle-based anticancer drug delivery systems can transport therapeutic drugs directly to the tumor site, thereby reducing side effects such as toxicity and drug resistance associated with intratumoral molecular heterogenicity [50]. This approach is called passive targeting strategy and consists of intratumoral accumulation of nanoparticles (Figure 8A) [48,50]. Nanoparticles can protect the drug from degradation and increase the half-life of the drug [50]. Moreover, the cytotoxic drug concentration can be reduced [50]. Such qualities are advantageous for cancer treatment and are possible due to the unique physicochemical and biological features of nanoparticles that can easily be manipulated, e.g. polyethylene glycol (PEG)- ylation (Figure 9B) [50].

The most unique features of nanoparticles are their size (range between 100 and 1000nm) and surface charge [48,50,51]. They are smaller then their target cells, which makes it

[48] Jiang W, Roemeling C.A, Chen Y, Qie Y, Xiujie L, Chen J, Kim B.Y.S: Designing nanomedicine for immune-oncology. Nature Biomedical Engineering 2017, **1(0029)**: 1-11

[49] Pardoll D.M: The blockade of immune checkpoints in cancer immunotherapy. Nature Review Cancer 2012, **12(4)**: 252-264

[50] Hosseini Maryam, Haji-Fatahaliha M, Jadidi-Niaragh F, Majidi J, Yousefi M: The use of nanoparticles as a promising therapeutic approach in cancer immunotherapy. Artificial Cells, Nanomedicine, and Biotechnology 2016, **44(4)**: 1051-1061

[51] Griffiths G, Nyström B, Sable S.B, Khuller G.K: Nanobead-based interventions for the treatment and prevention of tuberculosis. Nature Reviews Microbiology 2010, **8(11)**: 827-834

possible to transport high doses of the drug to either the surface or inside of the target cell via endocytic pathway without disturbing their biological functions [48,50,51]. On the other hand, their surface charge (highly positive) improves their uptake by the targets, usually APCs [48,50]. After uptake, nanoparticles can release its cargo in a sustained manner, which can both enhance and prolong the activation of professional APCs such as macrophages and dendritic cells [48,50]. It can also induce cytokine production [48,50]. In this way, nanoparticles can be used to initiate antitumor activity far from the tumor site by targeting the phagocytic and cytotoxic immune cells that can migrate to the tumor [48,50]. This active targeting strategy implies attaching recognition molecules on the surface of nanoparticles that can be recognized by the target-receptors (Figure 8B) [48].

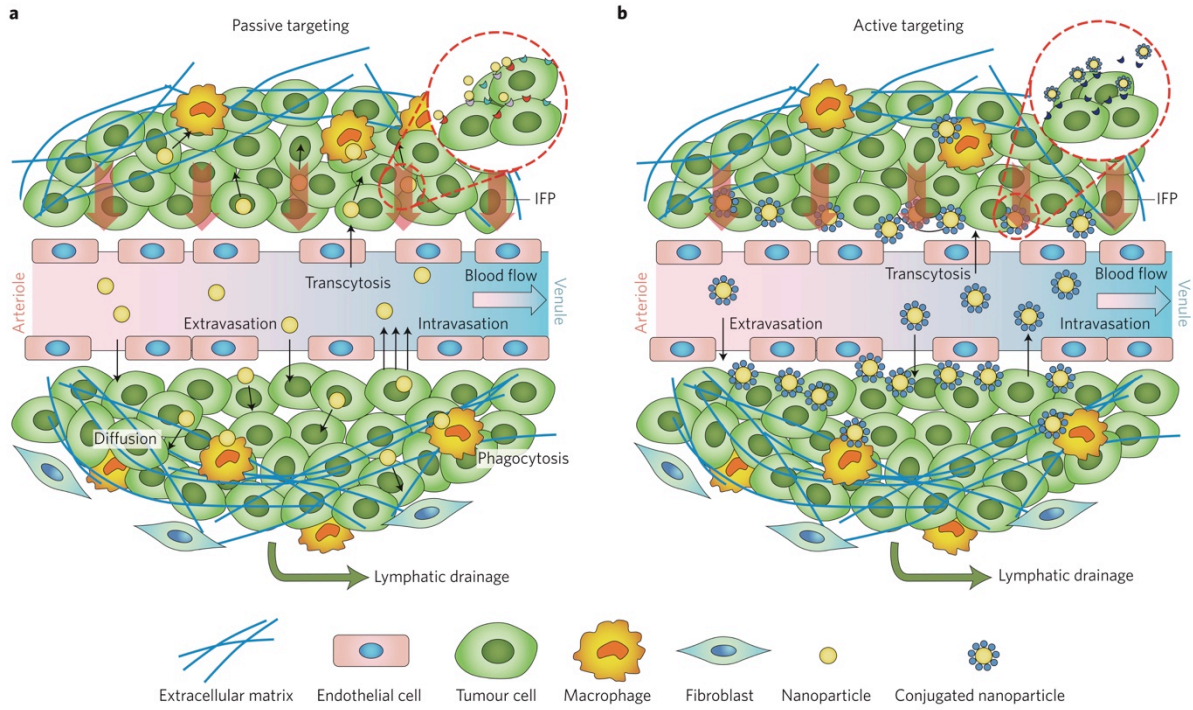

Figure 8. Active and passive nanoparticle delivery strategy. A)Passive targeting: nanoparticles interact in a non-specific manner with target cell-membrane receptors. Since tumors have disorganized and leaky vasculatures, it is easier for nanoparticles to diffuse and be retained within the tumor. B) Active targeting: Conjugation with target ligand makes it possible for nanoparticles to bind specific receptors thereby enhancing the therapeutic effects. Figure modified and adopted from [48].

[48] Jiang W, Roemeling C.A, Chen Y, Qie Y, Xiujie L, Chen J, Kim B.Y.S: Designing nanomedicine for immune-oncology. Nature Biomedical Engineering 2017, **1(0029)**: 1-11

[50] Hosseini Maryam, Haji-Fatahaliha M, Jadidi-Niaragh F, Majidi J, Yousefi M: The use of nanoparticles as a promising therapeutic approach in cancer immunotherapy. Artificial Cells, Nanomedicine, and Biotechnology 2016, **44(4)**: 1051-1061

[51] Griffiths G, Nyström B, Sable S.B, Khuller G.K: Nanobead-based interventions for the treatment and prevention of tuberculosis. Nature Reviews Microbiology 2010, **8(11)**: 827-834

In addition to use of nanoparticles for inducing antitumor effect, they can also be designed to block immune-suppressive effects [48,52]. This approach could possibly replace immune-checkpoint inhibitors such as anti-CLTA-4 and anti-PD-1/PD-1 [48,52].

1.4.3.2 Polymeric nanoparticles

Among all members of the nanoparticle family, polymeric nanoparticles are the most used delivery systems due to easy and inexpensive production, biodegradable, non-immunogenic and water-soluble features [53]. Polymeric nanoparticles can be made with many different materials and methods, which can affect their size, surface charge and hydrophobicity [53]. The three main forms of polymeric nanoparticles are nanosphere, nanocapsule and nanomicelle (Figure 9A) [51]. The polymers used for making these nanoparticles are either synthetic or natural [53]. The most used polymers are poly (lactic-co-glycolic acid) (PLGA) and chitosan [53].

PLGA is a biodegradable polymer mostly used for encapsulating hydrophobic drugs [53]. Many studies have demonstrated the correlation between PLGA nanoparticles and increased IFN-γ or IL-4 production, which indicates a potential in inducing both Th1 and Th2 responses [53]. These nanoparticles are currently used in pre-clinical studies with vaccine carrier systems for Hepatitis B, malaria and tuberculosis [53,54]. The problem with PLGA nanoparticles is the use of highly toxic organic solvents necessary for their production, which can affect the encapsulated drug-efficiency [55].

On the other hand, chitosan is a characterized polyelectrolyte that does not require toxic solvents for drug encapsulation [53]. The chitosan-nanoparticle formation is based on electrostatic interactions or crosslinking between the positively charged chitosan amino groups and negatively charged groups of the drug [53]. Another widely used method is polyelectrolyte complexation where chitosan is cross-linked with polysaccharides or

[48] Jiang W, Roemeling C.A, Chen Y, Qie Y, Xiujie L, Chen J, Kim B.Y.S: Designing nanomedicine for immune-oncology. Nature Biomedical Engineering 2017, **1(0029)**: 1-11

[51] Griffiths G, Nyström B, Sable S.B, Khuller G.K: Nanobead-based interventions for the treatment and prevention of tuberculosis. Nature Reviews Microbiology 2010, **8(11)**: 827-834

[52] Saleh T, Shojaosadati S.A: Multifunctional nanoparticles for cancer immunotherapy. Human Vaccines & Immunotherapeutics 2016, **12(7)**: 1863-1875

[53] Bolhassani A, Javanzad S, Saleh T, Hashemi M, Aghasadeghi M.R, Sadat S.M: Polymeric nanoparticles. Human Vaccines & Immunotherapeutics 2014, **10(2)**: 321-332

[54] Gregory A.E, Titball R, Williamson D: Vaccine delivery using nanoparticles. Frontiers in Cellular and Infection Microbiology 2013, **3(13)**: 1-13

[55] De Koker S, Lambrecht B.N, Willart M.A, van Kooyk Y, Grooten J, Vervaet C, Remon J.P, De Geest B.G: Designing polymeric particles for antigen delivery. Chemical Society Reviews 2011, **40(1)**: 320-339

DNA/RNA [56]. The most recent studies have shown chitosan in combination with TLR ligand poly I:C for delivery and activation of macrophages [56].

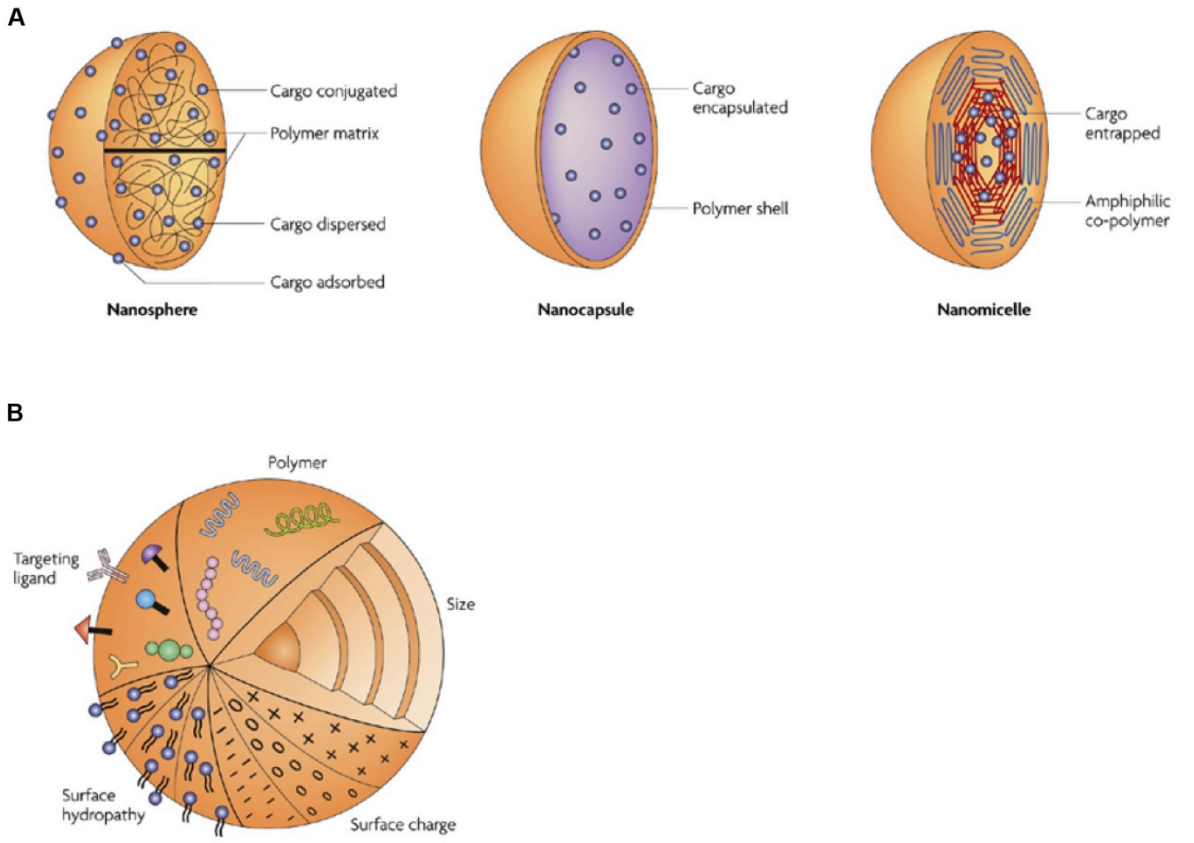

Figure 9. Characteristics of nanoparticles. A) Polymeric nanoparticles can be divided into three main groups: nanospheres, nanocapsules and nanomicelles. They differ how their cargo is placed in the particle. In a nanosphere, the cargo is found in a dissolved form in the matrix or it is attached to the surface of the polymer matrix. Nanocapsules contain their cargo in a solution, which is surrounded by a shell-like wall. The last form, a nanomicelle is made of amphiphilic co-polymers that interact with each other (hydrophobic and hydrophilic) to make the particle around the cargo. B) The unique features of nanoparticles that can be easily manipulated. The choice of the polymer can decide not only the nanoparticle biocompatibility and degradation rate but also its encapsulation efficiency, internalization and cargo release rate. The high positive charge of nanoparticles, can influence their internalization rate and route. Two different features of a nanoparticle, surface hydrophobicity and hydrophilicity, can lead to increased or decreased uptake of the nanoparticles by targets. By conjugating the particle with different target ligands, the delivery will be more specific thus increasing the therapeutic effect of the particle. Last but not least, the size of the particles is one of the most important features; the smaller the particle is, the better and faster is its uptake. Figure adopted and modified from [51]

[56] Speth M.T, Repnik U, Müller E, Spanier J, Kalinke U, Corthay A, Griffiths G: Poly (I:C)-encapsulating nanoparticles enhance macrophage response to BSG-vaccine via synergistic activation of Toll-like receptor signaling. (manuscript in preparation)

[51] Griffiths G, Nyström B, Sable S.B, Khuller G.K: Nanobead-based interventions for the treatment and prevention of tuberculosis. Nature Reviews Microbiology 2010, **8(11)**: 827-834

2 Aims of the study

Main objective: To identify new molecular combinations for rendering macrophage tumoricidal

Sub-goals:

1. To evaluate the therapeutic potential of the most promising *in vitro* molecular combination *in vivo*
2. To investigate the potential replacement of IFN-γ with a type I interferon for activation of macrophage tumoricidal activity
3. To test the combination of IFN-γ with the pro-inflammatory cytokine TNF-α for induction of tumoricidal activity in macrophages

3 Materials and Methods

3.1 Materials

3.1.1 Cell lines

3.1.1.1 Lewis Lung Carcinoma

Lewis Lung Carcinoma (LLC) is a spontaneous mouse C57BL/6 lung carcinoma cell line that was discovered by Dr. Margaret R. Lewis in 1951 [57]. However, the cell line itself was first established by Bertram in 1980 [57]. This cell line was used as the main target cells in this study and was obtained from CLS Cell Lines Service.

3.1.1.2 Bone marrow derived macrophages

In this study, two different types of primary effector cells were used: bone marrow derived macrophages (BMDM) from normal C57BL/6 mice and BMDM from non-obese diabetic severe combined immunodeficient gamma (NOD/SCID/IL2ry^{null} or NSG) mice [58]. NSG^{TM} have two main mutations, which make them highly immunodeficient [59]. They lack the IL-2 receptor common γ subunit, which leads to down-regulation of cytokine signaling and NK cell depletion [59]. The *Prkdc* or *scid* mutation leads to lack of development of B and T lymphocyte populations [59,60]. This severe immunodeficiency allows these mice or derived cell lines to be used for xenotransplantation procedures and for testing different immunotherapeutic factors in the absence of B, T and NK cells [58-61].

---

[57] Bertram J.S, Janik P: Establishment of a cloned line of Lewis Lung Carcinoma cells adopted to cell culture. Cancer Letters 1980, **11(1)**: 63-73

[58] Patton J, Vuyyuru R, Siglin A, Root M, Manser T: Evaluation of the efficiency of human immune system reconstitution in NSG mice and NSG mice containing a human HLA.A2 transgene using hematopoietic stem cells purified from different sources. Journal of Immunological Methods 2015, **422**:13-21

[59] Presa M, Chen Y.G, Grier A.E, Leiter E.H, Brehm M.A, Greiner D.L, Shultz L.D, Serreze D.V: The presence and preferential activation of regulatory T cells diminish adoptive transfer of autoimmune diabetes by polyclonal nonobese diabetic (NOD) T cells effectors into NSG versus NOD-scid mice. The Journal of Immunology 2015, **195(7)**: 3011-3019

[60] Shultz L.D, Brehm M.A, Bavari S, Greiner D.L: Humanized mice as a preclinical tool for infectious disease and biomedical research. Annals of the New York Academy of Sciences 2011, **1245**:50-54

[61] Simpson-Abelson M.R, Sonnenberg G.F, Takita H, Yokota S.J, Conway Jr T.F, Kelleher Jr R.J, Shultz L.D, Barcos M, Bankert R.B: Long-term engrafment and expansion of tumor-derived memory T cells following the implantation of non-disrupted pieces of human lung tumor into NOD-scid IL2Rγ^{null} mice. The Journal of Immunology 2008, **180(10)**: 7009-7018

3.1.2 Mice strains

Both mouse strains were bred at the Department of Comparative Medicine, at Rikshospital (Oslo University Hospital, Norway). The study was approved by the Norwegian National Committee for Animal Experiments and performed according to approved guidelines and regulations.

3.1.3 TLR agonists and cytokines

In this study, the following three TLR agonists (Table 3) were used to activate bone marrow-derived macrophages.

Table 3. An overview of all TLR agonists used in this study.

TLR receptor	TLR agonist	Source	Manufacture
TLR1/2	Pam3CSK4	Synthetic lipoprotein analog of triacylated lipopetide	InvivoGen, USA
TLR2; TLR4; RAGE	HMGB1	Bacterially expressed recombinant protein (*E.coli*). The protein used was calmodullin-binding protein (CBP)-tagged rat HMGB1	Peter Lundbäck, Karolinska Institutet, Stockholm, Sweden
TLR3	Poly (I:C) of low molecular weight	Synthetic analog of double-stranded RNA	InvivoGen, USA

The TLR agonists were used alone or in combinations with either another TLR agonists or with the following cytokines (Table 4):

Table 4. An overview of all used cytokines in this study.

Receptor	Cytokine	Source	Manufacture
IFNGR1	rIFNγ	Mouse recombinant (produced in *E.coli*)	Peprotech, USA
IFNARI/IFNAR2	rIFNβ	Human embryonic kidney cell HEK293-derived Ille22-Asn182	Bio-Techne, UK
TNFR1/TNFR2	mTNFα	Mouse recombinant (produced in *E.coli*)	Peprotech, USA

3.1.4 Reagents

The following reagents were used in this study (Table 5):

Table 5. An overview of all reagents used in the study.

Reagents	Manufacture
Chitosan	Sigma-Aldrich, USA
Dimethyl sulfoxide (DMSO)	Amresco, USA
Dulbecco´s phosphate-buffered saline (DPBS) with Calsium and Magnesium chloride	Gibco, Life Technologies,USA
DPBS without Calsium and Magnesium chloride	Thermo Scientific, USA
Fetal bovine serum (FBS)	Biochrom GmbH, Germany
FBS	Sigma-Aldrich, USA
FITCH Annexin V Apoptosis Detection Kit with PI	BioLegend, Nordic BioSite
Glyserol	Applichnem Lifescience, Germany
[methyl- ^{3}H]-Thymidine (185 MBq/5mCi)	Hartmann Analytic, Germany
Mitomycin C from Streptomyces caespitosus	Sigma-Aldrich, USA
N-(1-napthyl)ethylenediamine dihydrochloride >98% (NED)	Sigma-Aldrich, USA
Penicillin/ Streptomycin (100X)	Thermo Scientific, USA
Phosphoric acid 85%	Sigma-Aldrich, USA
RPMI 1640 medium	Thermo Scientific, USA
S-Methylisothiourea hemisulfate salt (SMT)	Sigma-Aldrich, USA
Sulfanilamide >99%	Sigma-Aldrich, USA
Trypan Blue Stain 0.4%	Life technologies, USA
Trypsin-EDTA solution 0.25%	Sigma-Aldrich, USA

3.1.5 Cell culturing medium and equipment

The cell culturing media used in this study are shown in Table 6.

Table 6. An overview of the different cell culturing media used in this study and its compositions.

Cell culturing medium/buffer	Composition
Complete bone marrow-derived macrophage (BMDM) growth medium	RPMI 1640, 10% FBS Biochrome, 10% L929-derived conditioned medium and 1% Penicillin/Streptomycin
Complete bone marrow-derived macrophage (BMDM) medium	RPMI 1640, 10% FBS Biochrome and 10% L929-derived conditioned medium
Flow buffer	Cold PBS without Calsium and Magnesium chloride, and 10%FBS Sigma
LLC medium	RPMI 1640 and 10% FBS Sigma

The required cell culturing equipment for this study is shown in Table 7.

Table 7. An overview of the equipment used in the study.

Equipment	Characteristics	Manufacture
Cell counting chamber slides	Countess, Invitrogen	Thermo Fisher Scientific, USA
Cell culture cluster	96 wells; round bottom with lid; tissue culture treated; nonpyrogenic; polystyrene; sterile	Corning Incorporated, USA
Cell culture cluster	96 wells; flat bottom with low evaporation lid; tissue culture treated; nonpyrogenic; polystyrene; sterile	Corning Incorporated, USA
Cell culture cluster	24 wells; flat bottom with lid; tissue culture treated; nonpyrogenic; polystyrene; sterile	Corning Incorporated, USA
Cell culture cluster	24 wells; flat bottom with lid; non-tissue culture treated; nonpyrogenic; polystyrene; sterile	Corning Incorporated, USA
Cell culture dishes	90 mm; non-tissue treated; ribbed design	VWR, USA
Cell culture flasks	75cm^2, 175cm^2; Nunc Cell Culture treated EasYFLask; angled neck; vent cap; sterile	Thermo Fisher Scientific, USA
Centrifuge tubes	15mL; 50mL; RNase-/DNase-free, nonpyrogenic, sterile	Corning Incorporated, USA
Multichannel pipettes	5-50µL; 30-300 µL	Thermo Fisher Scientific, USA
Pipettes	10µL; 100µL; 200µL; 1000µL; single channel	Eppendorf, Germany
Pipette	0.2µL-2µL; single channel	Thermo Fischer Scientific, USA
Pipette tips	0.1-10µL; 1-200µL; 100-1250µL; ultrafine point	VWR, USA
Serological pipette	5mL; disposable; sterile	Fisher Scientific, USA
Serological pipette	10mL; 25mL; disposable; sterile	Aktiengesellschaft&Co, Germany

3.1.6 Surgery equipment

The surgery-equipment used in the mice-study is shown in Table 8.

Table 8. An overview of the equipment used in the mice-study.

Equipment	Characteristics	Manufacture
Anesthesia machine	Matrix VIP 3000 Isoflurane Vaporizer	Midmark Corporation, USA
Disinfectant	Ethanol 75%	Antibac A.S, Norway
Heading pad	White, quadrant	OBH Nordica, Norway
Isoflurane	Fluid; 100% isoflurane	Zoetis, Finland
Needle	Gauge 27 x 3/4^{II}; 0.4x19mm	BD Microlance ^{TM}3, Ireland

Equipment	Characteristics	Manufacture
Needle	Gauge 18; hydrodemic needle; 1.2x25mm	NIPRO Corporation Japan/ NIPRO Europe, Belgium
Syringe	1mL, terumo syringe without needle	Terumo Corporation Philippines/ Terumo Europe N.V. Belgium

3.1.7 Laboratory safety equipment

An overview of the laboratory safety equipment is shown in Table 9.

Table 9. An overview of the laboratory safety equipment used in the study.

Equipment	Characteristics	Manufacture
Gloves	Nitrile examination gloves; lung cuff, blue; powder free; non-sterile	Klinion, Netherlands
Gloves	Vinyl, white, powder free medical examination gloves; non-sterile	Abena, Denmark
Lab coats	White, long sleeves	Rikshospital, Oslo, Norway
Surgical face mask	Surgical face mask with ties; not made with natural rubber latex; white/blue	MedLine, France
Surgical face mask	3M™ Aura™ Health Care Respirator; fluid resistant and disposable; flat-fold design; white	3M OH&ES, UK

3.1.8 Hardware and software

The different hardware and software used during the study are listed in Table 10.

Table 10. An overview of the different hardware and software used in the study**.**

Hardware	Type	Manufacture
Centrifuge	KUBOTA 5930	Kubota Corporation, Japan
CO_2 incubator	Forma Scientific	Thermo Scientific, USA
Flow cytometer	FACS Aria II	BD Biosciences, USA
Freezer	Forma Scientific	Thermo Scientific, USA
Harvester	96	TOMTEC, USA
Heat sealer	Wallac 295-012	PerkinElmer, Wallac, USA
Water purification system	Mili-Q direct	Merck, Germany
Software	**Developer**	
Gen 5	Biotek Instruments, Inc	
FlowJo 10.3	FlowJo, LLC	
GraphPad Prism7	Graph Pad Software, Inc	

3.2 Methods

3.2.1 *In vitro* methods

3.2.1.1 Preparation and characterization of Poly (I:C) encapsulating chitosan-nanoparticles (pIC-NPs)

Poly (I:C) encapsulating chitosan-nanoparticles (pIC-NPs) were made by using polyelectrolyte complexation between the anionic poly (I:C) and the cationic chitosan defined as a non-toxic and biodegradable natural polymer [56].

This easy and widely use method does not require any auxiliary molecules such as catalysts since the reaction is based on the electrostatic attraction between the cationic amino groups of chitosan and the anionic groups of poly (I:C). Based on this, pIC-NPs should form spontaneously by mixing these two polyelectrolytes in aqueous solution.

The polyelectrolyte complexation for making pIC-NPs was carried out according to the following protocol and by Martin Tobias Speth, a PhD student at the University of Oslo (UiO, Blindern):

Preparation of solutions

- Kitozyme Chitosan

1. Over night, the stock solution of endotoxin-free low molecular chitosan with the concentration of 5 mg/mL was dissolved in endotoxin-free distillated water (hereafter dH_2O) / 1% acetic acid.
2. The dissolved chitosan solution was then diluted to a concentration of 2 mg/mL by using dH_2O.
3. The pH of the solution was adjusted to a value of 6 with 5M NaOH.
4. The chitosan-solution was at the end, sterile filtered with a 0.2 μm filter.

- Poly (I:C)

1. The low-molecular weight poly (I:C) with a stock concentration of 2.5 mg/mL was dissolved with endotoxin-free 0.9% NaCl to 1mg/mL.

[56] Speth M.T, Repnik U, Müller E, Spanier J, Kalinke U, Corthay A, Griffiths G: Poly (I:C)-encapsulating nanoparticles enhance macrophage response to BSG-vaccine via synergistic activation of Toll-like receptor signaling. (Manuscript in preparation)

2. The dissolved poly (I:C) solution was incubated at approximately 60°C for 10 min.
3. After the incubation, the solution was cooled down for reannealing, at room temperature.

Preparation of Chitosan/pIC nanoparticles

1. 500 µL of the chitosan solution was added to one well of a 24-well non-tissue treated plate containing a magnet.
2. 500 µL of the prepared poly (I:C) solution was added drop wise (100-200 µL at a time) with a 200 µL pipette to the chitosan solution, under continuous stirring for 20 min (~500 rpm).
3. The obtained solution was transferred to a 1.5mL eppendorf tube containing a 20 µL glycerol bed.
4. The solution was centrifuged at 10.000g for 20 min.
5. The supernatant (hereafter SN) was resuspended in 0.45% NaCl by pipetting, followed by a 10 min water-bath sonication before use in the cancer cell growth inhibition assay (Section 2.2.1.2).

Table 11. Summery of the unique characteristics of poly(I:C) encapsulating chitosan-nanoparticles (pIC-NPs) from [56].

Characteristics	**pIC-NPs**	**Method used to determine the defined characteristics**
Hydrodynamic size	384 ± 46 nm	Nano ZS Zeta-sizer instrument
ζ- potential; the surface charge	+37.7± 1.8 mV	Nano SZ Zeta-sizer instrument
Encapsulation efficiency; the amount of encapsulated poly (I:C) in pIC-NPs	88.7± 2.6 % ≈ 60% poly (I:C) in pIC-NPs	Measuring unbound poly (I:C) after making NPs by using the absorbance of free poly (I:C) at 260nm on a Nanodrop
The amount of chitosan in pIC-NPs	≈ 40% chitosan in pIC-NPs	Calculated by using the amount of free chitosan in the supernatant. To determine the amount of free chitosan, fluorescamine assay was used.
Morphology	A loose irregularly shaped core and fiber-like polymer-structures protruding from the core	Transmission electron microscopy (TEM)
Uptake	Phagocytic pathway or receptor-mediated endocytosis	Flow Cytometry Confocal microscopy

[56] Speth M.T, Repnik U, Müller E, Spanier J, Kalinke U, Corthay A, Griffiths G: Poly (I:C)-encapsulating nanoparticles enhance macrophage response to BSG-vaccine via synergistic activation of Toll-like receptor signaling. (Manuscript in preparation)

3.2.1.2 Cancer cell growth inhibition assay

Cancer cell growth inhibition assay was used as an *in vitro* method to test different combinations of immunostimulating factors to induce macrophage cytotoxic and cytostatic activity toward LLC cells. The rate of proliferating LLC cells was reflected by the incorporation of the radioactive thymidine after co-culturing of LLC with BMDM.

Cancer cell growth inhibition assay was performed by the following protocol:

Preparation

1. One ampule of BMDM either from C57BL/6NRj or NSG mice; containing 10 million cells/mL was defrosted.
2. The cells were washed with 30 mL of cold PBS without Calcium and Magnesium chloride (hereafter PBS -/-) and centrifuged at 400g for 5 min.
3. The cell pellet was resuspended with medium consisting of RPMI 1640, 10% FBS Biochrome and 10% L929-derived conditioned medium (CM) (hereafter complete BMDM medium).
4. The murine BMDM were seeded out in five 90mm non-treated Petri dishes and left for 3 days in the incubator at +37°C in a humidified 5% CO_2 –incubator.

Day I Macrophage harvesting and plating

1. BMDM were harvested by first collecting all culture medium from each non-treated Petri dish into a common 50mL Flacon tube.
2. 10 mL of cold PBS-/- was added to each plate and incubated for 10 min at +4°C to detach the remaining cells.
3. After the incubation, each plate was washed twice with 10ml of cold PBS -/-.
4. All cell suspensions were collected and centrifuged at 400g for 5 min.
5. Supernatants were discarded and the cell pellets were resuspended with 3-5mL of complete BMDM medium and incubated with Mitomycin C with at concentration of 10 mg/mL for 2 h at + 37°C in a humidified 5% CO_2 –incubator, to block the cell proliferation of BMDMs.
6. After incubation, the cells were washed twice with 20 mL of cold PBS -/- and centrifuged at 400g for 5 min.
7. The cell pellet was resuspended in 3-5mL of complete BMDM medium and cells were prepared for counting.

- The following formula was used to calculate the cell concentration: average(cell number/square)x dilution x180.000 (squares/mL)= cells/mL.

8. BMDM effector cells were seeded out at three different concentrations (Table 12) in a 96-well flat bottom tissue culture treated plate. BMDM cell suspension was applied in triplicates in a volume of 200µL to each well.
9. The plates were incubated for 24h at +37 °C in a humidified 5% CO_2 –incubator.

Table 12. Overview of macrophage: LLC rations plating-strategy.

BMDM: LLC ratio	**20:1**	**10:1**	**1:1**
BMDM cells/mL	300 000	150 000	15 000
BMDM suspension volume/well	200 µL	200 µL	200 µL
BMDM cells/well	60 000	30 000	3 000
LLC cells/well added after 48h	3 000	3 000	3 000

Day II Activation of BMDM with different immunostimulating factors

1. After 24h of incubation, 100µL of medium was replaced with different immunostimulating factors either alone or in combination.
2. Each immunostimulating factor was added in a volume of 50µL to the appropriate well.
3. 50µL of complete BMDM medium was added to wells that contained only one immunostimulating factor.
4. The plate(s) were incubated for 24h at +37°C in a humidified 5% CO_2- incubator.

Day III LLC co-cultivation and measurement of Nitric Oxide (NO) production

1. LLC cells were cultivated in medium consisting of RPMI 1640 and 10% FBS Sigma (hereafter LLC medium) in either 175 or 75cm ^{2} cultivation flasks (at +37°C in a humidified 5% CO_2 –incubator).
2. LLC suspension with $3x10^4$ cells/mL was made with complete BMDM medium.
3. For all wells, 100µL of cell supernatants was removed. The supernatants from the highest macrophage density was used in Nitric Oxide (NO) assay (Section 3.2.1.3) while the rest was discarded.

4. 100μL of the LLC cell suspension was added to all wells except to the macrophage-alone wells and thereby creating different effector: cancer target cells ratios (20:1; 10:1 and 1:1).
5. Fresh complete BMDM medium was added to macrophage-alone wells, which served as a control for the effector cell growth.
6. The cells were co-cultured with LLC for 24h at +37°C in a humidified 5% CO_2 incubator before adding radiolabeled thymidine.

Day IV [Methyl – ^{3}H]-Thymidine

1. After 24h of co-culture, 10 μL containing 20μCi of [Methyl -^{3}H]-Thymidine was added to each well and incubated for another 24h before harvesting at +37°C in a humidified 5% CO_2 –incubator.

Day V Measurement of radiolabeled DNA

1. Before analyzing the plate(s), it was necessary to first freeze down the samples at -80°C and then defrost the samples at room temperature in order to burst the cells.
2. The samples were harvested onto filters by using a Tomtec-96 cell harvester.
3. LLC growth was determined by analyzing the amount of radiolabeled DNA expressed as counts per minutes (cpm) on 1450 MicroBeta Trilux Microplate Scintillation counter.
4. The results were analyzed with Graph Pad Prism 7 where the average value of the triplicates and the standard error of mean (SEM) were calculated.
5. The layout design was made with Adobe Illustrator.

3.2.1.3 Nitric Oxide (NO) assay-measurement of nitric oxide production by activated macrophages

Nitric Oxide (NO) production from 24 h activated macrophages was determined by measuring the levels of NO metabolite nitrite (NO_2^-) in the cell-free supernatants obtained from the wells with the highest macrophage densities. NO_2^- was quantified by using the colometric Griess assay. This assay is based on the Griess diazotization reaction of NO_2^- which leads to the formation of the azo dye (Figure 10).

The Griess assay was performed according to the following protocol:

1. Sodium nitrite ($NaNO_2$) solution was used to produce the standard curve for nitrite absorbance. The standard curve was made as a two-fold dilution starting at 100μM (100-50-25-12.5-6.25-3.13-1.56 μM). Distilled water was used as the blank in the standard curve.
2. Two different Griess reagents were prepared: Griess reagent A consisting of dH_2O with 1% sulphanilamide and 5%phosphoric acid whereas Griess reagent B consisted of dH_2O with 0.1% N-(1-napthyl) ethylenediamine.
3. The cell supernatants from the wells with the highest macrophage densities were centrifuged in the 96 well round bottom plate at 1400 rpm for 2 min to remove all cellular debris.
4. 50 μL of the supernatants were transferred to a 96 well flat bottom plate where the standard curve was already made.
5. 50 μL of Griess reagent A was added to all wells and the samples were incubated at room temperature for 10 min, in the dark which gave the opportunity to convert sulfanilic acid into diazionium salt.
6. After the incubation, 50 μL of Griess reagent B was added to all samples to induce the formation of the azo dye.
7. The level of nitrite in the samples was measured on Gen5- microplate reader at 540 nm.
8. The results were analyzed and mean and standard deviation (SD) calculated using Graph Pad Prism 7, and the layout design was made with Adobe Illustrator.

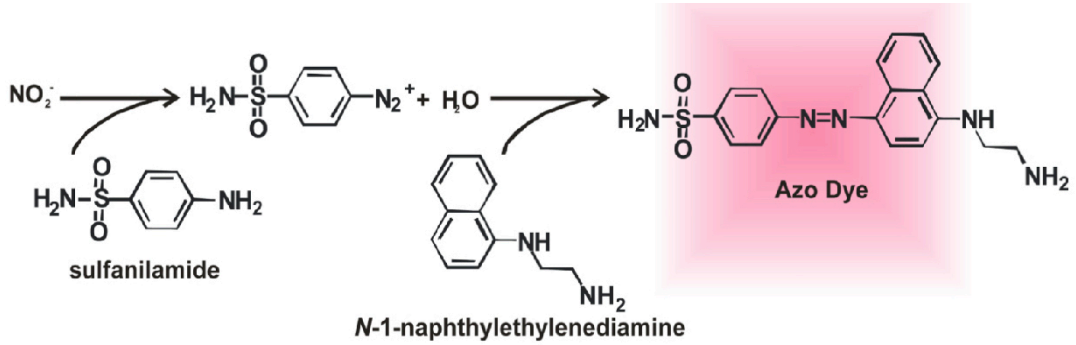

Figure 10. Griess Assay. The reaction between NO_2^- with Griess reagents leads to the formation of the Azo dye. Figure adopted and modified from [62].

[62] Coneski P.N, Schoenfisch M.H: Nitric oxide release: part III. Measurement and reporting. Chemical Society reviews 2012, **41(10)**: 3753-3758.

3.2.1.4 Detection of pIC-NPs-induced apoptosis in bone marrow derived macrophages (BMDM), using the Annexin V and PI binding assay

In order to determine whether high concentration of NPs-pIC is toxic to macrophages and thereby induce apoptosis, Annexin V and Propidium Iodide (PI) binding assay was used. This assay is a sensitive and rapid method, and is based on the observation that phosphatidylserine (PS), a negatively charged phospholipid normally found on the cytoplasmic leaflet of the plasma membrane, is translocated to the cell surface during apoptosis due to the membrane asymmetry lost [63,64,65].

Externalization of PS to the cell surface makes it easier for fluorochrome-labeled FITC Annexin V, a Ca^{2+} dependent phospholipid-binding protein with high affinity for PS, to specifically target and identify early/late apoptotic cells. Only FITC Annexin positive cells are early apoptotic cells while only PI positive are indication on primary necrotic cells. Dual staining with Annexin V and PI allowed further characterization of the different stages of apoptosis and distinction between necrotic and apoptotic cells [63,64,65].

Annexin V and PI binding assay was carried out according to the following protocol:

Preparation

1. One ampule of BMDM from C57BL/6 mice containing $1x10^6$ cells/mL in 90%FBS and 10% DMSO, was defrosted.
2. The cells were washed with 20 mL cold PBS -/-.
3. The cell suspension was centrifuged at 400g for 5 min.
4. The cell pellet was resuspended with complete BMDM growth medium containing PRMI 1640, 10% FBS Biochrome, 10% L929-derived conditioned medium (CM) and 1% Penicillin/ Streptomycin (P/S).
5. The cells were seeded out in five 90mm non-cell culture treated Petri dishes, 10mL/dish.

[63] Sawai H, Domae N: Discrimination between primary necrosis and apoptosis by necrostatin-1 in Annexin V-positive/propodium iodide-negative cells. Biochemical and Biophysical Research Communications 2011, **411(3)**: 569-573

[64] Vermes I, Haanen C, Steffens-Nakken H, Reutelingsperger C: A novel assay for apoptosis. Flow cytometric detection of phosphatidylserine expression on early apoptotic cells using fluorescein labelled Annexin V. Journal Immunological Methods 1995, **184(1)**: 39-51

[65] Schuttle B, Nuydens R, Geerts H, Ramaekers F: Annexin V binding assay as a tool to measure apoptosis in differentiated neuronal cells. Journal of Neuroscience Methods 1998, **86(1)**: 63-69

6. The cells were left growing in the incubator for 2 days at +37°C in a humidified 5% CO_2 – incubator.

Day I BMDM plating and treatment

1. BMDM cells were harvested from the non-treated Petri dishes by first removing all supernatants.
2. 10 mL of cold PBS -/- was added to each plate and incubated for approximately 20-30 minutes at +4°C, to detach the remaining cells on the plates.
3. After the incubation, the cells were harvested and transferred to a 50mL Falcon tube and kept on ice. 5 mL of new cold PBS -/- was added to each plate in order to harvest and transfer any remaining cells.
4. All cell suspensions were centrifuged at 400g for 5 min at 4°C.
5. The cell pellets were resuspended by adding 1 mL of complete BMDM medium per tube, and transferred to one common 50mL Falcon tube giving a total volume of 10 mL.
6. The cells were counted manually by using disposable plastic chamber slides and trypan blue stain. The cell concentration was calculated by using the following formula:

   average (cell number/square) x dilution x 180.000 (squares/mL)= cells/mL.

   - For non-Mitomycin C treated cells, the needed cell number was $2.56x10^6$ or 160.000 cells/well for a 24-well tissue culture treated plate
   - For Mitomycin C-treated cells, the needed cell number was $3.52x10^6$ or 220.000 cells/well for a 24-well tissue culture treated plate
7. The two different BMDM cell suspensions were prepared with complete BMDM medium.
8. The cells were plated in duplicates on both 24-well tissue culture treated plates at the desired concentrations.
9. The plates were incubated for 2 hours at +37°C in a humidified 5% CO_2 – incubator.
10. After the incubation:
    - All media from each well was removed by using suction on the non-Mitomycin C treated plate and 500µL of complete BMDM medium including the different treatment-factors in the desired concentrations, were added to the appropriate wells (Table 13).

- All media from each well on the Mitomycin C-treated plate was also removed with suction and washed twice with 1mL of warm PBS with Calsium and Magnesium chloride (hereafter PBS +/+).

  After the washing steps, 500μL of the different treatment-factors were added to the appropriate wells (Table 13).

11. The plates were incubated for 24h at + 37 °C in humidified 5% CO_2 – incubator.

Day II Annexin V and PI staining and Flow Cytometry analysis

1. After 24h treatment-incubation, the media (cell supernatants) from each well was transferred to the respective Falcon tubes and kept on ice.
2. Each well was washed with 1mL warm PBS +/+.
3. The PBS was removed carefully with suction and 150 μL of Trypsin was added to each well for approximately 10-15 minutes at +37 °C.
4. 1 mL of fresh Biochrome medium was added to each well to inactivate Trypsin.
5. By pipetting, the cells were transferred to the respective falcon tubes containing the media from the first step and kept on ice.
6. The cell suspensions were centrifuged at 400g for 5 min.
7. The supernatants were discarded and 5 mL of Flow Buffer (cold PBS and 10%FBS Sigma) was added to each tube on ice, to resuspend the pellets.
8. The cell suspensions were once more centrifuged at 400g for 5 min.
9. The supernatants were discarded by using vacuum.
10. The cell pellets were resuspended in 100 μL Annexin V Binding Buffer and transferred to Flow tubes on ice.
11. 3 μL of FITC Annexin V and 6 μL of PI solutions were added to the appropriate Flow tubes.
12. The solutions were gently vortexed and incubated for 15 min on ice, in the dark.
13. After the incubation, 200μL of Annexin V Binding Buffer was added to each tube and the cell suspensions were analyzed by Flow Cytometry analysis without further washing steps.

Table 13. Overview of different treatments used in the experiment

		1	2	3	4	5	6	
MØ alone	**A**							**NPs 2µg/mL**
Staurosporine 1µM	**B**							**NPs 10µg/mL+Pam3 100ng/mL**
NPs 10µg/mL	**C**							**NPs 5µg/mL+ Pam3 100ng/mL**
NPs 5µg/mL	**D**							**NPs 2µg/mL + Pam3 100ng/mL**

3.2.2. *In vivo* methods

3.2.2.1 Lewis Lung Carcinoma (LLC) titration experiment

LLC titration experiment was carried out in order to find the number of LLC cells required for development of specific tumor sizes in a acceptable time frame.

Mice included in the experiment were all age matched that were bread at the KPM animal facility at Rikshospital by the PhD student, Branislava Stankovic. The total number of mice included in this experiment, was 34; 17 males and 17 females. Both males and females were marked and randomly assigned to a given group by the PhD student Elisabeth Müller. These strategies lead to the formation of different groups consisting of both male and female mice. Each group was consisting of 7 mice except group nr 1 which had 8 mice.

Mycoplasma free LLC cells were cultivated for one week in 175 cm^2 cultivation flask at +37° , in a humidified 5% CO_2 atmosphere. The cells were cultivated in medium consisting of RPMI 160 with 10% FBS Sigma and 1% Penicillin/ Streptomycin.

In order to make the LLC single cell suspensions for injection into C57BL/6 mice, the cultured LLC cells were scraped from the 175mm^2 cultivation flasks bottom using a cell scraper. The LLC cells were transferred to a 50mL Falcon tube and centrifuged at 400g for 5 min. The cell pellet was first washed with PBS -/- and then centrifuged once more at 400g for 5 min before resuspending it in 3mL of old PBS -/-. The resuspended LLC cells were prepared for counting. The following formula was used to calculate the cell concentration: average (cell number/square) x dilution x 180.000 (squares/mL) = cells/mL.

LLC suspensions containing different cell numbers (Table 14) were made with PBS -/- and resuspended well in order to get single cell suspensions. All single LLC cell suspensions

were kept on ice before injecting a total volume of 100 µL subcutaneously (s.c) into isoflurane gas anesthetized mice.

The injection site was made in the right flank by first sterilizing the injection site with 70% Ethanol. The skin on the right flank was pulled up with forceps to give excess to inject the LLC suspension s.c. After the injection, the opening of the injection site was hold with forceps before pulling the 18-gauge needle out.

Table 14. The experimental set-up for LLC-titration.

Group nr	Males (nr)	Females (nr)	Number of LLC injected
1	4	4	1.000
2	2	5	10.000
3	4	3	20.000
4	3	4	50.000
5	4	3	100.000

The mice were checked one day post injection, and the growing tumors were measured three times per week (Monday-Wednesday-Friday). The study was blinded, so that the mice were not marked with which study group they belonged to. The width and length of each tumor was measured by vernier calipers. Tumors with irregular shapes and visually consisting of two lobes, were measured separately until they merged to become one. When the tumor size reached 15 mm or a volume of 700 mm^2 , the mice were sacrificed by neck dislocation. Tumor growth was observed for 47 days post injection.

Tumor measurements, length and width, were used to calculate the tumor volume according to the following formula: tumor volume (V)= (length x $width^2$) x π /6.

The data were analyzed with Graph Pad Prism 7 (using Student T test). The layout design was made with Adobe Illustrator.

3.2.2.2 In vivo Poly(I:C) treatment on implant Lewis Lung Carcinoma tumors

Poly (I:C) was reported to induce antitumor immune responses in vivo when administrated intraperitoneally or subcutaneously to Lewis Lung Carcinoma tumor-implanted mice [66].

The aim of this experiment was to reproduce the finding by Shime at all [66].

Mycoplasma-free LLC cells were cultivated for 2 weeks in 175cm^2 cultivation flask containing RPM1 160 medium with 10% FBS Sigma and 1% Penicillin/ Streptomycin. The LLC cells were cultivated at +37°C in a humidified 5% CO_2-incubator. The cells were harvested from the cultivation flasks using a cell scraper and centrifuged at 400g for 5 min and resuspended in cold PBS -/- and prepared for counting. LLC cell suspension with a concentration of 1x10^7 cells/mL was prepared with 15mL of cold PBS-/- and kept on ice until injecting a volume of 100μL into each mouse.

10 female and 3 male C57BL/6 mice were included in this experiment. All mice were age matched and bread in KPM animal facility at Rikshospital.

Prior to injection, all mice were anesthetized with isoflurane gas. The mice were shaved and injected s.c with 100μL of the prepared LLC cell suspension on the right flank.

The treatment started 9 days post LLC injections when the average tumor volume per group was approximately 55 mm^3. The control group that received only 100 μL of cold PBS -/-consisted of 6 mice while the treatment group that received 0.25 mg poly (I:C) consisted of 7 mice. The injections were given twice a week, intraperitoneally (i.p) by placing the mice on their backs, spraying the injection site with 70% Ethanol. After the injection, the injection site was hold with forceps to give an easier excess to pull out the 18-gauge needle.

The tumor measurements were taken the same days as the injections were administrated. The tumors were measured in two dimensions, length and width, with caliper. Irregular shaped-tumors were measured separately until merged. Tumor volume was calculated using the following formula: Tumor volume (V) = V= (length x width^2) x π /6.

Mice that developed necrosis or exceeded the 15 mm limit of tumor size were eliminated with neck dislocation. The experiment was terminated 30 days after LLC injections.

[66] Shime H, Matsumoto M, Oshiumi H, Tanaka S, Nakane A, Iwakura Y, Tahara H, Inoue N, Seya T: Toll-like receptor 3 signaling converts tumor-supporting myeloid cells to tumoricidal effectors. Proceedings of the National Academy of Sciences of the United States of America (PNAS) 2012, **109(6)**: 2066-2071.

3.2.2.3 Acute-toxicity study of pIC-NPs in combination with Pam3 to determinate the safest dose of pIC-NPs for in vivo approach for tumor immunotherapy

In order to determine if administration of pIC-NPs in combination with Pam3 is toxic or would lead to acute inflammation, four different doses of pIC-NPs were used on total thirteen C57BL/6 mice. The decided four doses of pIC-NPs used in this experiment were based on the in vitro results of pIC-NPs in cancer cell growth inhibition. All the mice included in this study were males and age matched.

The mice were divided into five groups where each treatment group (Groups 1-4; Table 15) received 9 μg of Pam3 in combination with different pIC-NPs dose. The different test-treatment solutions were administrated s.c in a total volume of 100μL. The treatment injections were given as a 50 μL saline solution containing appropriate dose of pIC-NPs and 50μL of PBS containing 9 μg Pam3. The control group (Group 5, Table 15) received only 100 μL of cold PBS -/-.

The treatments were administrated only once, whereafter the mice were monitored daily for two weeks for any clinical signs of local acute inflammation such as redness and swelling. Besides of local acute inflammation signs, body weight and water-consumption was also monitored as well in order to investigate if administration of pIC-NPs resulted in failure to thrive.

Table 15. The experimental set-up. Group 5 was the control group.

Group nr	Number of mice	Amount of pIC-NPs	Amount of Pam3	Volume of PBS
1	3	2μg	9μg	
2	3	20μg	9μg	
3	3	50μg	9μg	
4	3	100μg	9μg	
5	1	-	-	100μL

The observed local inflammation at the injection site was monitored closely to see if it increases or decreases over time. Both length and width for each local inflammation was measured with vernier calipers. To calculate the volume (V) of the local inflammation, the following formula was used: $V = (\text{length} \times \text{width}^2) \times \pi / 6$, the same formula used for

calculating tumor volumes (Section 2.2.2.1). The results were analyzed with Graph Pad Prism 7.

4 Results

4.1 Results from *in vitro* experiments

4.1.1 The TLR1/TLR2 ligand, Pam3CSK4, synergizes with IFN-γ for activation of C57BL/6 BMDMs towards an antitumor macrophage phenotype

The *in vitro* assay, growth inhibition assay, was used to investigate which signals are required to activate BMDMs towards an antitumor macrophage phenotype which is able to inhibit cancer cell growth. First we needed to reproduce the previous successful experiments, which had established that two signals, delivered by Pam3CSK4 (Pam3) and IFN-γ could activate macrophages towards this phenotype [67].

Pam3 is a synthetic lipoprotein analog recognized by TLR1 and TLR2, and able to induce an antitumor macrophage phenotype which is able to inhibit the cancer cell growth and produce NO, however only when combined with a second signal [67].

BMDMs from C57BL/6 mice were first treated with Mitomycin C in order to inhibit their proliferation rate. Then, the macrophages were activated with different concentrations (1000-100-10 ng/mL) of Pam3 either alone or in combination with the second stimulus, IFN-γ (40 ng/mL), for 24h. Control wells contained macrophages that were left untreated. After 24h of activation, the cell supernatant from the highest macrophage density was used to measure the NO-production of activated macrophages. LLC cells ($3x10^3$ cells/well) were added to the wells containing macrophages and co-cultured for 24h. In order to determine the amount of proliferation rate of LLC cells, [^{3}H]-Thymidine was added to all samples 24h before harvesting the cells (Figure 11A).

The Mitomycin C successfully blocked BMDMs from proliferating as seen by a low cpm, which indicated that the proliferation rate was successfully inhibited (Figure 11B, the 3 first columns to the left). The co-culture of LLCs and unstimulated BMDMs displayed strong

[67] Müller E, Christopoulos P, Halder S, Lunde A, Beraki K, Speth M, Øyenbråten I, Corthay A: Two signals are required for optimal induction of tumoricidal M1 macrophage phenotype (Manuscript in preparation)

proliferation, similar to LLCs alone, and indicated that BMDMs do not inhibit cancer cell growth in the absence of activation (Figure 11B, second group of columns from the left). Similarly, Pam3 or IFN-γ alone did not induce any LLC growth inhibition by BMDMs (Figure 11B, the four groups of columns in the middle). Furthermore, there was no direct inhibitory effect of the activating factors, Pam3 or IFN-γ, on LLC growth (Figure 11A, the four groups of columns in the middle).

However, upon activation of BMDMs with both Pam3 and IFN-γ simultaneously, the BMDMs inhibited the growth of LLC almost completely (Figure 11B, the 3 groups of columns to the right). This growth inhibition was dependent on a sufficient ratio of BMDM to LLC cells, and 20:1 and 10:1 was seen to be efficient. These results are in agreement with previous reports from our group [67], which found that TLR ligands and IFN-γ synergize for activation of antitumor M1 macrophages.

The NO levels from the highest macrophage concentrations show a close correlation with the results from the cancer cell growth inhibition assay (Figure 11C). Significant NO levels were observed in samples where BMDMs were activated with both IFN-γ (40ng/mL) and Pam3 in all concentrations (Figure 11C, the three columns to the right). Non-stimulated BMDMs did not produce significant levels of NO (Figure 11B, the first column to the left), neither did single activated BMDMs.

[67] Müller E, Christopoulos P, Halder S, Lunde A, Beraki K, Speth M, Øyenbråten I, Corthay A: Two signals are required for optimal induction of tumoricidal M1 macrophage phenotype (Manuscript in preparation)

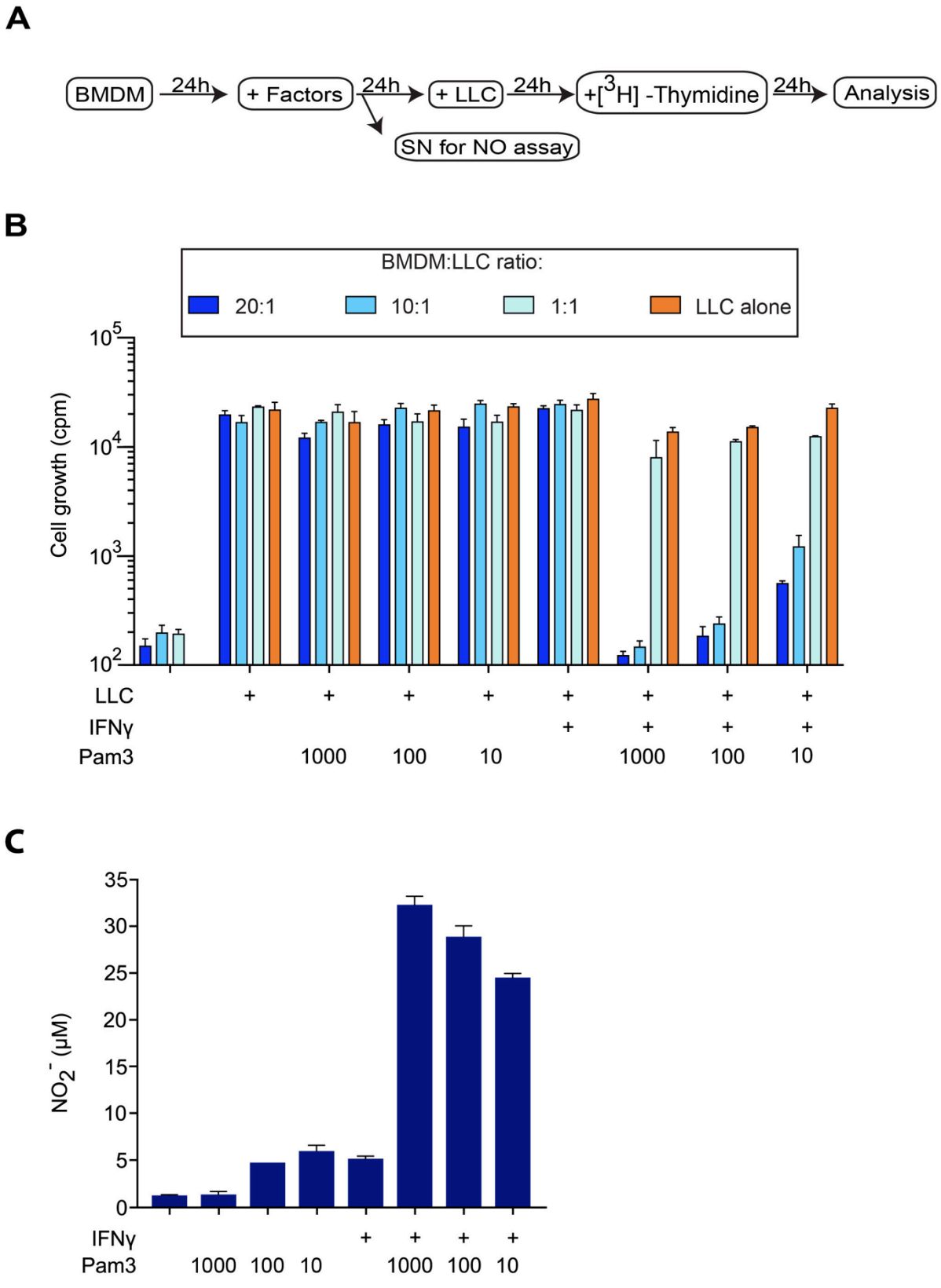

Figure 11. Macrophage activation by IFN-γ either alone or in combination with titrated concentration of TLR1/2 agonist Pam3CK4 (Pam3) A) The schematic overview of the experiment setup. B) Mitomycin C-treated C57BL/6 BMDMs at three different densities were left untreated or stimulated with the indicated factors (1000ng/mL, 100ng/mL and 10ng/mL Pam3, 40 ng/mL IFN-γ). After 24h of

activation, 100μL of cell medium was removed and LLC cells ($3x10^3$ cells/well) were added to different number of BMDMs in order to achieve the indicated BMDM:LLC cell ratio. [^{3}H]-Thymidine was added and cells were harvested after another 24h incubation. The amount of incorporated radiolabeled thymidine is shown on the y-axis as counts per minute (cpm). The data represents the mean values of triplicates ± SEM. C) NO-production by BMDMs after 24h activation with Pam3 at the indicated titrated concentrations (1000ng/mL, 100ng/mL and 10ng/mL) either alone or in combination with IFN-γ (40ng/mL). The NO_2^- levels (μM) are presented as the mean value of triplicates ± SEM. Unstimulated BMDMs and BMDMs stimulated with either Pam3 or IFN-γ alone, were used as negative controls.

4.1.2 pIC-NPs may replace IFN-γ in the synergy with the TLR1/2 agonist, Pam3, for activation of antitumor macrophage phenotype macrophages

The endosomal TLR3 is known to recognize viral double-stranded RNA. This receptor uses the TRIF-dependent signaling pathway in order to induce the production of type I interferons such as IFN-α and IFN-β. Previous study of Elisabeth Müller et al [67] demonstrated the synergy between the TLR3 agonist Poly (I:C) and IFNγ for M1 macrophages [67]. However, in this study we were interested in replacing IFNγ with poly(I:C) since this TLR3 ligand leads to IFN-α/-β production and these cytokines might work similar to IFN-γ. To investigate, if the combination of Poly(I:C) and Pam3 could induce the tumoricidal activity of macrophages, we used Poly(I:C) encapsulated in chitosan nanoparticles. These pIC-NPs have already demonstrated its potential in activating macrophages in combination with BCG in TB [56].

In order to test the potential of pIC-NPs to induce the tumoricidal activity in macrophages, we performed the *in vitro* assay, cancer cell growth inhibition assay. For this experiment we used the already tested concentration of pIC-NPs, 2 μg/mL [56], either alone or in combination with two Pam3 concentrations (1000ng/mL and 100ng/mL) to activate BMDMs from both C57BL/6 and NSG mice for 24h (Figure 12A,C). Some macrophages were left unstimulated or stimulated with pIC-NPs and Pam3 alone. The positive control for this experiment was Pam3 (100ng/mL) and IFN-γ (40ng/mL). After 24h of activation, the cell medium from the highest macrophage concentration was used for NO assay while LLC cells ($3x10^3$ cells/well) were added to the different number of BMDMs. pIC-NPs were also added to LLC alone in order to investigate any potential of direct toxicity on LLC cells

[56] Speth M.T, Repnik U, Müller E, Spanier J, Kalinke U, Corthay A, Griffiths G: Poly (I:C)-encapsulating nanoparticles enhance macrophage response to BSG-vaccine via synergistic activation of Toll-like receptor signaling. (Manuscript in preparation)

[67] Müller E, Christopoulos P, Halder S, Lunde A, Beraki K, Speth M, Øyenbråten I, Corthay A: Two signals are required for optimal induction of tumoricidal M1 macrophage phenotype (Manuscript in preparation)

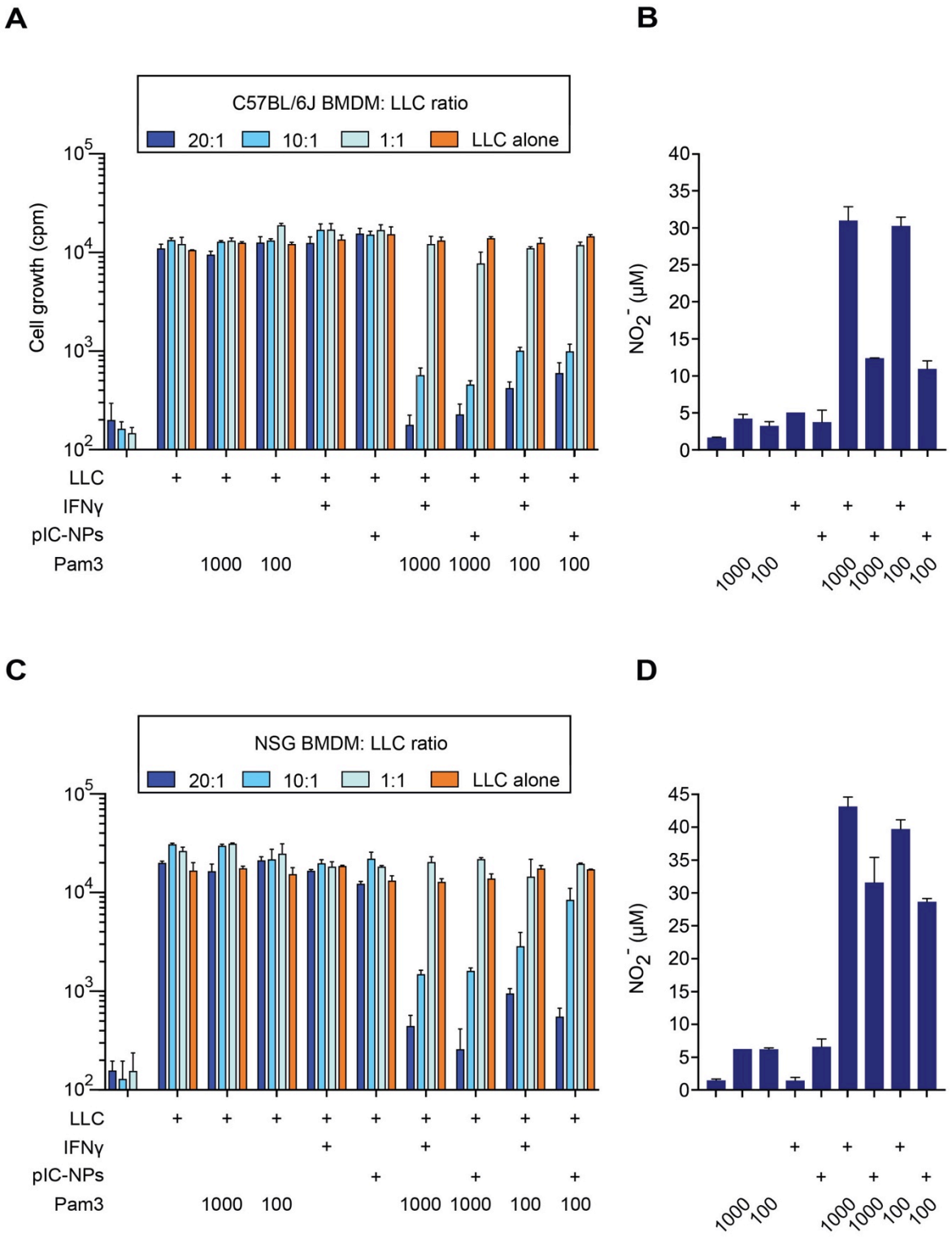

Figure 12. Activation of macrophages with pIC-NPs and Pam3. A) BMDMs from C57BL/6J mice were activated with pIC-NPs (2 μg/mL) either alone or in combination with two Pam3 concentrations (1000 ng/mL and 100 ng/mL) for 24h. After 24h activation, cell medium was removed and LLC cells ($3x10^3$ cells/well) were added to different number BMDMs in order to achieve the indicated BMDM:LLC cell ratio. [^{3}H]-Thymidine was added 24h before harvesting the cells. The amount of incorporated radiolabeled thymidine is presented as cpm on the y-axis. B) NO production by C57BL/6J BMDMs after 24h of stimulation with the same combinations of factors as in *A*. The NO_2^- levels were measured in supernatants from the highest macrophage density by Griess assay. C) Same

experiment set-up as in *A* but with NSG BMDMs as effector cells. D) Same Griess assay for determining NO levels in supernatants from the highest macrophage density as in *B* only from the NSG BMDMs this time. All data (A-D) are presented as the mean of triplicates ± SEM.

Finally, the proliferation rate of LLC cells was determined by the incorporation of radiolabeled thymidine, which was added 24h before harvesting the cells.

The BMDMs from C57BL/6 mice activated with Pam3 and pIC-NPs showed similar ability to inhibit LLC growth as when activated with IFN-γ and Pam3 (Figure 12A, the four groups of columns from the right). The most significant growth inhibition of LLC cells was observed at 20:1 and 10:1 effector:target cell ration. Interestingly, pIC-NPs alone did not induce any growth inhibition of LLC cells and neither did they show any signs of inducing direct toxicity on the LLC cells (Figure 12A, orange columns in the middle of the graph). Despite that both pIC-NPs and IFN-γ combined with Pam3 gave a strong growth inhibition (Figure 12A, the four groups of columns from the right), activation by pIC-NPs in combination with Pam3 induced lower levels of NO than Pam3 combined with IFN-γ (Figure 12B).

BMDMs from NSG mice showed enhanced growth inhibition of LLC cells by BMDMs stimulated with pIC-NPs and Pam3 compared to Pam3 and IFN-γ (Figure 12C, the four groups of columns from the right). Moreover, the NO levels of NSG stimulated BMDMs with pIC-NPs and Pam3 are higher compared to those of C57BL/6 BMDMs (Figure 12B,C). Interestingly, the higher NO levels did not give an increased cancer cell growth inhibition, indicating that NO might not be the only factor contributing to the observed growth inhibition (Figure 12A,C the four groups of columns from the right).

All the respective controls in the experiments seem to be as expected as there is no growth inhibition observed with single-stimulated macrophages or in LLC alone cultivated samples.

4.1.3 pIC-NPs can induce the highest tumoricidal activity in macrophages at the concentration of 200ng/mL

Since pIC-NPs showed an inducing tumoricidal potential in both C57BL/6 and defective BMDMs like NSG, we wanted to determine the most potent concentration of pIC-NPs with the cancer cell growth inhibition assay.

In order to determine this efficiency range of pIC-NPs, the C57BL/6 BMDMs were stimulated with pIC-NPs in a variety of concentrations either alone or in combination with Pam3 (100ng/mL). Some macrophages were left unstimulated or received only one signal (either 100ng/mL Pam3 or the indicated concentrations of pIC-NPs in Figure 13) and used as negative controls. The positive control was Pam3 (100ng/mL) and IFN-γ (40ng/mL). After 24h stimulation, NO assay was carried out with macrophages from the highest concentration whereas LLC cells ($3x10^3$ cells/well) were added to the different number of macrophages. The radiolabeled thymidine was added to all samples 24h post co-cultivation. The cells were harvested 24h after and the incorporated thymidine into proliferation LLC cells was analyzed.

LLC cell growth inhibition was the strongest at pIC-NPs concentration of 200ng/mL (or 0.2 μg/mL) (Figure 13A, the fourth group of columns from the right). This observed growth inhibition was primarily at 20:1 effector:target cell ratio. However, the positive control induced a strong LLC growth inhibition at both 20:1 and 10:1 BMDM:LLC cell ratio, as expected. BMDMs stimulated with either pIC-NPs or Pam3 alone did not induce any growth inhibition of LLC cells (Figure 13A the left side of the graph) neither did they show any sings of direct toxicity on LLC cells (Figure 13A, orange columns). Based on the results, the effect of pIC-NPs is completely abolished at the concentrations of 0.2 ng/mL (0.0002 μg/mL) (Figure 13A, the first group of columns from the right).

These results (Figure 13A) correlate with those from the NO assay (Figure 13B). The highest NO production was observed in macrophages stimulated with pIC-NPs at 200ng/mL together with Pam3 (100ng/mL) (Figure 13B, the fourth bar from the right). Still, it is lower than the NO levels observed from the positive control (higher than 30 μM)

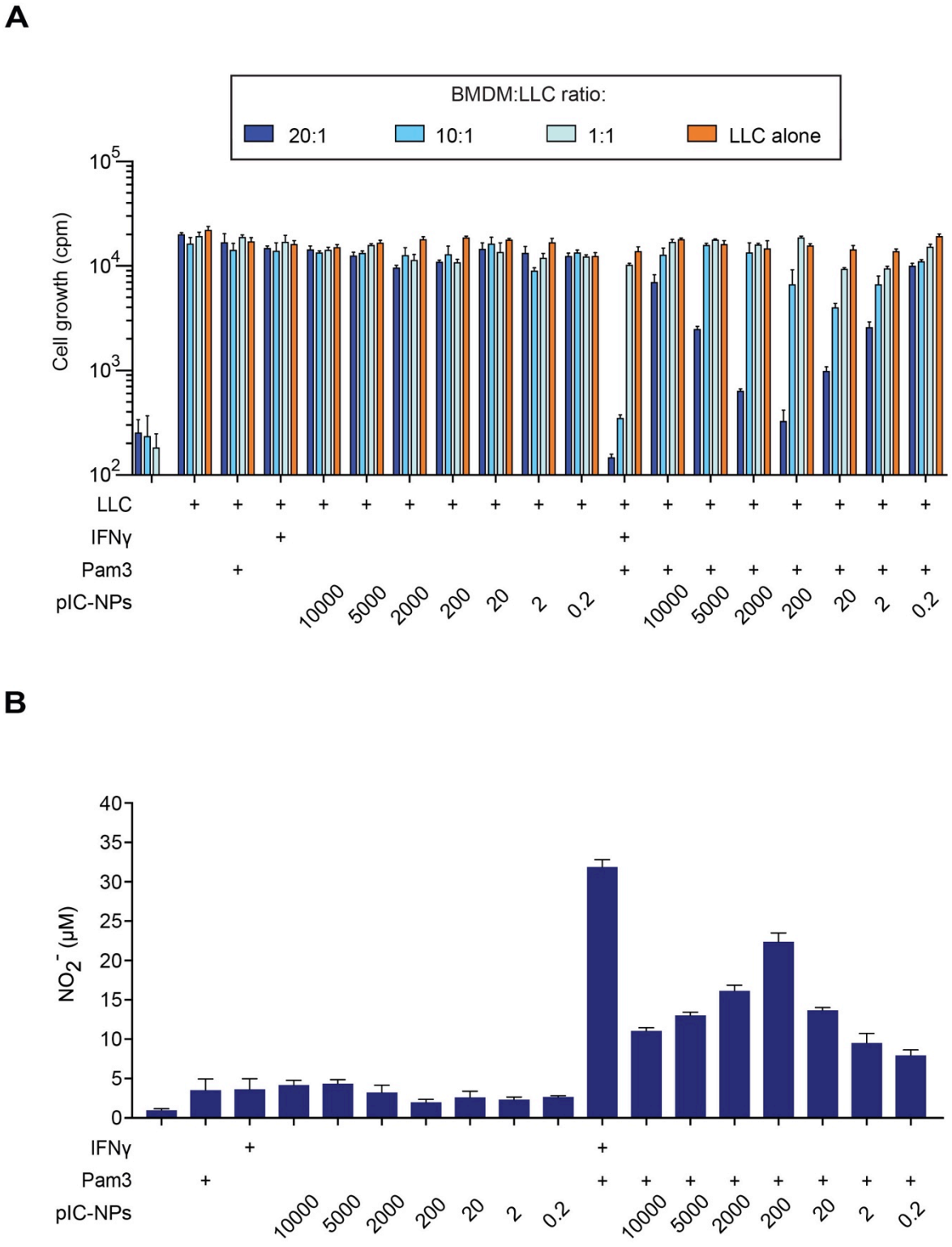

Figure 13. The titration of pIC-NPs in combination with Pam3. A) BMDMs from C57BL/6 mice were stimulated with a broad concentration range of pIC-NPs as indicated either alone or in conjugation with Pam3 (100ng/mL). After 24h of stimulation, LLC cells ($3x10^3$ cells/well) were added in order to achieve the indicated BMDM:LLC cell ratio. After 24h of co-cultivation, radiolabeled thymidine was added and cells were harvested after another 24h incubation. B) The NO-production by pIC-NPs-stimulated BMDMs determined by Griess assay. The data in *A* and *B* represent the mean values of triplicates ± SEM.

4.1.4 pIC-NPs may induce apoptosis in Mitomycin C-treated macrophages at high doses

Based on the pIC-NPs titration experiment (Figure 13A and B) we were interested in investigating the reason behind the abolished LLC growth inhibition at high pIC-NPs concentrations (10μg/mL and 5μg/mL). One possible hypothesis could be that high pIC-NPs concentrations are too toxic for macrophages and induce cell death.

In order to test if pIC-NPs are able to induce cell death at high concentrations, we performed the Annexin V and PI binding assay and analyzed the cells by using flow cytometry. Annexin V-FITC staining allows identifying early/late apoptotic cells due to the externalization of PS to the cell surface. Only Annexin V-FITC positive cells (Annexin V-$FITC^+/PI^-$) are early apoptotic cells whereas only PI positive (Annexin V-$FITC^-/PI^+$) are regarded as primary necrotic cells. Dual staining with Annexin V-FITC and PI gives further characterization of the different stages of cell death such as late apoptotic cells undergoing secondary necrosis (Annexin V-$FITC^+/PI^+$). Viable cells are double negative, Annexin V-$FITC^-/PI^-$.

For this experiment we used both C57BL/6 Mitomycin C-treated BMDMs to mimic the conditions in the cancer growth inhibition assay, and non-Mitomycin C treated BMDMs from the same mice strain. The non-Mitomycin C treated BMDMs were used in order to see how untreated or normal macrophages respond to pIC-NPs as in *in vivo* situations.

Both types of BMDMs were treated with three different concentrations of pIC-NPs (10 μg/mL, 5μg/mL and 2μg/mL) either alone or in combination with the second stimulus, Pam3 (100ng/mL) for 24h. Staurosporine (1μM) was added to certain BMDMs 6h before proceeding with the Annexin V and PI binding assay. The Staurosporine-treated BMDMs were used as the positive control whereas BMDMs that did not receive any stimulation (untreated BMDMs, Figure 14A and Figure 15A) were used as the negative control.

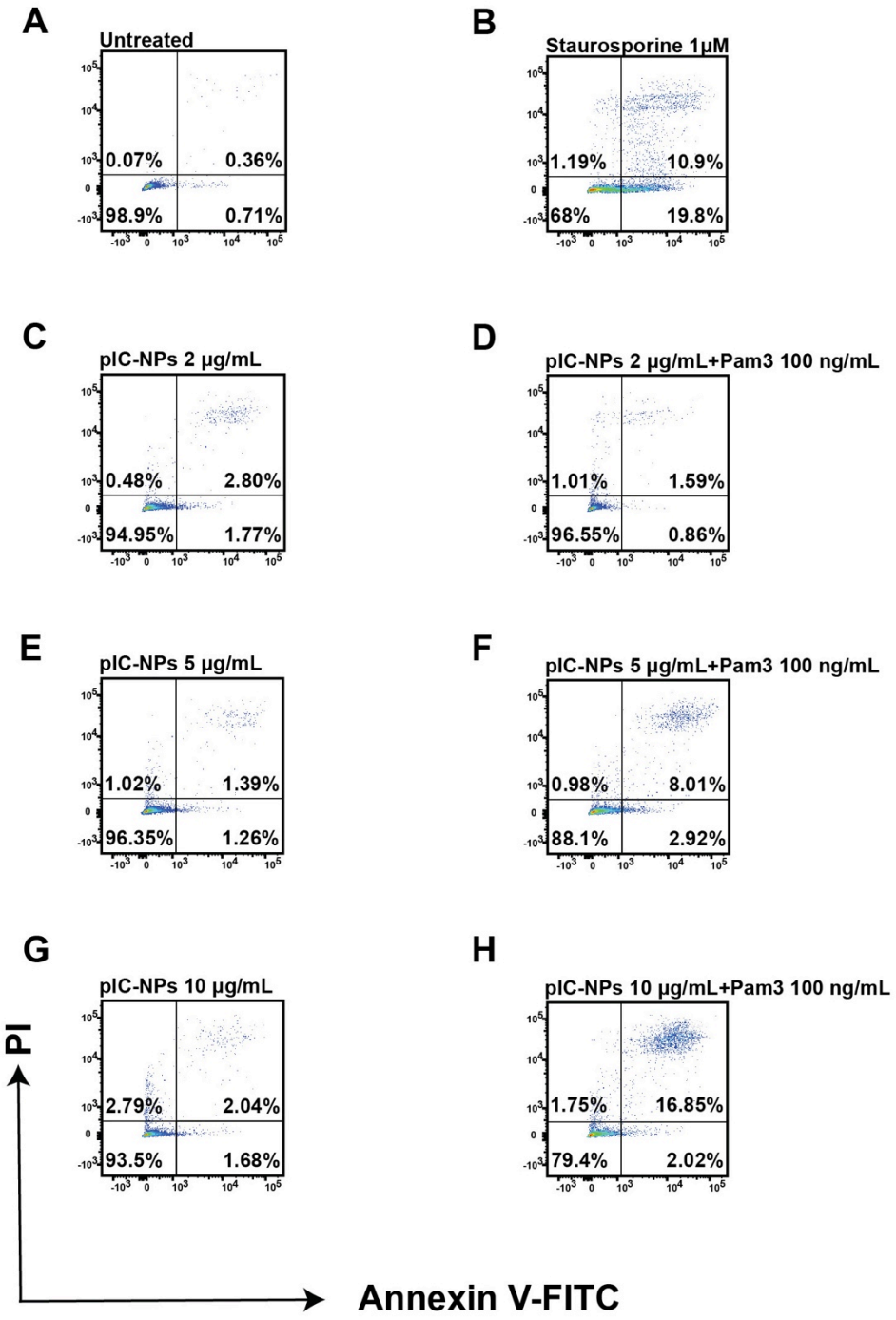

Figure 14. Detection of pIC-NPs –induced apoptosis in Mitomycin C-treated BMDMs. Mitomycin C-treated BMDMs from C57BL/6 mice were stimulated with three different concentrations of pIC-NPs (10 µg/mL, 5 µg/mL and 2 µg/mL) either alone or in combination with Pam3 (100ng/mL) for 24h. Untreated BMDMs were used as negative control whereas staurosporine-treated BMDMs were the positive control. pIC-NPs-induced apoptosis in BMDMs was evaluated by using Annexin V and PI binding assay followed by flow cytometry analysis 24h after treatment. Cell staining with Annexin V-FITC is shown on the x-axis whereas PI staining on the y-axis. Annexin V-FITC^{+}/PI^{-} cells are early apoptotic cells while Annexin V-FITC^{-}/PI^{+} are primary necrotic cells. Late apoptotic cells undergoing secondary necrosis are Annexin V-FITC^{+}/PI^{+}. Double negative cells are regarded as live cells. The flow cytometry data of the four distinct populations are presented with percentage numbers which represent the average value of the duplicates ± SD.

Flow cytometry data from Mitomycin C-treated BMDMs revealed 16.85% of BMDMs treated with 10 μg/mL pIC-NPs and Pam3 (100ng/mL) to be late apoptotic cells undergoing secondary necrosis (Figure 14H, Table 16). The other two pIC-NPs concentrations (5 μg/mL and 2 μg/mL) did not revealed any significant percentage of apoptosis or necrosis (Figure 14C-F, Table 16) alone or in combination with Pam3.

Table 16. An overview of the flow cytometry analysis of Mitomycin C-treated BMDMs as percentage of the duplicates ± SD

Samples	**Annexin V /PI$^-$**	**Annexin V$^+$ / PI$^-$**	**Annexin V$^+$ / PI$^+$**	**Annexin V$^-$ / PI$^+$**
Untreated	98.9 %	0.71%	0.36%	0.07%
Staurosporine 1μM	68%	19.8%	10.9%	1.19%
pIC-NPs 2 μg/mL	94.95%	1.77%	2.80%	0.48%
pIC-NPs 2 μg/mL+Pam3 100ng/mL	96.55%	0.86%	1.59%	1.01%
pIC-NPs 5 μg/mL	96.35%	1.26%	1.39%	1.02%
pIC-NPs 5 μg/mL+Pam3 100ng/mL	88.1%	2.92%	8.01%	0.98%
pIC-NPs 10 μg/mL	93.5%	1.68%	2.04%	2.79%
pIC-NPs 10 μg/mL+ Pam3 100ng/mL	79.4%	2.02%	16.85%	1.75%

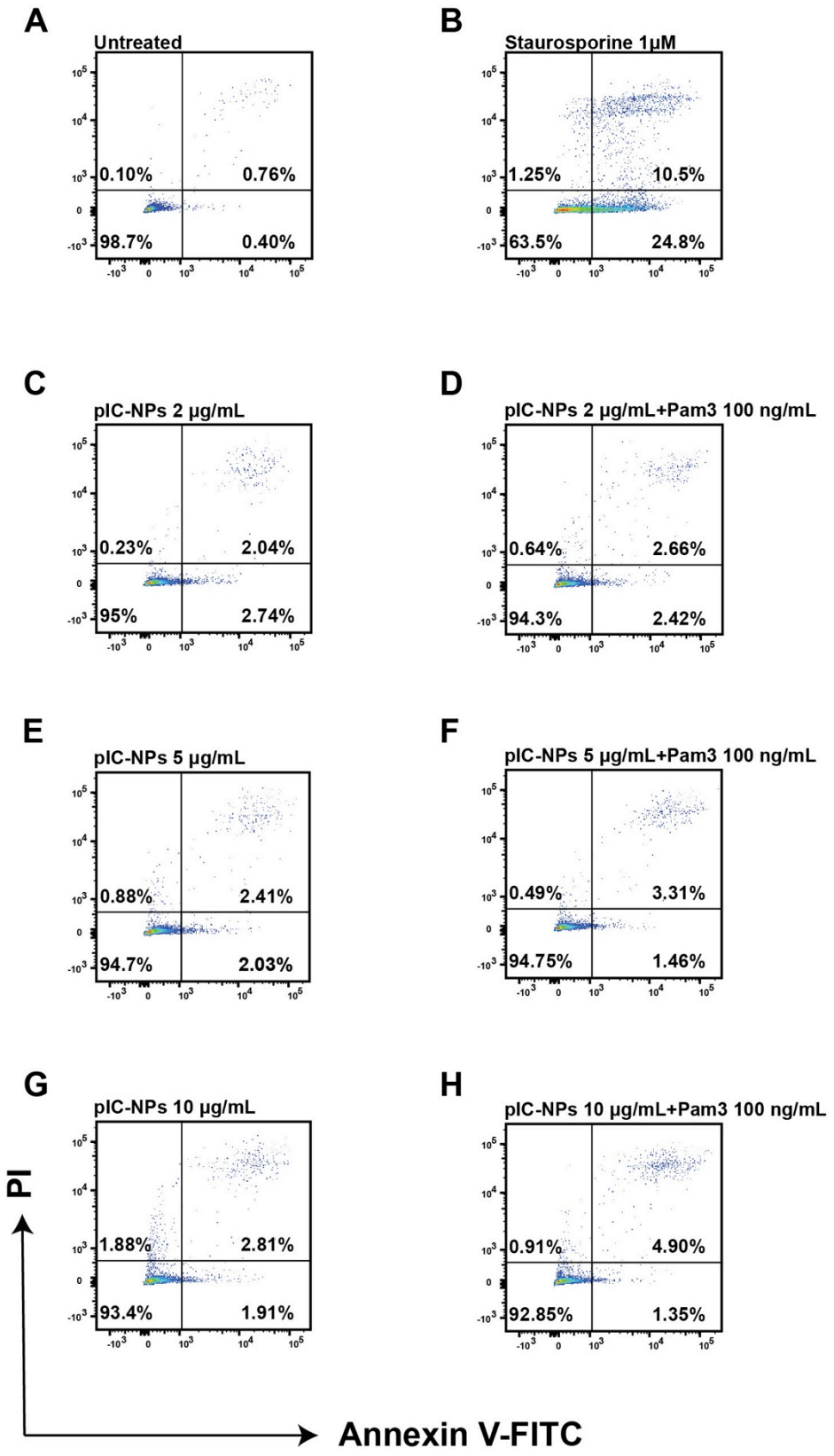

Figure 15. Detection of pIC-NPs-induced apoptosis in non-Mitomycin C treated BMDMs. C57BL/6 BMDMs were treated with the same concentrations of pIC-NPs as Mitomycin C-treated BMDMs (Figure 14). Staurosporine (1µM)-treated BMDMs were the positive control while untreated BMDMs were used as the negative control. After 24h of co-stimulation, Annexin V and PI binding assay was carried out. The cells were analyzed with flow cytometry. Annexin V-FITC staining is shown on the

x-axis and PI staining on the y-axis. Viable cells were determined by being Annexin V-FITC$^-$/PI$^-$ whereas double positive (Annexin V-FITC$^+$/PI$^+$) represent apoptotic cells that are undergoing secondary necrosis. Annexin V-FITC$^+$/PI$^-$ cells are early apoptotic cells whereas Annexin V-FITC$^-$/PI$^+$ cells are primary necrotic cells. Each of the four distinct cell populations is presented as percentage numbers. The data presents the average value of the duplicates ±SD.

Interestingly, we did not observe any signs of apoptosis or necrosis in non-Mitomycin C treated BMDMs stimulated with pIC-NPs (Figure 15C-H, Table 17). The positive control showed 24.8% of early apoptotic cells, which is a higher percentage than in Mitomycin C-treated BMDMs (Figure 14B, Figure 15B, Tables 16 and 17).

From the flow cytometry data it is possible to conclude that pIC-NPs neither alone nor in combination with Pam3 (100ng/mL) are able to induce apoptosis/necrosis in non-Mitomycin C treated BMDMs. However, we have observed some late apoptosis, secondary necrosis in Mitomycin C-treated BMDMs stimulated with the highest pIC-NPs concentration (10 μg/mL) together with Pam3 (100ng/mL) (Figure 14H). This observed apoptosis/necrosis could also be due to the macrophage stress response towards Mitomycin C treatment.

Table 17. An overview of the flow cytometry analysis of non-Mitomycin C treated BMDMs as percentage of the duplicates ± SD

Samples	**Annexin V$^-$ / PI$^-$**	**Annexin V$^+$ / PI$^-$**	**Annexin V$^+$ / PI$^+$**	**Annexin V$^-$ / PI$^+$**
Untreated	98.7 %	0.40%	0.76%	0.10%
Staurosporine 1μM	63.5%	24.8%	10.5%	1.25%
pIC-NPs 2 μg/mL	95%	2.74%	2.04%	0.23%
pIC-NPs 2 μg/mL+Pam3 100ng/mL	94.3%	2.42%	2.66%	0.64%
pIC-NPs 5 μg/mL	94.7%	2.03%	2.41%	0.88%
pIC-NPs 5 μg/mL+Pam3 100ng/mL	94.75%	1.46%	3.31%	0.49%
pIC-NPs 10 μg/mL	93.4%	1.91%	2.81%	1.88%
pIC-NPs 10 μg/mL+ Pam3 100ng/mL	92.85%	1.35%	4.90%	0.91%

4.1.5 pIC-NPs effect on cancer cell growth inhibition is NO mediated

Based on the work of Speth el al it seems that the TRIF-dependent signaling pathway induced by pIC-NPs is essential for the observed synergistic action of pIC-NPs with another TLR agonist [56]. It is know that auto-/paracrine stimulation of type I IFN induced by the TRIF-signaling pathway leads to amplified activation of innate immune cells such as macrophages [68,69].

In our experiments where we combined the TLR1/2 agonist Pam3 with pIC-NPs, we emerged the MyD88- and TRIF-signaling pathway. The next question was if the observe growth inhibition effect is NO mediated.

In order to determine if the pIC-NPs growth inhibition effect on LLC cells is in fact dependent on NO, we used the NO production inhibition SMT [70] at the concentration 10mM in cancer cell growth inhibition assay.

C57BL/6 BMDMs were stimulated with two pIC-NPs concentrations (2μg/mL and 0.2μg/mL) alone or in combination with Pam3 (100ng/mL) for 24h. Pam3 (100ng/mL) co-stimulation with IFN-γ (40ng/mL) was used as the positive control in the experiment. Negative controls included single-stimulated and unstimulated macrophages. SMT (10mM) was added only to macrophages that were stimulated with two signals; either Pam3 with IFN-γ or to the combination of Pam3 and pIC-NPs (Figure 16A, the three groups of columns from the right). The LLC cell suspension in a total volume of 100μL/well was added 24h after stimulation whereas the radiolabeled thymidine was added 24h before harvesting the cells.

The observed growth inhibition of LLC cells by pIC-NPs was completely abolished with SMT present (Figure 16A, the two groups of columns from the right). The same observation was seen for the positive control (Figure 16A, the third group of columns from the right).

The NO production was also reduced with the presence of SMT; from more than 25μM to less than 5μM for pIC-NPs (0.2μg/mL) in combination with Pam3 (100ng/mL) (Figure

[56] Speth M.T, Repnik U, Müller E, Spanier J, Kalinke U, Corthay A, Griffiths G: Poly (I:C)-encapsulating nanoparticles enhance macrophage response to BSG-vaccine via synergistic activation of Toll-like receptor signaling. (Manuscript in preparation)
[68] Decker T, Müller M, Stockinger S: The Yin and Yang of type I interferon activity in bacterial infection. Nature Review Immunology 2005, **5(9)**: 675-687
[69] Zhang X, Alley E.W, Russel S.W, Morrison D.C: Necessity and sufficiency of beta interferon for nitric oxide production in mouse peritoneal macrophages. Infection and immunity 1994, **62(1)**: 33-40
[70] Southan G.J, Szabo C, Thiemermann C: Isothioureas: potent inhibitors of nitric oxide synthases with variable isoform selectivity. British journal of pharmacology 1995, **114(2)**: 510-516

16B). These results are also reflected in the abolished cancer cell growth inhibition (Figure 16A). Taken together, these results indicate that NO is one of the essential components for pIC-NPs inhibitory effect on LLC cell growth.

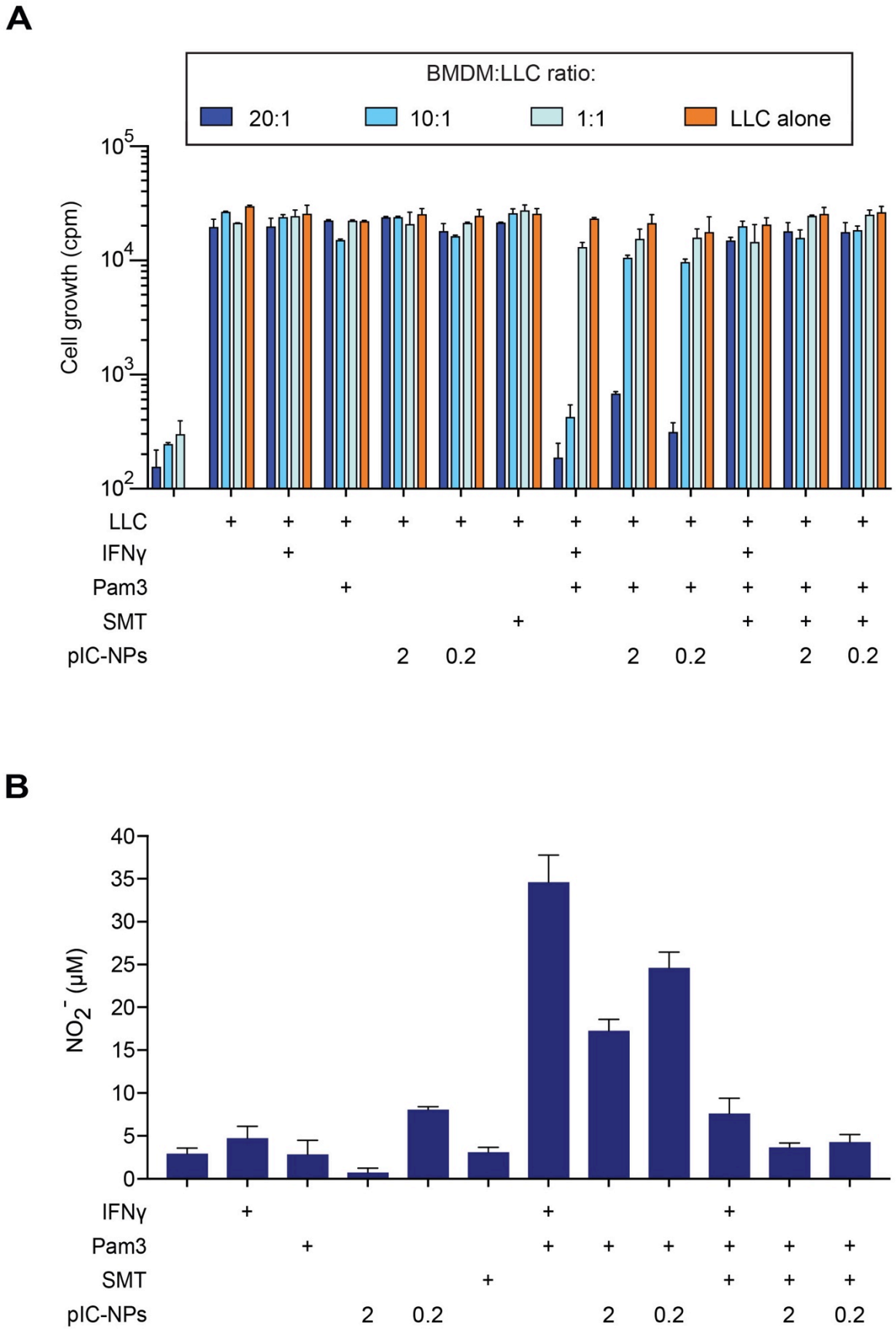

Figure 16. pIC-NPs effect on LLC cell growth inhibition is mediated by NO. A) BMDMs from C57BL/6 mice at three different densities were left untreated or activated with the indicated factors (2 μg/mL and

0.2 μg/mL pIC-NPs, 100ng/mL Pam3, 40ng/mL IFN-γ) for 24h. The positive control for the experiment was Pam3 (100ng/mL) in combination with IFN-γ (40ng/mL). SMT (10μM) was present in samples where BMDMs were stimulated with two signals as indicated in the graph (the three groups of columns from the right). After 24h activation, LLC cells ($3x10^3$ cells/well) were added to different number of BMDMs in order to achieve the indicated BMDM:LLC cell ratio. The radiolabeled thymidine was added 24h after co-cultivation. The incorporation of radiolabeled thymidine is presented as cpm-values on the y-axis. B) NO production was measured in the supernatants of BMDMs from the highest density wells by Griess assay. The data in *A* and *B* are presented as the mean of triplicate ± SEM.

4.1.6 IFN-γ can be replaced by IFN-β, a type I interferon, for rendering macrophages tumoricidal

Type I interferons can exert both direct and indirect antitumor effects [71, 72]. In the tumor microenvironment, type I interferons are known for its antineoplastic effects such as inhibition of tumor cell proliferation and enhanced apoptosis [71,72]. Cultivated breast tumor cell lines showed enhanced apoptosis upon IFN-β and TLR3 agonist Poly(I:C) stimulation [71]. This stimulation leads to enhanced expression of the TNF-related apoptosis-inducing ligand (TRAIL), which leads to the observed enhanced cell death [71]. Moreover, type I interferons can activate both innate and adaptive immune cells to amplify the antitumor effects [71,72].

The increased interest in using IFN-β as an immunotherapeutic agent drew our attention to test IFN-β ability to render macrophages tumoricidal *in vitro*.

In the *in vitro* cancer cell growth inhibition assay, C57BL/6 BMDMs were stimulated with five different concentrations of IFN-β (Figure 17A). IFN-β was administrated either alone or in combination with Pam3 (100ng/mL). At the same time, some macrophages were stimulated with IFN-γ at the same concentrations as IFN-β in order to compare the two cytokines activation ability. IFN-β as well as IFN-γ was added to LLC cell alone to test potential direct toxicity. LLC cells ($3x10^3$ cells/well) were added 24h post co-stimulation and was followed by addition of radiolabeled thymidine 24h before harvesting the cells.

Based on our *in vitro* results, IFN-β induces stronger LLC cell growth inhibition at both 20:1 and 10:1 effector:target cell ration compared to IFN-γ (Figure 17A). Interestingly, we observed some toxicity upon IFN-β stimulation on LLC cells alone (Figure 17A, the fifth

[71] Parker B.S, Rautela J, Hertzog P.J: Antitumor actions of interferons: implications for cancer therapy. Nature Review Cancer 2016, **16(3)**: 131-144

[72] Zitvogel L, Galluzi L, Kepp O, Smyth M.J, Kroemer G: Type I interferons in anticancer immunity. Nature Reviews Immunology 2015, **15(7)**: 405-414

orange bar from the right). This observation makes it clear to exclude the use of IFN-β at the concentration of 40 ng/mL in further experiments. IFN-β and IFN-γ at 40 ng/mL in conjugation with Pam3 (100 ng/mL) showed similar inhibitory effect at 20:1 effector:target cell ratio. However, no inhibitory effects were observed with IFN-β or IFN-γ single-stimulation (Figure 17A).

IFN-β at 40 ng/mL in combination with Pam3 (100ng/mL) induced higher NO production (above 60 μM) than IFN-γ (above 30 μM). The inhibitory effects and NO production by IFN-β co-stimulation with Pam3 are concentration-dependent where the highest IFN-β concentration (40 ng/mL) seems to have a toxic effect on LLC cells (Figure 17A and B). Taken together, we can conclude that IFN-β in combination with Pam3 (100 ng/mL) is able to induce the tumoricidal ability of macrophages to a similar degree as IFN-γ.

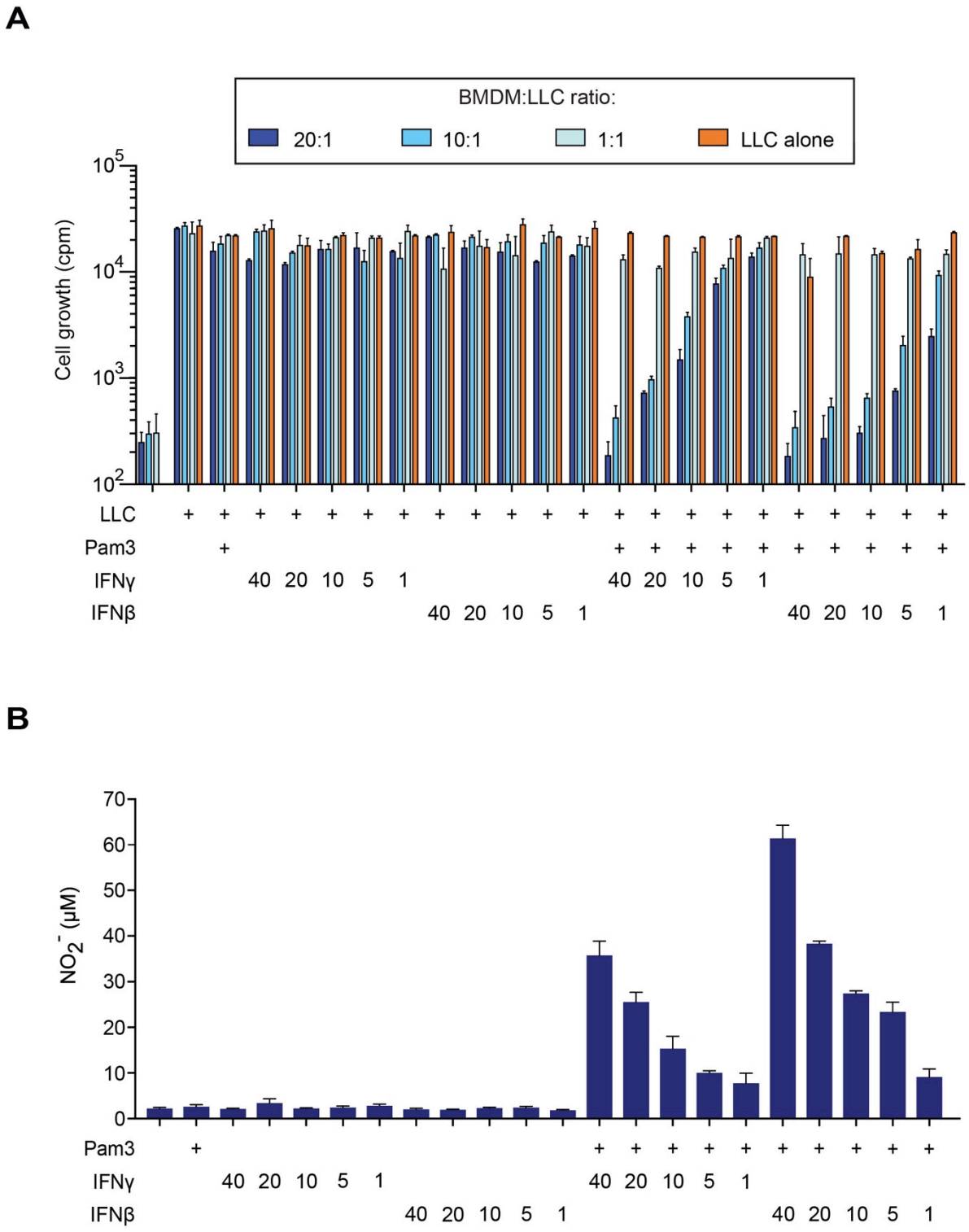

Figure 17. The activation of macrophages by type I interferon. A) C57BL/6 BMDMs at three different densities were left untreated or stimulated with the indicated concentrations of IFN-γ and IFN-β; either alone or in combination with Pam3 (100 ng/mL). LLC cells ($3x10^3$ cells/well) were added 24h after activation. After 24h of co-cultivation, radiolabeled thymidine was added and cells were harvested after another 24h incubation. The amount of incorporated radiolabeled thymidine is shown on the y-axis as cpm. B) The NO-production by IFNγ- and IFNβ-stimulated BMDMs. The NO production was measured by using Griess assay. The data presented in both *A* and *B*, are mean values of triplicates ± SEM.

4.1.7 TNF-α is not an efficient macrophage activator

Previous *in vitro* studies demonstrated TNF-α synergistic action with IFN-γ, which enhanced the tumoricidal activity of murine macrophages [28]. Results from cancer cell growth inhibition assay using TNF-α as the activating factor on murine peritoneal macrophages revealed an inhibitory effect on MOPC315 cell growth [73]. This inhibition was comparable to LPS-stimulated macrophages when the concentration of TNF-α was either 200 U/mL or 2 000 U/mL [73].

In this study, we wanted to investigate if TNF-α could also activate murine BMDMs in a similar was as TLR1/2 agonist Pam3.

Using the *in vitro* cancer cell growth inhibition assay, C57BL/6 BMDMs were stimulated with a broad concentration range of TNF-α. This stimulation was done either with TNF-α alone or in combination with IFN-γ (40ng/mL). The effector cell co-activation was done in a 24h time frame, which was followed by the addition of LLC target cells ($3x10^3$ cells/well). After 24h co-cultivation, radiolabeled thymidine was added and the cells were analyzed after another 24h incubation.

The results revealed that only at the highest used concentration (1000ng/mL) TNF-α induced an inhibitory effect on LLC growth (Figure 18A the seventh group of columns from the right). Moreover, this inhibitory effect was primarily at 20:1 effector:target cell ratio where BMDMs were activated with TNF-α (1000ng/mL) and IFN-γ (40ng/mL). TNF-α did not show any direct toxicity on LLC alone (Figure 18A, the orange columns). The positive control in the experiment, Pam3 (100ng/mL) in combination with IFN-γ (40ng/mL) gave the expected growth inhibition of LLC cells as in previous experiments (Figure 18A, the fifth group of columns from the left). All the other controls are as expected; no growth inhibition in unstimulated BMDMs co-cultured with LLC cells or from BMDMs stimulated with only one signal (Figure 18A).

The NO-assay revealed some NO production when combining the different concentrations of TNF-α with IFN-γ (40ng/mL). Moreover, this observed NO-production is concentration dependent as indicated in the Figure 18B. The highest NO-levels detected were above 20 μM (Figure 18B), but it gave a decreased inhibitory effect (Figure 18A).

---

[28] Haabeth O.A.W, Bogen B, Corthay A: A model for cancer-suppressive inflammation. Oncolmmunology 2012, **1(7)**: 1146-1155

[73] Stavna A: Activation of macrophages for inhibition of cancer cell growth. Master in Science thesis, Oslo and Akershus University College of Applied Science, 2013

This experiment was repeated three times with the same outcome. Thus, it is possible to conclude that TNF-α is not suitable to replace the TLR1/2 agonist Pam3 in the synergistic action with IFN-γ.

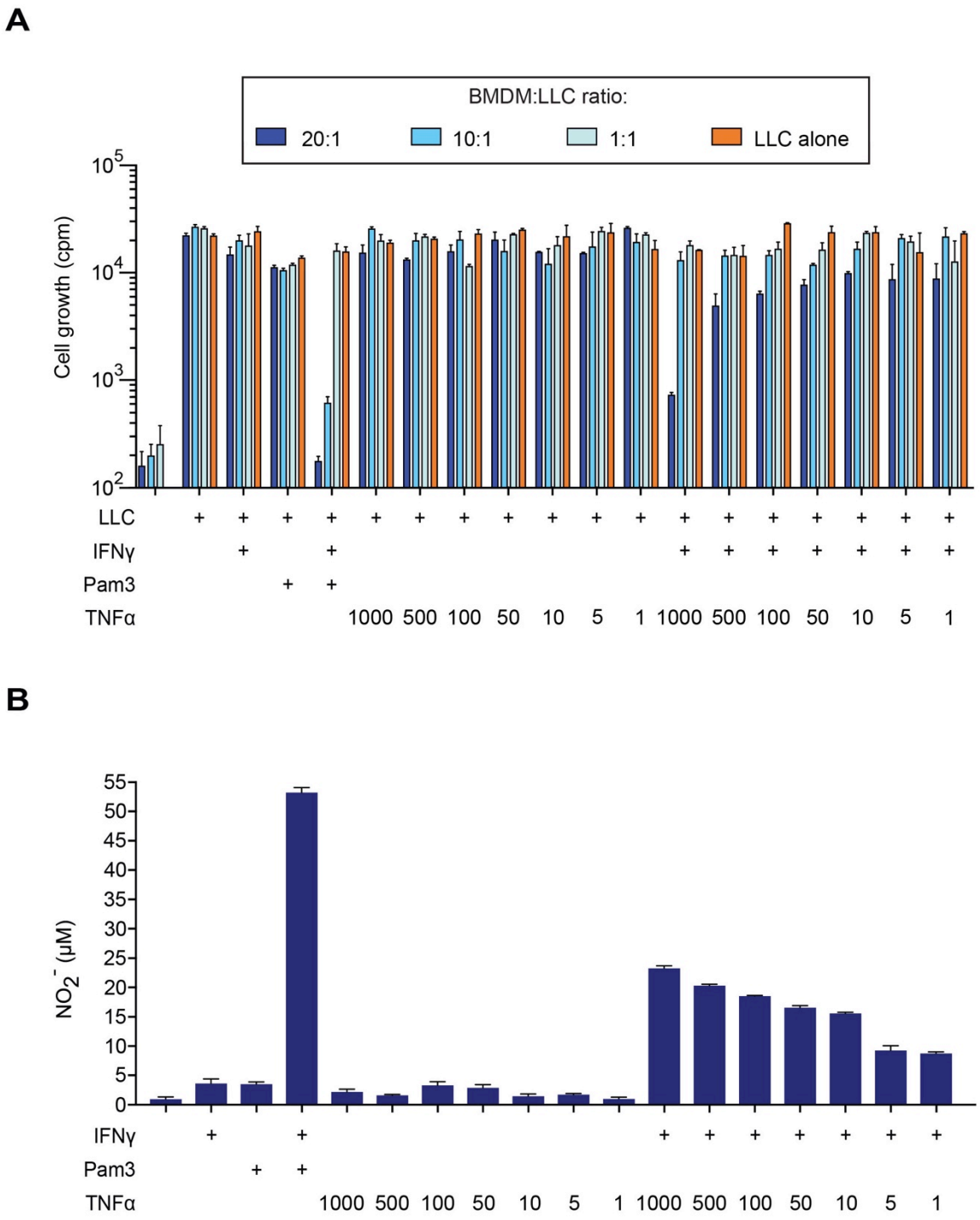

Figure 18. TNF-α-stimulated murine BMDMs in combination with IFN-γ. A) C57BL/6 BMDMs at three different densities were left untreated or stimulated with the indicated broad concentration range of TNF-α. After 24h activation, LLC cells ($3x10^3$ cells/well) were added. Radiolabeled

thymidine was added after 24h of co-cultivation and cells were harvested after another 24h incubation. The incorporated thymidine into proliferation LLC cells is presented as cpm-values, depicted on the y-axis. B) NO levels produced by BMDMs from the highest macrophage concentration. The NO production was measured in the supernatants by Griess assay. Data shown in both *A* and *B* represent the mean values of triplicates ± SEM.

4.1.8 HMGB1 acts in synergy with Pam3 to induce the tumoricidal activity in murine BMDMs

The protein HMGB1 is well documented as an enhancer of proinflammatory cytokine production when combined with TLR ligands such as LPS (TLR4 agonist) and Pam3 (TLR1/2 agonist) [33]. Based on the work of Hreggvidsdottir et al [33] on HMGB1 synergistic effects with TLR ligands for enhanced proinflammatory cytokine production, our became interested in testing HMGB1-induced tumoricidal ability in macrophages.

HMGB1 at three different concentrations (10ng/mL, 5ng/mL and 1 ng/mL) was used in order to activate murine BMDMs either alone or together with Pam3 (100ng/mL). The positive control used in this experiment was Pam3 (100ng/mL) combined with IFN-γ (40ng/mL). HMGB1 was also added to LLC alone wells to rule out the toxicity effect on LLC cells. The co-stimulation time was 24h followed by addition of LLC cells ($3x10^3$ cells/well) to all stimulated macrophages. The co-cultivation between BMDMs and LLC cells was followed by the incorporation of radiolabeled thymidine.

According to the *in vitro* results from the cancer cell growth inhibition assay, HMGB1 is able to induce an inhibitory effect on the LLC cell growth (Figure 19A). Moreover, this observed LLC cell growth inhibition is primarily at 20:1 effector:target cell ratio and is concentration dependent (Figure 19A, the three groups of columns from the right). The HMGB1-induced inhibitory effect is not strong as the induced inhibitory effect by the positive control. No indication of growth inhibition was detected with HMGB1 alone or any signs of toxicity on LLC cells.

BMDMs stimulated with both HMGB1 and Pam3 produced NO levels that were lower compared to the positive control (Figure 19B). Furthermore, the HMGB1-induced NO-production is concentration dependent where the highest concentration (10ng/mL) together

[33]Hreggvidsdottir H.S, östberg T, Wähämaa H, Schierbeck H, Aveberger A-C, Klevenvall L, Palmblad K, Ottosson L, Andersson U, Harris H.E: The alarmin HMGB1 acts in synergy with endogenous and exogenous danger signals to promote inflammation. Journal of Leukocyte Biology 2009, **86(3)**: 655-662

with Pam3 (100ng/mL) gave the highest NO levels (above 20 μM). The data from NO assay correlate with those from the cancer cell growth inhibition assay.

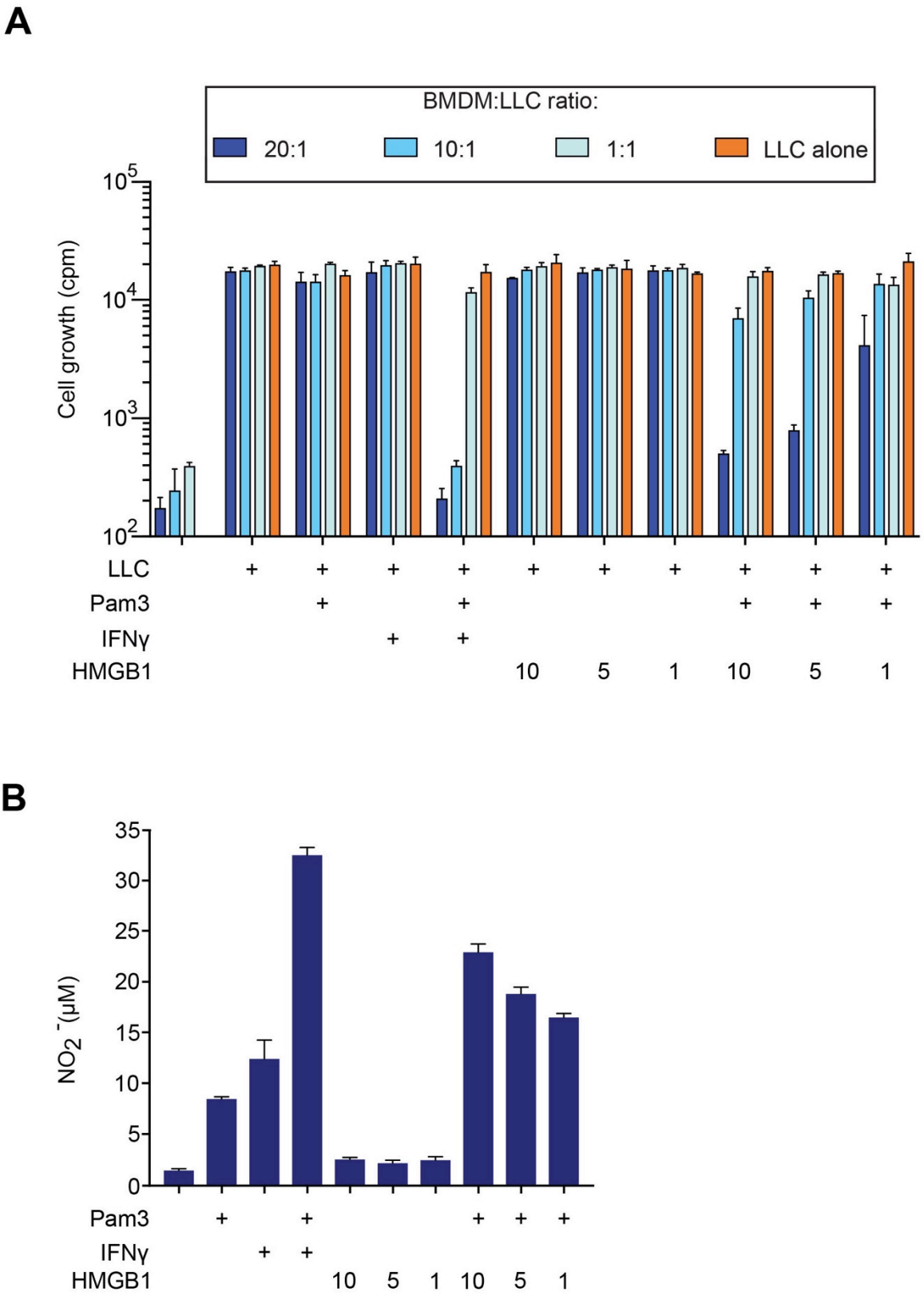

Figure 19. Macrophage activation by HMGB1 and Pam3. A) BMDMs from C57BL/6 mice at three different densities were left untreated or stimulated with the indicated factors (10ng/mL, 5ng/mL and 1ng/mL HMGB1, 100ng/mL Pam3, 40ng/mL IFN-γ). The 24h activation was followed by the addition of LLC cells ($3x10^3$ cells/well).

[^{3}H]-Thymidine was added after the 24h co-cultivation and cells were harvested after another 24h incubation. B) The indirect measurement of NO levels as NO_2^- was done with Griess assay. The NO levels were measured in the supernatants from the highest macrophage concentrations. All data in both *A* and *B* are presented as mean values of triplicates ± SEM.

4.2 Results from *in vivo* experiments

4.2.1 A small number of LLC is required for tumor development

In order to determine the specific number of LLC cells necessary for tumor development in an acceptable time frame, we performed the LLC titration experiments. In this experiment five different amounts of LLC cells (Table 14) were tested for the potential of inducing tumors in C57BL/6 mice. The LLC cells were injected s.c in a total of 34 C57BL/6 mice. The experiment was terminated 47 days post LLC injection.

During the experiment, some mice were sacrificed due to necrosis development before reaching the tumor size of 15 mm or the tumor volume of 700 mm^3. After the experiment termination, there were two mice (nr 1 and 32 from Group 1) that did not develop any tumors.

The results revealed that it is possible to induce tumor development in mice after 18 days post injection with only 1000 LLC cells (Figure 20, red line). Groups with 50 000 and 100 000 injected LLC cells developed tumors much faster compared to the other groups (Figure 20, purple and black line).

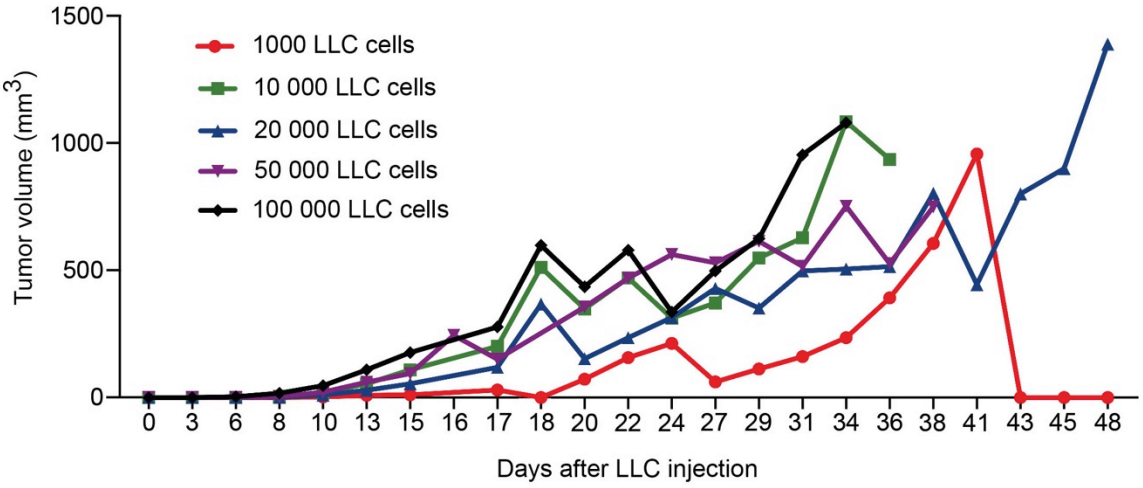

Figure 20. Average tumor development per group. Each line represents one group as indicated. The tumor volume is presented on the y-axis as mm^3 while the time for tumor development after LLC injection is depicted on the x-axis. The different lines represents each groups mean values.

4.2.2. Intraperitoneally administrated Poly (I:C) might reduce tumor volume in LLC-bearing C57BL/6 mice

Our *in vitro* results on Poly(I:C) in the form of nanoparticles, revealed pIC-NPs ability to stimulate the cytotoxic ability of macrophages towards LLC cells thus making them a potential immunotherapy candidate. In the literature, there are many reports on Poly (I:C) anti-tumor effects [66]. Shime et al [66] reported that intraperitoneally injected Poly (I:C) could reduce tumor volumes in LLC-bearing mice. We became interested in reproducing these findings for the benefit of proceeding with the pIC-NPs *in vivo*. In order to reproduce the results form Shime et al [66], we used 13 C57BL/6 mice and divided them into two groups: control group (PBS-group) and treatment group (Poly (I:C)-group). The injections were given twice a week after 9 days post LLC injection. The tumor measurements were taken the same day as administrated injections. During this 30-days experiment, some mice were sacrificed due to necrosis development or reaching the 15 mm tumor size limit.

The results revealed a potential trend of effect of Poly(I:C) alone on LLC tumors. However, we did not see significant survival benefit (Figure 21) or significant tumor reduction (Figure 22 A,B) as reported by Shime et al.

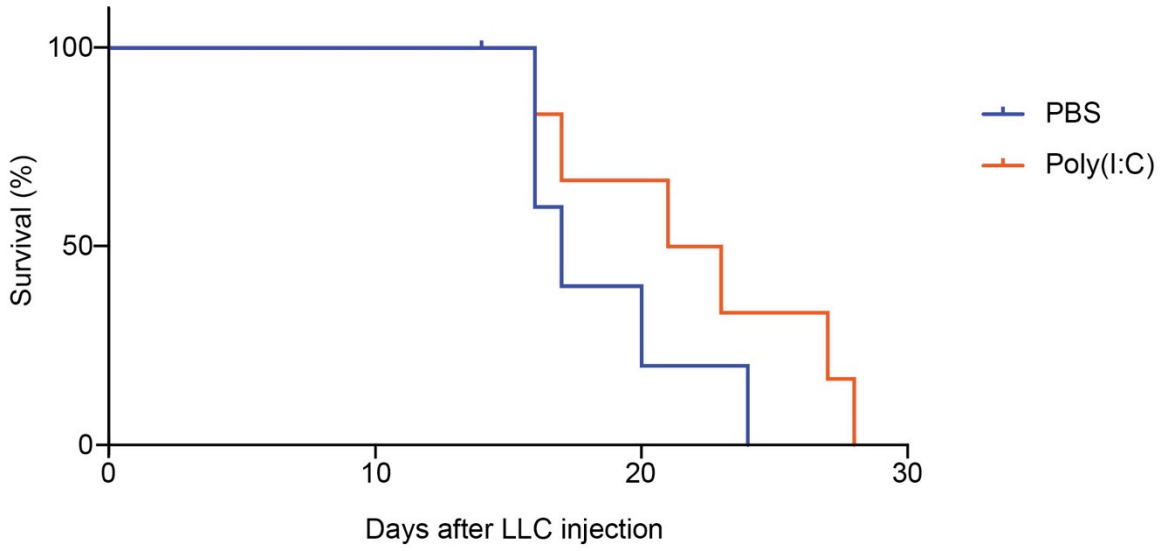

Figure 21. The survival curve of the two treatment groups after LLC tumor challenge: n=6 per PBS group, n=7 per Poly(I:C) group. Mice were sacrificed when tumor volume exceeded 700mm^3.

[66] Shime H, Matsumoto M, Oshiumi H, Tanaka S, Nakane A, Iwakura Y, Tahara H, Inoue N, Seya T: Toll-like receptor 3 signaling converts tumor-supporting myeloid cells to tumoricidal effectors. Proceedings of the National Academy of Sciences of the United States of America (PNAS) 2012, **109(6)**: 2066-2071.

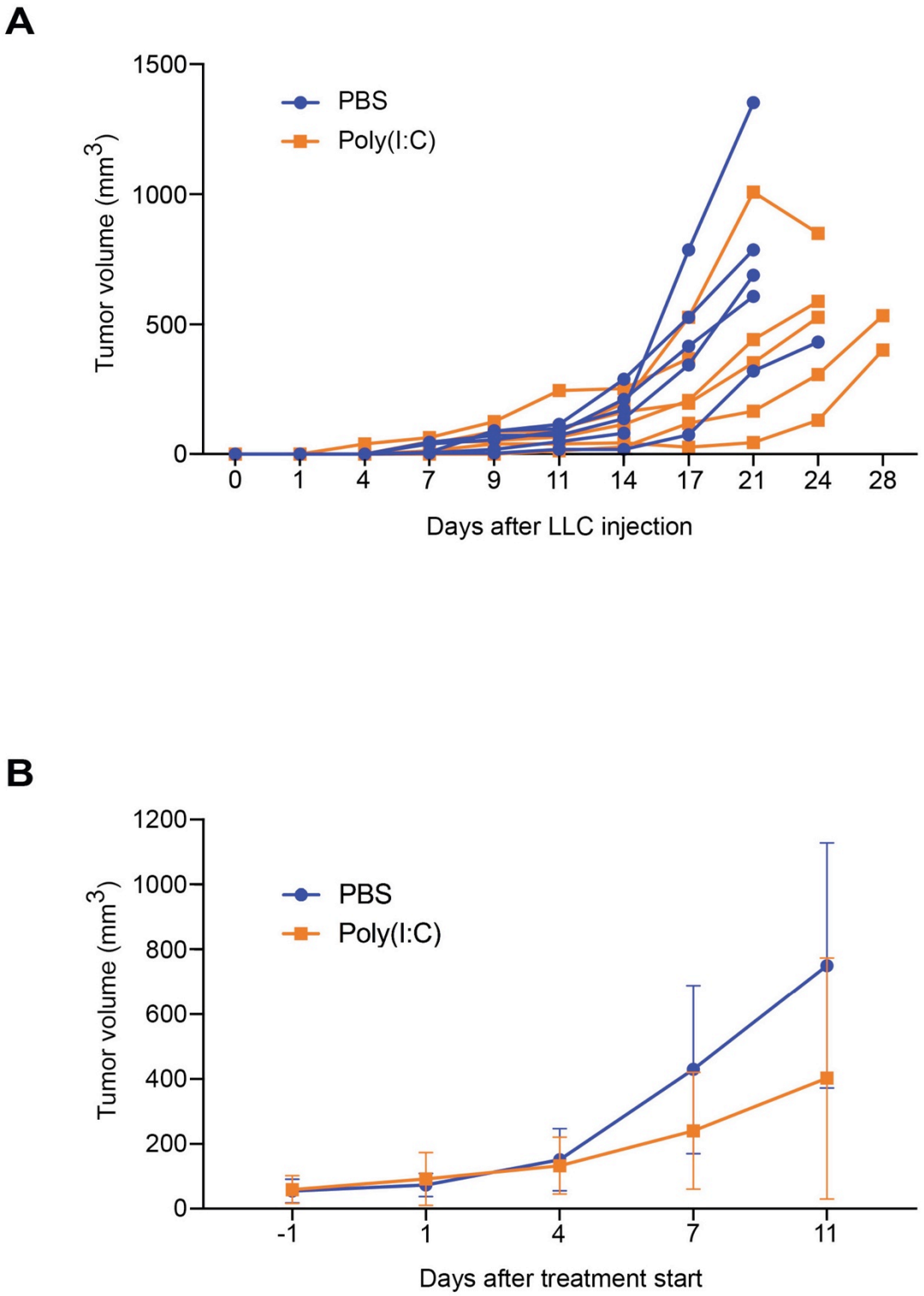

Figure 22. Tumor growth after treatment administration. C57BL/6 mice were injected s.c with LLC cells on day 0 while the treatment started at day 9. The control group received PBS (100µL) whereas the treatment group received 0.25mg Poly (I:C). All treatment injections were given intraperitoneally. A) the tumor volume of all individual mice B)The average tumor volume per treatment group. All data are presented as mean value ± SD.

4.2.3 The safes pIC-NPs dose for *in vivo* approach is 2 µg/m

Our *in vitro* results using cancer cell growth inhibition assay revealed pIC-NPs ability to induce tumoricidal activity in macrophages. Next, we saw a potential trend of effect of Poly(I:C) alone in the LLC mice model. Finally, we wanted to investigate if Poly (I:C) in the form of nanoparticles, could lead to reduced tumor development as well. In order to proceed with this, we needed first to investigate if pIC-NPs could be toxic or induce local acute inflammation in mice before using them as immunotherapeutic factors.

In order to determine the possible toxicity of pIC-NPs, we performed the acute-toxicity study on thirteen C57BL/6 mice with four different doses of pIC-NPs (Table 15). The mice received the different doses of pIC-NPs together with Pam3 only once while being monitored daily for clinical signs of acute inflammation for two weeks. The control group was administrated with PBS.

Local inflammation was observed at the site of the injection in mice treated with high doses of pIC-NPs (20µg, 50µg and 100µg) (Figure 23, blue, red and purple lines). This observed inflammation in form of swelling was visible already one day post injection. In order to keep track of possible increase of subsiding of the inflammation, we used the volume of swelling (Figure 23). Another particular observation was skin irritation at the site of the injection site in the form of small red colorations. This skin irritation or rash was visible in some mice three days after administrated pIC-NPs treatment.

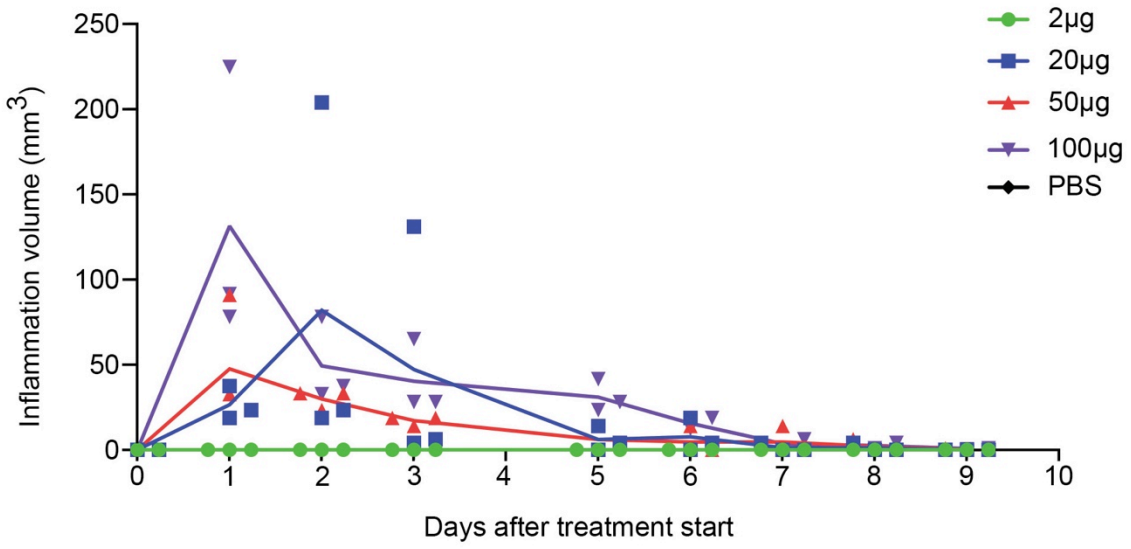

Figure 23. The swelling volume at the injection site after administrated pIC-NPs. Each dot represents one individual mouse whereas each color represents one group. The lines are representing each group mean values.

However, some subsiding in the swelling and skin irritation was visible at day six post treatment. Overall, all mice seem to be in a good heath condition despite the local inflammation. There were active and did not show any significant body weight loss outside the normal range [74] (Table 18).

Table 18. An overview of the body weighs of the 13 mice during the two-weeks acute toxicity study. AS(x): animal sacrificed due to open wound.

Group number		**Body weight (g)**								
	Day	0	1	2	3	5	6	7	8	9
Group 1	Mouse 1	28.7	27.7	27.9	28.4	28.1	28	28.6	28.4	28.2
	Mouse 2	26.5	25.3	26.2	26.6	26.3	26.6	26.1	26.1	25.6
	Mouse 3	30	29	29	29.5	29.1	28.9	28.7	29.1	29.1
Group 2	Mouse 4	33.5	31.5	31.8	31.2	31.7	31.4	31.4	31.8	31.3
	Mouse 5	27.9	26	26.4	25.2	26.1	26.1	26	26.5	25.9
	Mouse 6	26	24.1	24	23.8	24.3	24.2	23.8	24.1	23.7
Group 3	Mouse 7	29.5	27.9	28.4	28	28.5	28.3	28.4	28.4	28.4
	Mouse 8	32.5	31	30.9	30.8	31	31	30.1	29.9	29.4
	Mouse 9	31	30.6	30.1	29.6	29.7	29.7	28.8	29.9	29.6
Group 4	Mouse 10	27.7	26.3	26	26	26.6	25.9	25.8	26.1	25.8
	Mouse 11	31.2	28	28.5	28.9	28.6	28.4	27.8	27.9	27.5
	Mouse 12	32.2	30.3	30.2	30.5	30.2	AS x	x	x	x
Group 5	Mouse 13	26.5	25.7	25.7	25.5	25.9	25.7	25.7	27.9	25.8

No signs of inflammation were observed in mice treated with 2μg of pIC-NPs. This mice group showed also a good general heath without body weigh-loss or increased water consumption (Table 18). All mice had a healthy fur and showed normal behavior and responses to the environment. These observations were comparable to those of the control mice. Taken together, the safest dose of pIC-NPs for *in vivo* approach is 2 μg.

[74] Laboratory, T.J Body weight information for C57BL/6J (000604) 2017. Access to the information at the web-side: https://www.jax.org/jax-mice-and-services/strain-data-sheet-pages/body-weight-chart-000664#

5 Discussion

5.1 Pam3 as a potent inducer of macrophage tumoricidal activity

Sorgi et al demonstrated that Pam3, a synthetic lipoprotein analog, activated macrophages against bacterial infections [75]. In the study of Elisabeth Müller et al a broad range of TLR agonists were shown to render macrophages tumoricidal when combined with IFN-γ [67]. In our study, we were interested in reproducing the macrophage activation potential of Pam3 in order to determine the positive control for further experiments.

Our study showed that Pam3 at 1000ng/mL and 100ng/mL together with IFN-γ (40ng/mL) is able to induce the tumoricidal ability of BMDMs toward LLC cells as demonstrated by Elisabeth Müller et al [67]. However, no effect on cancer cell growth was observed with Pam3 or IFN-γ alone, which is in agreement with this previous study.

Moreover, IFN-γ in combination with Pam3 at 1000ng/mL lead to an NO-production more than 30μM while the combination with Pam3 at 100ng/mL gave 30μM of NO. Taken together, the results from cancer cell growth inhibition assay and NO production (Figure 11) indicate that Pam3 at both 1000ng/mL and 100ng/mL is a potent inducer of macrophage tumoricidal activity when combined with IFN-γ. The high levels of NO correlated with increased cancer cell growth inhibition. Since there is no significant difference between the two highest concentrations of Pam3, we decided to use Pam3 at 100ng/mL in combination with IFN-γ (40ng/mL) as a positive control for further experiments. Furthermore, we became interested in finding potential molecular combinations that could replace either Pam3 or IFN-γ and still gave the same observed cancer cell growth inhibition. In this study a few new candidates arise such as pIC-NPs, IFN-β and HMGB1.

[67] Müller E, Christopoulos P, Halder S, Lunde A, Beraki K, Speth M, Øyenbråten I, Corthay A: Two signals are required for optimal induction of tumoricidal M1 macrophage phenotype (Manuscript in preparation)

[75] Sorgi C.A, Rose S, Court N, Carlos D, Paula-Silva F.W.G, Assis P.A, Frantz F.G, Ryffel B, Quesniaux V, Faccioli L.H: GM-CSF priming drives bone marrow-derived macrophages to a pro-inflammatory pattern and downmodulates PGE_2 in response to TLR2 ligands. PloS one 2012, **7(7)**:e40523; 1-13.

5.2 pIC-NPs potential for cancer immunotherapy

The work by Speth et al on enhancing the immunogenicity of Bacillie Calmete-Guérin (BCG) vaccine by using pIC-NPs, lead us to test the same pIC-NPs for potential activation of macrophages towards an antitumor phenotype [56]. These pIC-NPs showed increased NO, which can be used in our studies on macrophage activation. In our study we combined these Poly (I:C) encapsulated chitosan-based nanoparticles with the TLR1/2 agonist, Pam3. By using pIC-NPs, the Type I interferon auto-/paracrine feedback loop can amplify the NO production (Figure 23). The current results show the potential of pIC-NPs for inducing the tumoricidal activity in both C57BL/6 and NSG BMDMs (Figure 12). Interestingly, this observed cancer cell growth was dependent on (i) sufficient ratio of BMDM to LLC cells where 20:1 showed to be most efficient and (ii) simultaneous Pam3 stimulation. No inhibition of LLC was observed with pIC-NPs alone suggesting that the auto-/paracrine feedback loop alone is not sufficient for the induced inhibitory effect but rather amplifies the Pam3-induced MyD88-dependent pathway and NO production (Figure 23). This hypothesis is further supported by NO-results from both C57BL/6 and NSG macrophages. The NO results revealed that simultaneous activation of macrophages with pIC-NPs and Pam3 induces higher NO levels compared to individual factors. Interestingly, these NO levels were higher in NSG BMDMs than in C57BL/6 (Figure 12).

Further investigations revealed that pIC-NPs induced macrophage tumoricidal activity is pIC-NPs concentration-dependent (Figure 13). The highest pIC-NPs induced tumoricidal activity seems to be at pIC-NPs concentration of 200ng/mL whereas the reduced effects are observed at 2 and 0.2 ng/mL.

Using flow cytometry we were able to detect that pIC-NPs induced apoptosis in Mitomycin C-treated BMDMs. The induced cell death was detected at high pIC-NPs concentrations (10ng/mL) in combination with Pam3 (Figure 14H). The results revealed 16.85% of the treated macrophages to be apoptotic cells undergoing secondary necrosis (Figure 14H, Table 16). However, this observed pIC-NPs toxicity can also be due to Mitomycin C since no significant percentage of apoptosis or necrosis was detected in non-Mitomycin C treated macrophages (Figure 15, Table 17). Taken together, these results suggest that high concentrations of pIC-NPs in synergy with Pam3 might lead to saturation of

[56] Speth M.T, Repnik U, Müller E, Spanier J, Kalinke U, Corthay A, Griffiths G: Poly (I:C)-encapsulating nanoparticles enhance macrophage response to BSG-vaccine via synergistic activation of Toll-like receptor signaling. (Manuscript in preparation)

the two involved signaling pathways and thereby to reduced or abolished cancer cell growth inhibition.

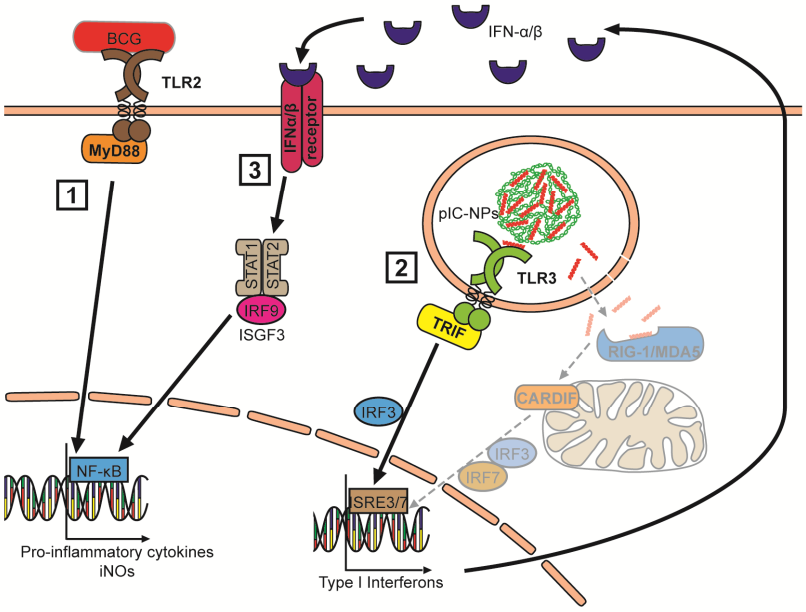

Figure 23. The signaling pathways induced by the synergistic action of the TLR3 and TLR2 agonist. In our study, we used Pam3 instead of BCG as the TLR2 agonist. Figure adopted from [56]

In our study with pIC-NPs we further investigated the importance of NO for the inhibitory effect. Müller et al reports demonstrated that the growth inhibitory ability of classical activated macrophages is NO-mediated [67]. The importance of NO production for pIC-NPs growth inhibitory ability was determined with the use of pharmacological iNOS inhibitor SMT (Figure 16). The presence of SMT completely abolished the cancer cell growth inhibition induced by pIC-NPs in combination with Pam3. These results suggest once more the NO mediated growth inhibition as a result of the synergistic action between the two immunostimulatory factors.

In all presented results the NO levels produced by pIC-NPs + Pam3 stimulated C57BL/6 macrophages were always lower compared to the positive control (Pam3 in combination with IFN-γ). However, pIC-NPs induced growth inhibition was comparable to the positive control (Pam3 stimulation with IFN-γ). These findings suggest that the peak of pIC-NPs induced NO production might not be after 24h of macrophage activation. Therefore, further experiments involving NO measurements at different time-points can be relevant.

[56] Speth M.T, Repnik U, Müller E, Spanier J, Kalinke U, Corthay A, Griffiths G: Poly (I:C)-encapsulating nanoparticles enhance macrophage response to BSG-vaccine via synergistic activation of Toll-like receptor signaling. (Manuscript in preparation)
[67] Müller E, Christopoulos P, Halder S, Lunde A, Beraki K, Speth M, Øyenbråten I, Corthay A: Two signals are required for optimal induction of tumoricidal M1 macrophage phenotype (Manuscript in preparation)

Furthermore, no toxicity of pIC-NPs towards LLC target cells was observed. Therefore we can conclude that the observed cancer cell growth inhibition is exclusively macrophage-mediated. The TLR1/2 agonist Pam3 seems to be the priming agent for the subsequent pIC-NPs stimulus. Since we demonstrated the synergy between two TLR agonists using the MyD88- and TRIF-depended pathway respectively, it would be of great interested if other TLR agonists could synergize in a similar way, as well.

Based on our promising *in vitro* results, pIC-NPs could be considered as a potential immunotherapeutic agent *in vivo*. Han el al reported the use of chitosan nanoparticles for enhanced immunogenicity of DCs *in vivo* [76]. The incorporated Poly (I:C) is protected against ribonuclease degradation leading to increased half life of the drug. Furthermore, they can easily be internalized through phagocytosis, by the target cells such as macrophages, without disturbing the biological features of the cell.

There is increased interest and reports of potential of TLR3 agonist Poly (I:C) as a beneficial treatment option for cancer and hepatitis B virus [66,77]. Shime et al documented the reduction of LLC implanted tumors with i.p injections of Poly (I:C) in WT mice [66]. This study and others will form the base for future *in vivo* experiments with pIC-NPs. In our pilot study, we did not observe significant tumor growth reduction or survival benefit between the two groups, just potential trends of effect of Poly(I:C) alone (Figure 21 and 22) [66]. Finally, the last step before using pIC-NPs in treatment experiment, was to perform the acute toxicity study which revealed that 2 μg of pIC-NPs is the safest dose in terms of avoiding inflammation or other experimental complications.

5.3 Type I interferon versus type II interferon

In their study on relapsing-remitting multiple sclerosis, Tao el al reported a synergy between TLR7 and TLR9 agonists with exogenous IFN-β leading to up-regulation of B cells

[66] Shime H, Matsumoto M, Oshiumi H, Tanaka S, Nakane A, Iwakura Y, Tahara H, Inoue N, Seya T: Toll-like receptor 3 signaling converts tumor-supporting myeloid cells to tumoricidal effectors. Proceedings of the National Academy of Sciences of the United States of America (PNAS) 2012, **109(6)**: 2066-2071.

[76] Han H.D, Byeon Y, Jang J-H, Jeon H. N, Kim G.H, Kim M.G, Pack C-G, Kang T.H, Jung I.D, Lim Y.T, Lee Y.J, Lee J.W, Shin B.C, Ahn H.J, Sood A.K, Park Y.M: In vivo steptwise immunomodulation using chitosan nanoparticles as a platform nanotechnology for cancer immunotherapy. Scientific reports 2016, **6 article number 38348**; 1-13

[77] Wu J, Huang S, Zhao X, Chen M, Lin Y, Xia Y, Sun C, Yang Xuecheng, Wang J, Guo Y, Song J, Zhang E, Wang , Zheng X, Schlaak J.F, Lu Mengji, Yang D: Poly (I:C) Treatment Leads to Interferon-Dependent Clearance of Hepatitis B Virus in a Hydrodynamic Injection Mouse Model. Journal of Virology 2014, **88(18)**: 10421-10431.

immunoregulatory cytokines [78]. Furthermore, type I interferons-based treatment can also be found in cancer [71,72]. New developing cancer immunotherapies are using type I interferons as a standard therapy for different cancer types such as CML, hairy cell leukemia, melanoma and Kaposi´s sarcoma [71,72,79]. Type I interferons, produced by most cells, are know for its involvement in antiviral immunity [71]. In the case of cancer, there is increasing number of reports on type I interferon showing their role in maturation of DC and their ability for Ag presentation by enhancing MHC- and co-stimulatory molecule expression [72,80,81].

In our study we were interested in replacing IFN-γ with IFN-β in the synergy with Pam3. Our *in vitro* results showed IFN-β to be more potent in activating macrophages compared to IFN-γ. Beside the proved synergy between IFN-β and Pam3, one more interesting finding was IFN-β direct cytotoxicity on LLCs. This observation can be seen as a disadvantage of using high concentrations of IFN-β in further experiments since it is not clear if the observed inhibitory effects is due to IFN-β or simply macrophage-mediated. Experiments involving IFN-β testing with other TLR agonists can be relevant for further investigation of this direct cytotoxicity.

[71] Parker B.S, Rautela J, Hertzog P.J: Antitumor actions of interferons:implications for cancer therapy. Nature Review Cancer 2016, **16(3)**: 131-144

[72] Zitvogel L, Galluzi L, Kepp O, Smyth M.J, Kroemer G: Type I interferons in anticancer immunity. Nature Reviews Immunology 2015, **15(7)**: 405-414

[78] Tao Y, Zhang X, Markovic-Plese S: Toll line receptor (TLR)7 and TLR9 agonist enhance interferon (IFN) beta-1a´s immunoregulatory effects on B cells in patients with relapsing-remitting multiple sclerosis (RRMs). Journal of Neuoroimmunology 2016, **15(298)**: 181-188

[79] Trinchieri G:Type I interferon: friend or foe? The Journal of Experimental Medicine 2010, **207(10)**: 2053-2063

[80] Simmons D.P, Wearsch P.A, Canaday D.H, Meyerson H.J, Liu Y.C, Wang Y, Boon W.H, Harding C.V: Type I interferon drives a distinctive dendritic cell maturation phenotype that allows continued class II MHC synthesis and antigen processing. Journal of Immunology 2012, **188(7)**: 3116-3126

[81] Le Bon A, Etchart N, Rossmann C, Ashton M, Hou S, Gewert D, Borrow P, Tough D.F: Cross-priming of CD8+ T cells stimulated by virus-induced type I interferon. Nature Immunology 2003, **4(10)**: 1009-1015

5.4 TNF-α and macrophage activation

The pleiotropic cytokine TNF-α uses two transmembrane receptors TNFR1 and TNFR2 to induce NF-κB and lymphocyte activation, respectively[28,29]. Several studies have reported anti-tumor properties of TNF-α where the cytokine synergizes with IFN-γ [28,73]. This synergy can lead to the activation of tumoricidal activity in murine peritoneal macrophages towards cancer cells [73]. Therefore, it was expected that TNF-α could also induce potentiation of murine BMDMs to a similar degree as in peritoneal macrophages. We used a broad concentration range of TNF-α in order to determine the best suitable concentration for macrophage activation. However, the results revealed that TNF-α ability for rendering macrophages tumoricidal is not efficient (Figure 18). The highest used concentration gave the observed growth inhibition primarily at the highest ratio of effector cells to target cells. Moreover this inhibitory effect was not strong as Pam3 induced inhibition. The same pattern was observed for NO production. The repeated experiments showed the same negative results, leading to the conclusion that TNF-α is not a potent activator of BMDMs.

5.5 HMGB1 activates macrophage towards an anti-tumor phenotype

The alarmin HGB1 has been reported by Hreggvidsdottir et al to function as an inflammatory enhancer [33]. This enhancing ability depends on HMGB1s interaction with other proinflammatory molecules [33]. The resulting complex formation gives a strong synergistic effect on the cytokine production [31-33]. Furthermore, Su et al in 2016 demonstrated HMGB1

[28] Haabeth O.A.W, Bogen B, Corthay A: A model for cancer-suppressive inflammation. Oncolmmunology 2012, **1(7)**: 1146-1155

[29] Parameswaran N, Patial S: Tumor Necrosis Factor-α Signaling in Macrophages. Crit Rev Eukaryot Gene Expr. 2010, **20(2)**: 87-103

[31] Lotze M.T, Tracey K.J: High-mobility group box 1 protein (HMGB1): nuclear weapon in the immune arsenal. Nature Reviews Immunology 2005, **5(4)**: 331-342

[32] Harris H.E, Andersson U, Pisetsky D.S: HMGB1: A multifunctional alarmin driving autoimmune and inflammatory disease. Nature Reviews Rheumatology 2012, **8(4)**: 195-202

[33] Hreggvidsdottir H.S, östberg T, Wähämaa H, Schierbeck H, Aveberger A-C, Klevenvall L, Palmblad K, Ottosson L, Andersson U, Harris H.E: The alarmin HMGB1 acts in synergy with endogenous and exogenous danger signals to promote inflammation. Journal of Leukocyte Biology 2009, **86(3)**: 655-662

[73] Stavna A: Activation of macrophages for inhibition of cancer cell growth. Master in Science thesis, Oslo and Akershus University College of Applied Science, 2013

and TLR4 involvement in macrophage reprogramming towards M1 phenotype [82]. This drew our attention towards testing the ability of HMGB1 to activate murine BMDMs towards an anti-tumor phenotype.

In our study we used calmodulin-binding protein (CBP)-tagged rat HMGB1 protein expressed by *E.coli*. This recombinant HMGB1 form contains both the disulfide bond between C23 and C45, and the thiol form of C106. It is these unique biochemical features, which allow HMGB1 to bind to TLR4. We combined this TLR4 ligand with TLR1/2 agonist in order to activate C57BL/6 BMDMs. Our results show that HMGB1 alone is ineffective in inducing the tumoricidal activity in C57BL/6 macrophages (Figure 19). However, when macrophages were activated with HMGB1and Pam3 we could observe a strong inhibition of cancer cell growth. This growth inhibition seems to be dependent on the number of BMDMs present with LLC cells since 20:1 ratio gave the strongest inhibitory effect. Similarly, higher NO production was observed upon HMGB1 co-stimulation with Pam3. Another important aspect about HMGB1 according to the *in vitro* results is that it does not induce direct toxicity on LLC. Therefore the observed cancer cell growth inhibition is macrophage-mediated.

5.6 LLC-induced tumor development

In our in vivo LLC titration experiment, we determined that 1000 LLC cells are sufficient for tumor development. However, higher LLC cell numbers such as 50.000 and 100.00 induced much faster tumor development leading to mice having to be sacrificed early due to necrosis development. The other experimental complication was the development of skin irritation and fighting scars, which made it sometimes difficult to determine the exact tumor size. Mice with either skin irritation or scars were separated from the others to avoid further complications.

[82] Su Z, Zhang P, Yu Y, Lu H, Liu Y, Ni P, Su X, Wang D, Liu Y, Wang J, Shen H, Xu W, Xu H: HMGB1 facilitated macrophage reprogramming towards a proinflammatory M1-like phenotype in experimental autoimmune myocarditis development. Scientific reports 2016, **6 (21884)**: 1-10

6 Concluding remarks

The main objective of this master thesis was to identify new molecular combinations for rendering macrophages tumoricidal. The presented *in vitro* data demonstrated that pIC-NPs and HMGB1 as potential candidates for activating macrophages towards an antitumor phenotype. However, both of these TLR agonists require synergizing with the TLR1/2 agonist Pam3 in order to give the proper macrophage activation. These new molecular combinations indicate that IFN-γ is not always needed for the induction of macrophages tumoricidal ability. Our *in vivo* studies demonstrated a trend for the antitumor potential of Poly (I:C) whereas the safest dose of pIC-NPs should be 2μg. Furthermore, we demonstrated the potential replacement of IFN-γ with type I interferon, IFN-β.

All the data presented in this thesis can be summarizes as followed:

1. The type I interferon, IFN-β, can replace IFN-γ for synergy with Pam3 and thereby inducing macrophage tumoricidal activity.
2. pIC-NPs was shown by Speth to yield IFN-β and can indeed replace IFN-γ as a second signal with Pam3.
3. The strongest tumoricidal activity is induced at pIC-NPs concentration of 200 ng/mL.
4. Higher pIC-NPs concentrations might lead to either apoptosis or saturation of the signaling pathway.
5. The observed cancer cell growth inhibition by pIC-NPs stimulated macrophages is NO mediated.
6. The safest *in vivo* dose of pIC-NPs is 2 μg.
7. The alarmin HMGB1 can also replace IFN-γ for synergy with Pam3. This might indicate that HMGB1 also induce IFN-β since HMGB1 is a TLR4-ligand.
8. LLC *in vivo* tumors can be induced with 1000 s.c injected LLC cells in C57BL/6 mice.
9. There are potential trends of effect of Poly(I:C) alone in LLC model
10. TNF-α does not replace Pam3 well for synergy with IFN-γ.

7 REFERENCES

1. Murphy K: *Janeway´s Immunobiology* 9th Edition: Garland Science; 2017
2. Akira S, Uematsu S, Takeuchi O: Pathogen recognition and innate immunity. *Cell* 2006, **124 (4)**: 783-801
3. Schenten, D. and R. Medzhitov: Chapter 3 : The control of adaptive immune responses by the innate immune system. *Advances in Immunology* 2011, **109**: p. 87-124.
4. Takeuchi O, Akira S: Pattern recognition receptors and inflammation. *Cell* 2010, **140 (6)**: 805-820
5. McComb S, Thiriot A, Krishnan L, Stark F: Chapter 1: Introduction to the Immune System. *Methods in Molecular Biology* 2013, **1061**: 1-20.
6. Murray P.J, Wynn T.A : Protective and pathogenic functions of macrophage subsets. *Nature Reviews Immunology* 2011, **11(11)**: 723-737.
7. Billack B: Macrophage Activation: Role of Toll-like Receptors, Nitric Oxide and Nuclear Factor kappa B. *Americal Journal of Pharmaceutical Education* 2006, **70(5)** Article 102; 1-10
8. Hume D.A : The Many Alternative Faces of Macrophage Activation. *Frontiers in Immunology* 2015, **6 (370)**: 1-10
9. Mosser D.M, Edwards J.P: Exploring the full spectrum of macrophage activation. *Nature Review Immunology* 2008, **8 (12)**: 958-969
10. Biswas S.K, Mantovani A: Macrophage plasticity and interaction with lymphocyte subsets: cancer as a paradigm. *Nature Review Immunology* 2010, **11 (10)**: 889-896
11. Porta C, Riboldi E, Ippolito A, Sica A: Molecular and epigenetic basis of macrophage polarized activation. *Seminars in Immunology* 2015, **27(4)**: 237-248
12. Botos I, Segal D.M, Davies D.R: The Structural Biology of Toll-like Receptors. *Structure* 2011, **19(4)**: 447-459
13. Pandey S, Kawai T, Akira S: Microbial Sensing by Toll-like Receptors and Intracellular Nucleic Acid Sensors. *Cold Spring Harbor Perspectives in Biology* 2015, **7 (1)**:a016246; 1-18
14. Trinchieri G, Sher A: Cooperation of Toll-like receptor signals in innate immune defense. *Nature Reviews Immunology* 2007, **7(3)**: 179-190
15. Joosten L.A.B, Abdollahi-Roodsaz S, Dinarello C.A, O´Neill L, Netea M.G: Toll-like receptors and chronic inflammation in rheumatic diseases: new developments. *Nature Reviews Rheumatology* 2016, **12(6)**: 344-357.
16. Blasius A.L, Beutler B: Intracellular Toll-like Receptors. *Immunity* 2010, **32(3)**: 305-315
17. Rakoff-Nahoum S, Medzhitov R: Toll-like receptors and cancer. *Nature Reviews Cancer* 2009, **9(1)**: 57-63
18. Rahat M.A, Hemmerlein Bernhard : Macrophage-tumor cell interactions regulate the function of nitric oxide. *Frontiers in Physiology* 2013, **4(144)**: 1-15
19. Bogdan C : Nitric oxide synthase in innate and adaptive immunity: an update. *Trends in immunology* 2015, **36(3)**: 161-178
20. Lee S, Margolin K: Cytokines in Cancer Immunotherapy. Cancers 2011, **3(4)**: 3856-3893
21. Ikram N, Hassan K, Tufail S: Cytokines. International Journal of Pathology 2004, **2(1)**: 47-58
22. Dranoff G: Cytokines in cancer pathogenesis and cancer therapy. Nature Reviews Cancer 2004, **4 (1)**: 11-22

23. Dunn G.P, Koebel C.M, Schreiber R.D: Interferons, immunity and cancer immunoediting. Nature Reviews Tumor Immunology 2006, **6(11)**: 836-848
24. Hervas-Stubbs S, Perez-Gracia J.L, Rouzat A, Sanmamed M.F, Le Bon A, Melero I: Direct Effects of Type I Interferons on Cells of the Immune System. Clinical Cancer Research 2011, **17(9)**: 2619-2627
25. Marschall Z, Scholz A, Cramer T, Schafer G, Schirner M, Oberg K, Wiedenmann B, Höcker M, Rosewicz Stefan: Effects of Interferon Alpha on Vascular Endothelial Growth Factor Gene Transcription and Tumor Angiogenesis. Journal of the National Cancer Institute 2003, **95(6)**: 437-448
26. Liang S, Wei H, Sun R, Tian Z : IFNalpha regulates NK cell cytotoxicity through STAT1 pathway. Cytokine 2003, **23(6)**: 190-199
27. Boehm U, Klamp T, Groot M, Howard JC : Cellular responses to interferon gamma. Annual Review Immunology 1997, **15**:749-795
28. Haabeth O.A.W, Bogen B, Corthay A: A model for cancer-suppressive inflammation. Oncolmmunology 2012, **1(7)**: 1146-1155
29. Parameswaran N, Patial S: Tumor Necrosis Factor-α Signaling in Macrophages. Crit Rev Eukaryot Gene Expr. 2010, **20(2)**: 87-103
30. Balkwill F: Tumor necrosis factor and cancer. Nature Reviews Cancer 2009, **9(5)**: 361-370
31. Lotze M.T, Tracey K.J: High-mobility group box 1 protein (HMGB1): nuclear weapon in the immune arsenal. Nature Reviews Immunology 2005, **5(4)**: 331-342
32. Harris H.E, Andersson U, Pisetsky D.S: HMGB1: A multifunctional alarmin driving autoimmune and inflammatory disease. Nature Reviews Rheumatology 2012, **8(4)**: 195-202
33. Hreggvidsdottir H.S, östberg T, Wähämaa H, Schierbeck H, Aveberger A-C, Klevenvall L, Palmblad K, Ottosson L, Andersson U, Harris H.E: The alarmin HMGB1 acts in synergy with endogenous and exogenous danger signals to promote inflammation. Journal of Leukocyte Biology 2009, **86(3)**: 655-662
34. Yang H, Lündbäck P, Ottosson L, Erlandsson-Harris H, Venereau E, Bianchi M.E, Al-Abed Y, Andersson U, Tracey K.J, Antoine D.J: Redox Modification of Cysteine Residues Regulates the Cytokine Activity of High Mobility Group Box-1 (HMGB1). Molecular Medicine 2012, **18**:250-259
35. Park J.S, Svetkauskaite D, He Q, Kim J.V., Strassheim D, Ishizaka A, Abraham E: Involvement of Toll-like receptors 2 and 4 in cellular activation by high mobility group box 1 protein. Journal of Biological Chemistry 2004, **279 (9)**: 7370-7377
36. Yang H, Wang H, Ju Z, Ragab A.A, Lündbäck P, Long W, Valdes-Ferrer S.I, He M, Pribis J.P, Li J, Lu B, Gero D, Szabo C, Antoine D.J, Harris H.E, Golenblock D.T, Meng J, Roth J, Chavan S.S, Andersson U, Billiar T.R, Tracey K.J, Al-Abed Y: MD-2 is required for disulfide HMGB1-dependent TLR4 signaling. The Journal of Experimental Medicine 2015, **212(1)**: 5-14
37. Kang R, Zhang Q, Zeh J.H III, Lotze M.T, Tang D: HMGB1 in Cancer: Good, Bad, or Both? Clinical Cancer Research 2013, **19(15)**: 4046-4057
38. Grivennikov S.I, Greten F.R, Karin M: Immunity, Inflammation and Cancer, Cell 2010, **140(6)**: 883-899
39. Corthay A: Does the immune system naturally protect against cancer? Frontiers in Immunology 2014, **5(197)**: 1-8
40. Pecorino L: Molecular biology of cancer-mechanisms, targets and therapeutics. **Fourth edition** 2016, Oxford University press
41. Hannah D, Weinberg R.A: Hallmarks of cancer: The next generation. Cell 2011, **144(5)**: 646-672

42. Dunn G.P, Old L.J, Schreiber R.D: The three Es of cancer immunoediting. Annual Review of Immunology 2004, **22**:329-360
43. Balkwill F, Mantovani A: Inflammation and cancer: back to Virchow? Lancet 2001, 357**(9255)**: 539-545
44. Mantovani A, Allavena P, Sica A, Balkwill F: Cancer-related inflammation. Nature 2008, **454 (7203)**: 436-444
45. Dunn G.P, Bruce A.T, Ikeda H, Old L.J, Schreiber R.D: Cancer immunoediting: from immunosurveillance to tumor escape. Nature Immunology 2002, 3(11): 991-998
46. Petty A.J, Yang Y: Tumor-associated macrophages: implications in cancer immunotherapy. Immunotherapy 2017, **9(3)**: 289-302
47. Mantovai A, Sozzani S, Locati M, Allavena P, Sica A: Macrophage polarization: tumor-associated macrophages as a paradigm for polarized M2 mononuclear phagocytes. Trends in Immunology Review 2002, **23(11)**: 549-555
48. Jiang W, Roemeling C.A, Chen Y, Qie Y, Xiujie L, Chen J, Kim B.Y.S: Designing nanomedicine for immune-oncology. Nature Biomedical Engineering 2017, **1(0029)**: 1-11
49. Pardoll D.M: The blockade of immune checkpoints in cancer immunotherapy. Nature Review Cancer 2012, **12(4)**: 252-264
50. Hosseini Maryam, Haji-Fatahaliha M, Jadidi-Niaragh F, Majidi J, Yousefi M: The use of nanoparticles as a promising therapeutic approach in cancer immunotherapy. Artificial Cells, Nanomedicine, and Biotechnology 2016, **44(4)**: 1051-1061
51. Griffiths G, Nyström B, Sable S.B, Khuller G.K: Nanobead-based interventions for the treatment and prevention of tuberculosis. Nature Reviews Microbiology 2010, **8(11)**: 827-834
52. Saleh T, Shojaosadati S.A: Multifunctional nanoparticles for cancer immunotherapy. Human Vaccines & Immunotherapeutics 2016, **12(7)**: 1863-1875
53. Bolhassani A, Javanzad S, Saleh T, Hashemi M, Aghasadeghi M.R, Sadat S.M: Polymeric nanoparticles. Human Vaccines & Immunotherapeutics 2014, **10(2)**: 321-332
54. Gregory A.E, Titball R, Williamson D: Vaccine delivery using nanoparticles. Frontiers in Cellular and Infection Microbiology 2013, **3(13)**: 1-13
55. De Koker S, Lambrecht B.N, Willart M.A, van Kooyk Y, Grooten J, Vervaet C, Remon J.P, De Geest B.G: Designing polymeric particles for antigen delivery. Chemical Society Reviews 2011, **40(1)**: 320-339
56. Speth M.T, Repnik U, Müller E, Spanier J, Kalinke U, Corthay A, Griffiths G: Poly (I:C)-encapsulating nanoparticles enhance macrophage response to BSG-vaccine via synergistic activation of Toll-like receptor signaling. (Manuscript in preparation)
57. Bertram J.S, Janik P: Establishment of a cloned line of Lewis Lung Carcinoma cells adopted to cell culture. Cancer Letters 1980, **11(1)**: 63-73
58. Patton J, Vuyyuru R, Siglin A, Root M, Manser T: Evaluation of the efficiency of human immune system reconstitution in NSG mice and NSG mice containing a human HLA.A2 transgene using hematopoietic stem cells purified from different sources. Journal of Immunological Methods 2015, **422**:13-21
59. Presa M, Chen Y.G, Grier A.E, Leiter E.H, Brehm M.A, Greiner D.L, Shultz L.D, Serreze D.V: The presence and preferential activation of regulatory T cells diminish adoptive transfer of autoimmune diabetes by polyclonal nonobese diabetic (NOD) T cells effectors into NSG versus NOD-scid mice. The Journal of Immunology 2015, **195(7)**: 3011-3019

60. Shultz L.D, Brehm M.A, Bavari S, Greiner D.L: Humanized mice as a preclinical tool for infectious disease and biomedical research. Annals of the New York Academy of Sciences 2011, **1245**:50-54
61. Simpson-Abelson M.R, Sonnenberg G.F, Takita H, Yokota S.J, Conway Jr T.F, Kelleher Jr R.J, Shultz L.D, Barcos M, Bankert R.B: Long-term engrafment and expansion of tumor-derived memory T cells following the implantation of non-disrupted pieces of human lung tumor into NOD-scid IL2Rγ^{null} mice. The Journal of Immunology 2008, **180(10)**: 7009-7018
62. Coneski P.N, Schoenfisch M.H: Nitric oxide release: part III. Measurement and reporting. Chemical Society reviews 2012, **41(10)**: 3753-3758.
63. Sawai H, Domae N: Discrimination between primary necrosis and apoptosis by necrostatin-1 in Annexin V-positive/propodium iodide-negative cells. Biochemical and Biophysical Research Communications 2011, **411(3)**: 569-573
64. Vermes I, Haanen C, Steffens-Nakken H, Reutelingsperger C: A novel assay for apoptosis. Flow cytometric detection of phosphatidylserine expression on early apoptotic cells using fluorescein labelled Annexin V. Journal Immunological Methods 1995, **184(1)**: 39-51
65. Schuttle B, Nuydens R, Geerts H, Ramaekers F: Annexin V binding assay as a tool to measure apoptosis in differentiated neuronal cells. Journal of Neuroscience Methods 1998, **86(1)**: 63-69
66. Shime H, Matsumoto M, Oshiumi H, Tanaka S, Nakane A, Iwakura Y, Tahara H, Inoue N, Seya T: Toll-like receptor 3 signaling converts tumor-supporting myeloid cells to tumoricidal effectors. Proceedings of the National Academy of Sciences of the United States of America (PNAS) 2012, **109(6)**: 2066-2071.
67. Müller E, Christopoulos P, Halder S, Lunde A, Beraki K, Speth M, Øyenbråten I, Corthay A: Two signals are required for optimal induction of tumoricidal M1 macrophage phenotype (Manuscript in preparation)
68. Decker T, Müller M, Stockinger S: The Yin and Yang of type I interferon activity in bacterial infection. Nature Review Immunology 2005, **5(9)**: 675-687
69. Zhang X, Alley E.W, Russel S.W, Morrison D.C: Necessity and sufficiency of beta interferon for nitric oxide production in mouse peritoneal macrophages. Infection and immunity 1994, **62(1)**: 33-40
70. Southan G.J, Szabo C, Thiemermann C: Isothioureas: potent inhibitors of nitric oxide synthases with variable isoform selectivity. British journal of pharmacology 1995, **114(2)**: 510-516
71. Parker B.S, Rautela J, Hertzog P.J: Antitumor actions of interferons:implications for cancer therapy. Nature Review Cancer 2016, **16(3)**: 131-144
72. Zitvogel L, Galluzi L, Kepp O, Smyth M.J, Kroemer G: Type I interferons in anticancer immunity. Nature Reviews Immunology 2015, **15(7)**: 405-414
73. Stavna A: Activation of macrophages for inhibition of cancer cell growth. Master in Science thesis, Oslo and Akershus University College of Applied Science, 2013
74. Laboratory, T.J Body weight information for C57BL/6J (000604) 2017. Access to the information at the web-side: https://www.jax.org/jax-mice-and-services/strain-data-sheet-pages/body-weight-chart-000664#
75. Sorgi C.A, Rose S, Court N, Carlos D, Paula-Silva F.W.G, Assis P.A, Frantz F.G, Ryffel B, Quesniaux V, Faccioli L.H: GM-CSF priming drives bone marrow-derived macrophages to a pro-inflammatory pattern and downmodulates PGE_2 in response to TLR2 ligands. PloS one 2012, **7(7)**:e40523; 1-13.
76. Han H.D, Byeon Y, Jang J-H, Jeon H. N, Kim G.H, Kim M.G, Pack C-G, Kang T.H, Jung I.D, Lim Y.T, Lee Y.J, Lee J.W, Shin B.C, Ahn H.J, Sood A.K, Park Y.M: In

vivo steptwise immunomodulation using chitosan nanoparticles as a platform nanotechnology for cancer immunotherapy. Scientific reports 2016, **6 article number 38348**; 1-13

77. Wu J, Huang S, Zhao X, Chen M, Lin Y, Xia Y, Sun C, Yang Xuecheng, Wang J, Guo Y, Song J, Zhang E, Wang , Zheng X, Schlaak J.F, Lu Mengji, Yang D: Poly (I:C) Treatment Leads to Interferon-Dependent Clearance of Hepatitis B Virus in a Hydrodynamic Injection Mouse Model. Journal of Virology 2014, **88(18)**: 10421-10431.
78. Tao Y, Zhang X, Markovic-Plese S: Toll line receptor (TLR)7 and TLR9 agonist enhance interferon (IFN) beta-1a´s immunoregulatory effects on B cells in patients with relapsing-remitting multiple sclerosis (RRMs). Journal of Neuoroimmunology 2016, **15(298)**: 181-188
79. Trinchieri G:Type I interferon: friend or foe? The Journal of Experimental Medicine 2010, **207(10)**: 2053-2063
80. Simmons D.P, Wearsch P.A, Canaday D.H, Meyerson H.J, Liu Y.C, Wang Y, Boon W.H, Harding C.V: Type I interferon drives a distinctive dendritic cell maturation phenotype that allows continued class II MHC synthesis and antigen processing. Journal of Immunology 2012, **188(7)**: 3116-3126
81. Le Bon A, Etchart N, Rossmann C, Ashton M, Hou S, Gewert D, Borrow P, Tough D.F: Cross-priming of CD8+ T cells stimulated by virus-induced type I interferon. Nature Immunology 2003, **4(10)**: 1009-1015
82. Su Z, Zhang P, Yu Y, Lu H, Liu Y, Ni P, Su X, Wang D, Liu Y, Wang J, Shen H, Xu W, Xu H: HMGB1 facilitated macrophage reprogramming towards a proinflammatory M1-like phenotype in experimental autoimmune myocarditis development. Scientific reports 2016, **6 (21884)**: 1-10